This is to certify that the
dissertation entitled

DEVELOPMENT OF TITANIUM PYRROLYL HYDROAMINATION CATALYSTS AND URANIUM PYRROLYL COMPLEXES

presented by

Douglas L. Swartz II

has been accepted towards fulfillment
of the requirements for the

Ph.D degree in Chemistry

Major Professor's Signature

7/1/09

Date

DEVELOPMENT OF TITANIUM PYRROLYL HYDROAMINATION CATALYSTS AND URANIUM PYRROLYL COMPLEXES

By

Douglas L. Swartz II

A DISSERTATION

Submitted to
Michigan State University
in partial fulfillment of the requirements
for the degree

DOCTOR OF PHILOSOPHY

Chemistry

2009

ABSTRACT

DEVELOPMENT OF TITANIUM PYRROLYL HYDROAMINATION CATALYSTS
AND
URANIUM PYRROLYL COMPLEXES

By

Douglas L. Swartz II

The primary focus of this thesis is the design and development of pyrrolyl based titanium hydroamination catalysts with applications towards multi-component coupling reactions involving a primary amine, alkyne, and isonitrile. Hydroamination is an atom efficient process for the production amines and imines from the formal addition of an N–H bond across a C–C unsaturated bond. Titanium-catalyzed hydroamination has seen an explosion of activity and has led to new methodologies in a variety of C–N containing molecules. The first chapter briefly discusses the types of ancillary ligands employed for titanium hydroamination catalysts with the main focus being on the development of titanium pyrrolyl complexes for the development of C–N bond forming reactions.

Since the first successful hydroamination of a primary amine and alkyne by a titanium pyrrolyl complex our goal has been to optimize the most promising catalysts that carry out these reactions to expand the scope of this methodology. Chapters 2 – 4 discuss the types of electronic features and steric profiles in catalyst design that encourage these useful C-N bond forming reactions.

Ligand isomerization in titanium dipyrrolylmethane complexes is common due to the different bonding hapticities the ligand can adopt. Methods for altering this barrier may provide clues to the active species in catalysis and allow control of complex structures. Chapter 5 discusses the effects 5,5-substitution has on dipyrrolylmethane

ligand isomerization and the parameters for pyrrolyl exchange.

Since the discovery of uranium bis(imido) analogues of the uranyl ion, UO_2^{2+}, actinide chemists have been intrigued with the bonding and reactivity of this functional group. Pyrrolyl ligands have proven to be a useful class of ancillary ligands for transition metals, however their employment in actinide chemistry is relatively scarce. The synthesis, structure, and reactivity of uranium bis(imido) dipyrrolylmethane complexes are discussed in Chapter 6.

To my wife, I hope it was all worth it

ACKNOWLEDGEMENTS

First and foremost I have to thank wife, Melesa, for all the love and support she has given to me over the past 11 years we have been together, especially the past 5 years during my time as a graduate student at Michigan State. I also want to thank my son, Lucelus, for being the best part of my day everyday when I get home, greeting me with the best hug and smile a dad can ever get.

I would like to thank my advisor, Aaron Odom, for all his patience, guidance and support during my time at Michigan State. Working under his direction provided me with wonderful opportunities that have lead to a satisfying graduate career. Among the many opportunities I was able to take part in, working with Dr. Jim Boncella at Los Alamos National Lab was an absolute pleasure and privilege. I would like to thank Jim for all his advice, patience, support he gave to my family and I while we were in Los Alamos.

I would also like to acknowledge all my past and present group members: Jim, Bala, Kapil, Sanjukta, Sam, Supriyo, Steve, and Eyal. I would like to give Supriyo a special "thank you" for being such a wonderful friend and colleague. I will miss working alongside him, "Absolutely."

I would like to acknowledge Professor Mitch Smith, Professor Jim McCusker, and Professor Bill Wulff for serving on my committee, for their guidance, and teaching me a degree of professionalism in presenting my research.

A special thanks goes to Dan Holmes for assisting me with all the NMR experiments I had to conduct throughout my graduate career.

Lastly, I would like to thank my parents for all the love, support and faith they put in me that helped me succeed in so aspects of life. I hope that I have made them proud.

Douglas L. Swartz II

TABLE OF CONTENTS

LIST OF TABLES

LIST OF FIGURES

LIST OF ABBREVIATIONS

Boc	*tert*-butyloxycarbonyl
Bu^tbipy	4,4'-di-*tert*-butyl-2,2'-bipyridine
Cod	1,5- cyclooctadiene
dap	2-((dimethyamino)methyl)pyrrolyl
H_2dpm	5,5-dimethyldipyrrolylmethane
GC/FID	Gas Chromotography Flame Ionization Detector
THF	tetrahydrofuran
DME	1,2-dimethoxyethane
dmpe	bis(dimethylphosphino)ethane
$Hpyrr^{mes}$	2-(mesityl)pyrrole
$Hpyrr^{3,5–CF3}$	2-(3,5-bis(trifluoromethyl)phenyl)pyrrole
$Hpyrr^{4–CF3}$	2-(4-(trifluoromethyl)phenyl)pyrrole
$Hpyrr^{tol}$	2-*p*-tolyl-1*H*-pyrrole
H_2dpm^{mes}	5,5'-(propane-2,2-diyl)bis(2-mesityl-pyrrole)
$H_2dpm^{3,5–CF3}$	5,5'-(propane-2,2-diyl)bis(2-(3,5-bis(trifluoromethyl)phenyl)pyrrole)
$3\text{-}dpm^{3,5–CF3}$	5,5'-(propane-2,2-diyl)bis(3-(3,5-bis(trifluoromethyl)phenyl)pyrrole)
$3\text{-}dpm^{C6F3}$	5,5'-(propane-2,2-diyl)bis(3-mesityl-pyrrole)
$3\text{-}Hpyrr^{3,5–CF3}$	3-(3,5-bis(trifluoromethyl)phenyl)pyrrole

3-Hpyrr^{C6F5}	3-(perfluorophenyl)pyrrole
Hpyrr$^{2\text{-}CF3\text{-}4\text{-}C6F5}$	2-(3,5-bis(trifluoromethyl)phenyl)-4-(perfluorophenyl)pyrrole
H_2cpm	1,1-bis(α-pyrrolyl)cyclohexane
H_2tmcpm	1,1-bis(α-pyrrolyl)-3,3,5,5-tetramethylcyclohexane
TFA	trifluoroacetic acid
RT	room temperature
EtOAc	ethyl acetate

LIST OF SCHEMES

CHAPTER 1

Titanium pyrrolyl catalysts in C–N bond formation

1.1 Introduction

The synthesis of C–N bonds is a significant process in organic chemistry. While a typical method for their preparation is the condensation of an amine or hydrazine with a ketone or aldehyde, titanium-catalyzed hydroamination is an attractive alternative when the desired product is not readily prepared using current carbonyl methodologies. While both methods are effective in preparing simple imine products, titanium-catalyzed hydroamination offers great synthetic utility in the selective generation of a variety of nitrogen containing products.

For example, the selective syntheis of α,β-unsaturated imines from the reaction of an α,β-unsaturated ketone with a primary amine can be problematic. Competing Michael addition reactions can lead to a mixture of products which can make isolation difficult. However, titanium-catalyzed hydroamination of a 1,3-enyne with a primary amine yields the desired product selectively without unwanted by-products (Scheme 1.1).

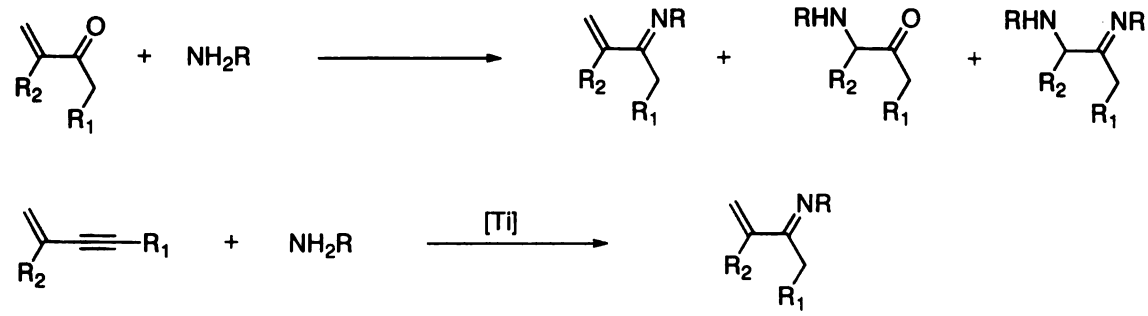

Scheme 1.1 Comparison between condensation and titanium-catalyzed hydroamination methodologies.

In addition to the synthesis of α,β-unsaturated imines, new methodologies in the synthesis of pyrroles, hydrazones, pyrimidines, and α,β-unsaturated β-iminoamines have been developed which use titanium-catalyzed hydroamination (*vide infra*). The development of titanium catalysts to carry out these transformations often use the hydroamination of alkynes with primary amines as a method for evaluating the efficacy of catalyst design.

While there are a plethora of titanium catalysts known to hydroaminate alkynes with primary amines, the development of catalysts through ancillary ligand studies to improve the substrate scope and enhance catalyst activity is an area of intense research. This chapter takes a cursory look at ancillary ligands for titanium catalysts with the main focus being on the enhancement of titanium pyrrolyl complexes towards the development of C–N bond forming reactions.

1.2 Hydroamination with titanium Cp complexes

Cyclopentadienyl (Cp) ligands are some of the most heavily studied ancilliaries for transition metals. Fittingly, some of the first reported examples of hydroamination with titanium catalysts were ligated with Cp-based ligands.[1]

Titanium-catalyzed hydroamination is believed to operate through a similar mechanism as the zirconocene-based system elucidated by Bergman and co-workers (Scheme 1.2).[2] A primary amine is a restriction of the Bergman mechanism for hydroamination and it is assumed that all the titanium catalysts in this chapter operate via this mechanism.

The first step in the catalytic cycle is the generation of a reactive metal imido species (**A**) which is formed from protonylsis of the precatalyst M–R bond. Introduction of an alkyne coordinates to **A** to yield complex **B** which undergoes a [2 + 2]-cylcoaddition to yield a azametallacyclobutene intermediate (**C**). Coordination of free primary amine to **C** in solution gives complex **D** which undergoes prontonlysis of the M–C bond to give bis(amido) metal complex **E**. Further protonation from the amide regenerates the active catalyst **A** and yields the imine product.

Chart 1.1 Cp based titanium catalysts

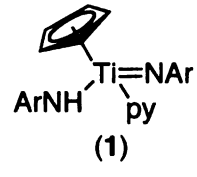

(1)

Bergman[3]

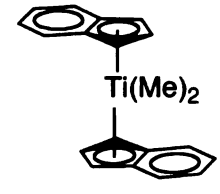

Doye

(2)

Doye[4]

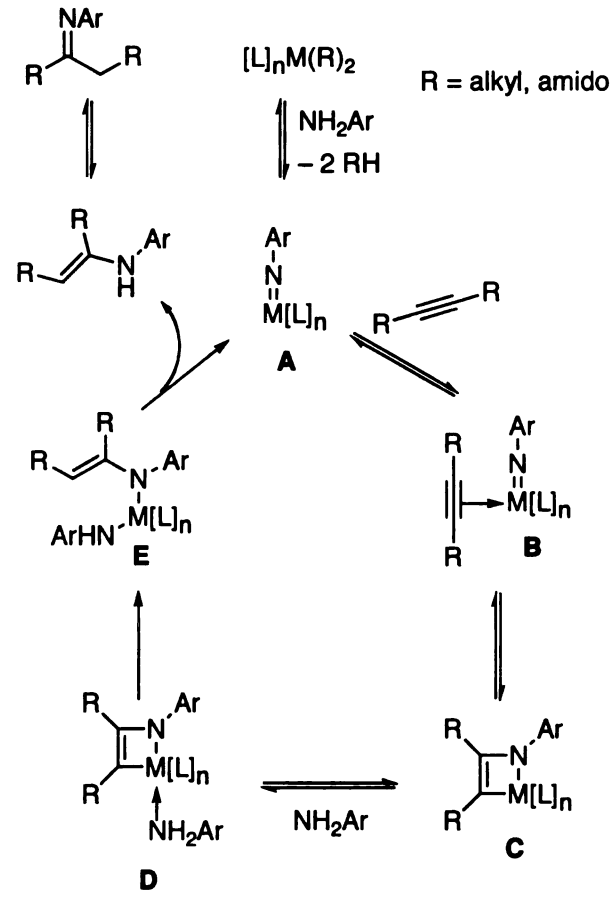

Scheme 1.2 Bergman mechanism for hydroamination

The groups of Doye and Bergman have pioneered Cp-based titanium catalysts, which have been shown to be fairly general catalysts for alkyne hydroamination (Chart 1.1).[4] Bergman and co-workers revealed that $TiCp_2Me_2$ undergoes cyclopentadienyl/amide ligand exchange, which enhances the reactivity towards alkyne hydroamination.

1.3 Hydroamination with titanium amido complexes

Since the first reports of hydroamination with titanium Cp catalysts, many groups have explored the use of amido ancillary ligands in hopes of generating more reactive catalysts and expanding the substrate scope. Odom reported that commercially available $Ti(NMe_2)_4$ (**3**) was a general hydroamination catalyst for aryl primary amines and alkynes (Scheme 1.3).[5]

Scheme 1.3 Hydroamination results with $Ti(NMe_2)_4$ (**3**) as catalyst.

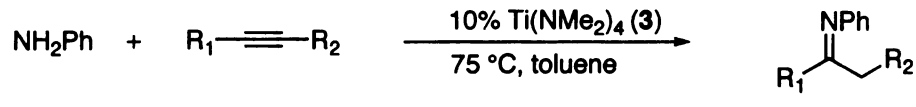

R_1, R_2 = (Bu^n, H), (Et, Et), (Ph,H)

87 - 92 %

Shortly after that report, Bergman and co-workers reported the hydroamination of amino allenes and amino alkynes with sulfonamido ancillary ligands on titanium (Chart 1.2).[6] It is also worthy to note, that the ligation of these chelating sulfonamido ligands on zirconium are relatively good asymmetric intramolecular alkene hydroamination catalysts with good yields and moderate ee's.[7]

Chart 1.2 Titanium sulfonamido complexes

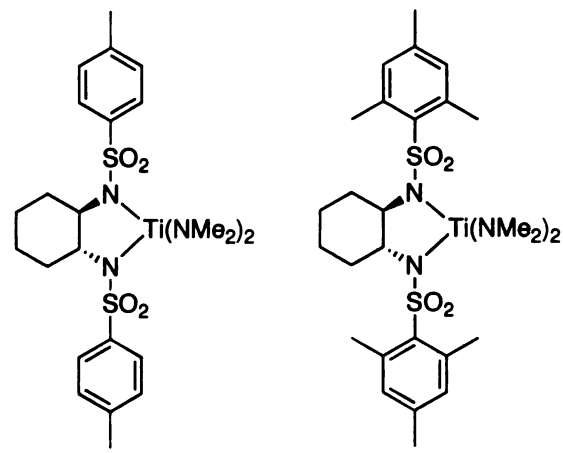

(**4**) (**5**)

Doye and co-workers reported a chelated Cp/amido titanium complex capable of hydroaminating an alkyne, followed by direct reduction via hydrosilylation with the same titanium precatalyst (Scheme 1.4).[8] This synthetic procedure allows for the production of secondary amines in a one-pot procedure, without having to use stoichmetric amounts of conventional reducing agents like $NaBH_3CN$ or $LiAlH_4$.

Scheme 1.4 Hydroamination/hydrosilylation by $Ti(NMe_2)_2(Cp\text{-}SiMe_2\text{-}NBu^t)$ (**6**).

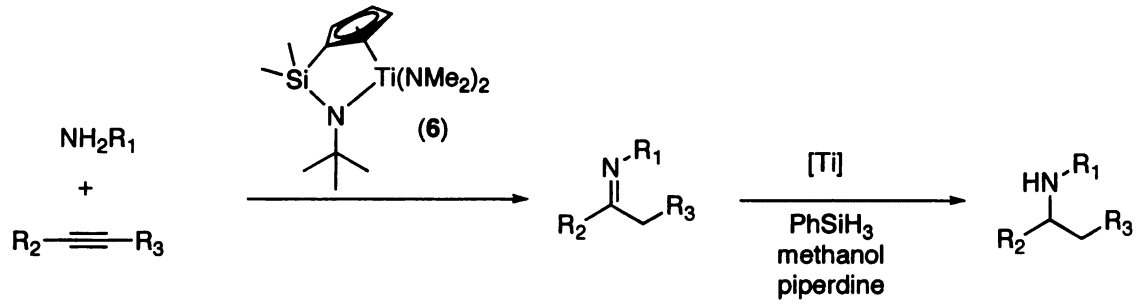

1.4 Hydroamination with titanium amidate complexes

The Schafer group has prepared a class of amidate titanium complexes capable of intermolecular hydroamination (Figure 1.1).[9] The development of electron deficient amidate ligands on titanium resulted in decreased catalytic performance and unexpected ligand reactivity.[10] There is supporting evidence that a more Lewis acidic metal center may facility greater hydroamination reactivity (*vide infra*).

Figure 1.1 Titanium amidate complex

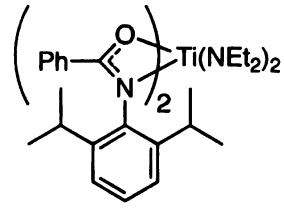

(7)

The strategy of using fluorine groups on the phenyl group rendered the arene susceptible to nucleophilic attack by primary amines at elevated temperatures. This resulted in the formation of HF during catalysis, which decomposed the catalyst (Equation 1.1). This observation shows there should be a judicious choice of electron-withdrawing substituents when selecting an ancillary ligand for titanium-catalyzed hydroamination.

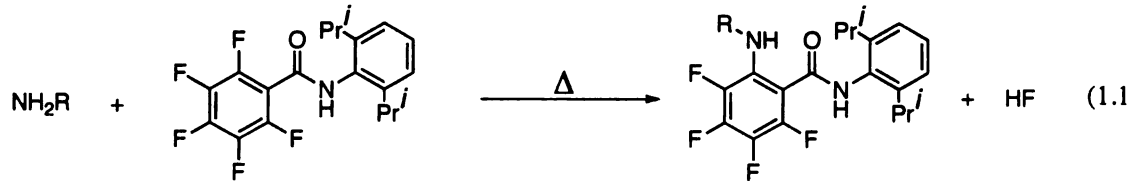

(1.1)

1.5 Hydroamination with titanium pyrrolyl complexes

Using deprotonated pyrroles as ancillary ligands is nothing new in transition metal chemistry. However, pyrrolyl ligands have seen increased attention as ancillaries in the field of catalysis. Among the many fields of catalysis, titanium catalyzed C–N and C–C bond forming reactions have probably been the largest application of pyrrolyl ligands.[12d]

Unlike many alkoxide, amide, or Cp ligands, pyrrole is not a strongly π-donating ligand. The nitrogen lone pair is delocalized around the ring to maintain aromaticity, which directly competes with π-donation to the metal center (The aromatic stabilization energy for pyrrole is ~21 kcal/mmol).[11] This decreased π-donation to the metal center results in a more Lewis acidic metal center that has proven useful in a variety of catalytic systems.[12]

One can easily draw analogies between the Bergman mechanism for hydroamination and the Chauvin mechanism for olefin metathesis. Both mechanisms include metal-ligand multiple bond intermediates and [2+2] cycloaddition processes with unsaturated substrates. One of the results from Schrock's olefin metathesis studies was that the reactivity increased in his d^0 molybdenum catalysts as the metal center was made more Lewis acidic.[13] Applying the same principle towards titanium catalysts for hydroamination using pyrrole-based ancillary ligands could be fruitful given the similarities in mechanisms and that pyrroles are weak π-donors. The increased Lewis acidity of the metal could result in stronger metal-alkyne binding, facilitating the [2+2] cycloaddition. In addition, the Brønsted acidity of a coordinated amine increases upon coordination to a metal center, which may speed up the rate-limiting protonolysis step.[14]

The first reported example of a pyrrolyl-based titanium catalyst for hydroamination was $Ti(NMe_2)_2$(dpma) (**8**), where dpma is *N*,*N*-di(pyrrolyl-α-methyl)-*N*-methylamine.[15] H_2dpma is readily prepared by reaction of 2 equivalents of pyrrole, 2 equivalents of formaldehyde, and an equivalent of methyl ammonium hydrochloride generating the ligand in good yield. H_2dpma can be placed on titanium by transamination with $Ti(NMe_2)_4$ (**3**) to yield precatalyst **8** in excellent yield (Scheme 1.5).

Scheme 1.5 Synthesis of H_2dpma and $Ti(NMe_2)_2$(dpma) (**8**).

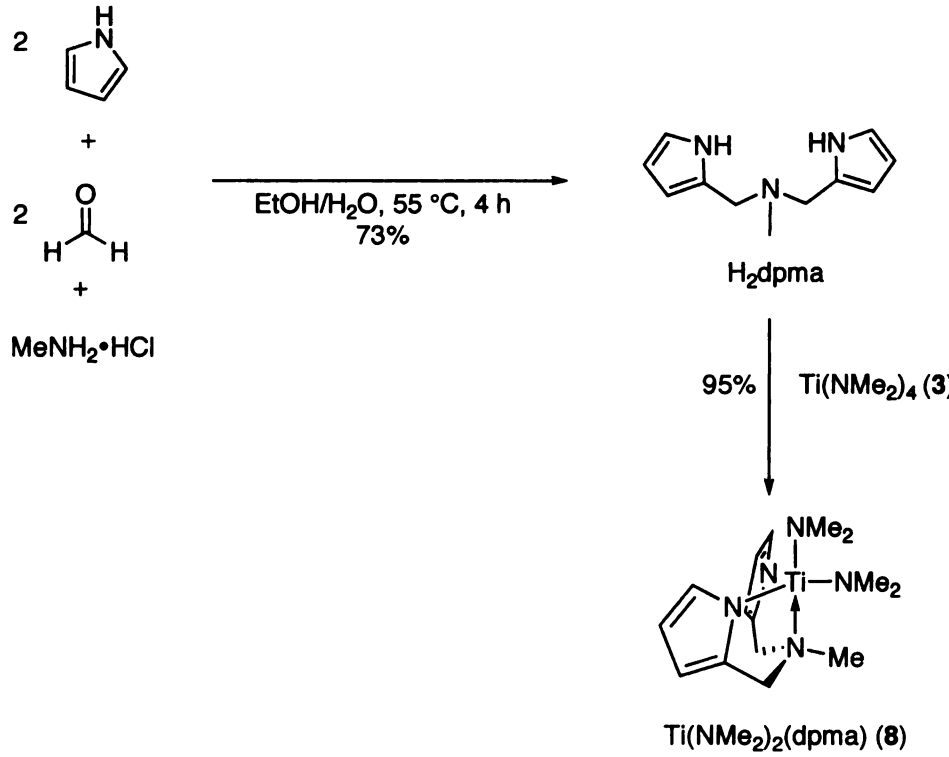

The hydroamination of aniline and 1-hexyne is carried out in 6 h at 75 °C with **8** at 10 mol% catalyst loading.[16] Complex **8** is a relatively good catalyst for the hydroamination of aryl and alkyl amines with alkynes (Table 1.1). While most of the reactions could be carried out at 75 °C with moderate reaction times, higher temperatures were required for more difficult substrates.

Table 1.1 Representative hydroamination results with 10 mol% $Ti(NMe_2)_2(dpma)$ (**8**).

Amine	Alkyne	Time (h) at 75 °C [130 °C]	% Yield at 75 °C [130 °C]	Selectivity (M: anti-M) at 75 °C [130 °C]
$PhNH_2$	Bu^n—≡—H	6	90	50:1
	Ph—≡—H	8	41	3.6:1
	Ph—≡—Me	144 [24]	99 [96]	1:24 [1:19]
	Et—≡—Et	72	63	
	Ph—≡—Ph	72 [74]	31 [99]	
$CyNH_2$	Ph—≡—H	20	50	1:6
	Ph—≡—Me	95 [29]	trace [99]	1:4
	Et—≡—Et	72 [24]	3 [57]	
	Ph—≡—Ph	72 [24]	0 [70]	

The dpma ligand architecture bears pyrrolyl ligands with an η^1,η^1-coordination in the solid state and in solution when bound to titanium. To date, this is the only bonding hapticity observed for the dpma ligand. Even though $Ti(NMe_2)_2(dpma)$ (**8**) was a relatively good hydroamination catalyst, alterations in ligand design to create a more Lewis acidic metal were explored. The most logical modification to the dpma ligand was removal of the donor amine in the dpma backbone, which lead to the use of dipyrrolylmethanes as ligands.

A variety of dipyrrolylmethanes can be prepared by reacting pyrrole with aldehydes or ketones in the presence of a catalytic amount of a Lewis or Brønstead acid.[17] The neat reaction of pyrrole and acetone with a catalytic amount of trifluoroacetic acid (TFA) yields 5,5-dimethyldipyrrolylmethane, H_2dpm. Reacting H_2dpm with $Ti(NMe_2)_4$ (**3**) affords $Ti(NMe_2)_2(dpm)$ (**9**) (Scheme 1.6).

Scheme 1.6 Synthesis of H_2dpm and $Ti(NMe_2)_2$(dpm) (**9**).

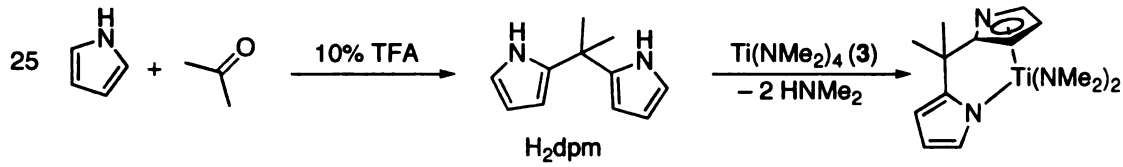

The solid-state structure of **9** has the pyrrolyls η^1,η^5-bound; however, in solution the ^{1}H NMR spectrum shows equivalent pyrrolyls, indicative of fast pyrroyl exchange on the NMR timescale. Using line shape analysis and spin saturation transfer experiments, our group has been able to place a barrier for pyrrolyl exchange at ~10 kcal/mol.[18,19]

$Ti(NMe_2)_2$(dpm) (**9**) catalyzes the reaction of aniline and 1-hexyne famously in ~5 minutes with a modest 5 mol% catalyst loading. The reaction of aniline and 1-hexyne is so rapid and exothermic that the reaction vessel is hot to the touch and refluxes the reagents, which results in the low yield for Entry 1 in Table 1.2.[19]

Table 1.2 Representative hydroamination results with $Ti(NMe_2)_2(dpm)$ (**9**) as the catalyst.

Amine	Alkyne	Conditions	% Yield	Selectivity (M: anti-M)
$PhNH_2$	Bu—≡—H	5%, 25 °C, 5 min	57	40:1
	Ph—≡—H	5%, 25 °C, 5 min	41	3.6:1
	Ph—≡—Me	5%, 50 °C, 6 h	83	50:1
	Et—≡—Et	5%, 50 °C, 24 h	94	
	Ph—≡—Ph	5%, 75 °C, 24 h	84	
$CyNH_2$	Ph—≡—H	5%, 25 °C, 10 min	54	1.6:1
	Ph—≡—Me	5%, 75 °C, 24 h	93	11:1
	Et—≡—Et	10%, 75 °C, 48 h	73	
	Ph—≡—Ph	10%, 100 °C, 48 h	72	

The results in Table 1.2 show that **9** is a good catalyst for the hydroamination of alkyl and aryl amines with alkynes and much more reactive than $Ti(NMe_2)_2(dpma)$ (**8**). A kinetic study comparing the various ligand architectures of **8**, **9**, and Cp-derived pyrrolyl complex (**10**), shows that the dipyrrolylmethane framework is quite a bit faster relative to the other pyrrole-based ligand frameworks (Table 1.3).

Table 1.3 Rate constants for $Ti(NMe_2)_2$(dpma) (**8**), $Ti(NMe_2)_2$(dpm) (**9**), $Ti(NMe_2)_2$(pyrr-Cp) (**10**) for the hydroamination of aniline and 1-phenylpropyne.

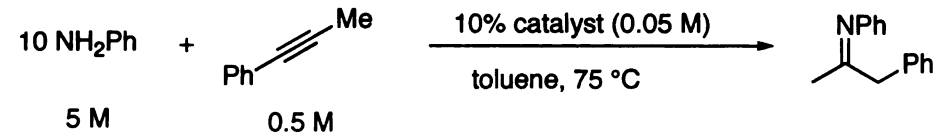

$$-\frac{d[\text{1-phenylpropyne}]}{dt} = k_{obs}t$$

Entry	Precatalyst	k_{obs} x 10^{-6} s^{-1} [a]
1	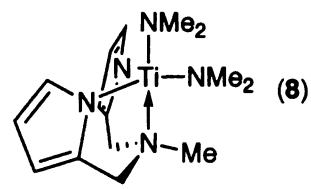 (**8**)	11 [7]
2	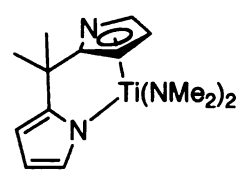 (**9**)	[157]
3	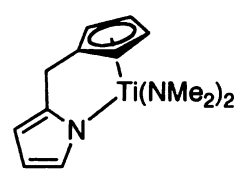 (**10**)	1

[a] Values in brackets are with chlorobenzene as solvent.

Complex **9** was about 20 times faster than $Ti(NMe_2)_2$(dpma) (**8**) and about a 100 times faster than **10**. It was proposed that $Ti(NMe_2)_2$(dpm) (**9**) can more readily access the η^1,η^1-isomer than **10**, accounting for the increase in catalysis rate.

Expanding the scope of hydroamination to include 1,3-enyne substrates allows for the synthesis of α,β-unsaturated imines, which can be difficult to prepare from a purely organic synthesis approach of reacting a primary amine with an α,β-unsaturated ketone.

Using titanium-catalyzed hydroamination avoids the competing Michael addition products which can occur in the latter procedure.

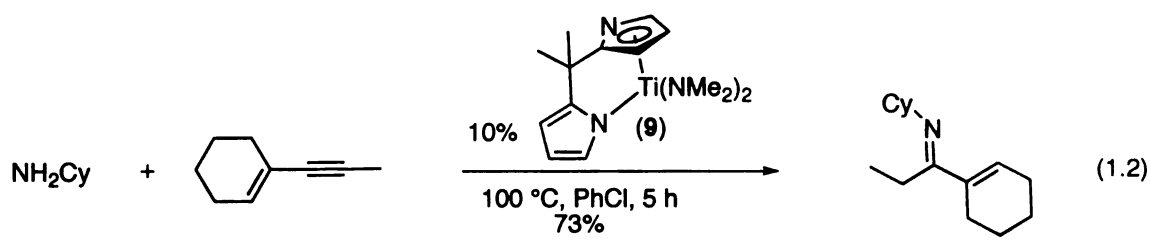

(1.2)

Complex **9** can conveniently hydroaminate a 1,3-enyne in 5 h at 100 °C (Equation 1.2).[20] Catalyst **9** showed good reactivity with less reactive alkyl amines; however, due to the rapidity of hydroamination, **9** was problematic with sensitive substrates where potential side reactions could occur (i.e. terminal alkynes). $Ti(NMe_2)_2(dap)_2$ (**11**) where dap is α-(dimethylaminomethyl)pyrrole proved to be the optimal catalyst for highly reactive substrates (Table 1.4). Catalyst **11** is prepared by reacting 2 equivalents of Hdap with $Ti(NMe_2)_4$ (**3**) (Equation 1.3).[21]

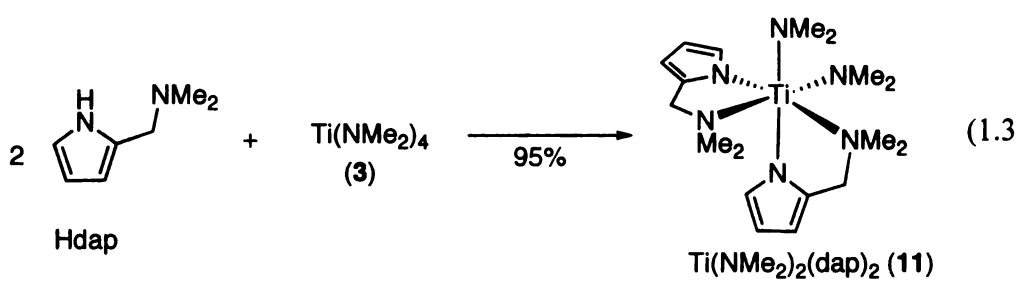

(1.3)

Table 1.4 Respresentative hydroamination results with $Ti(NMe_2)_2(dap)_2$ (**11**) at 10 mol% catalyst loading.

Amine	1,3-enyne	Conditions	% Yield	Product
$PhNH_2$	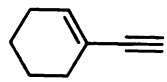	50 °C 16 h	88	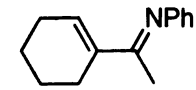
	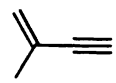	50 °C, 44 h	64	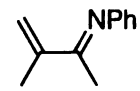
	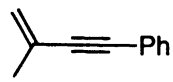	130 °C, 19 h	70	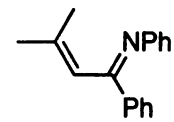
$CyNH_2$	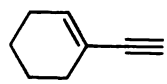	50 °C, 24 h	78	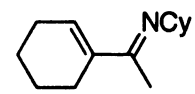
	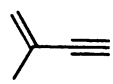	50 °C, 43 h	73	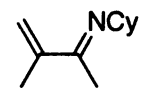

The ability to make new C–N bonds using hydroamination is a desirable alternative when the condensation of carbonyls with amines is problematic. The development of well-defined pyrrolyl-based catalysts provides the organic chemist with another synthetic tool to prepare a variety of imine products. In addition to imine products, new methodologies have been established for preparing pyrroles,[22] indoles,[9a] and hydrazones[9] via titanium-catalyzed reactions.

1.6 Iminoamination

Development of the hydroamination reaction to yield more elaborate imine products offers more potential in preparing valuable C–N containing products with broader applications. To expand on the scope of products obtained from the hydroamination mechanism, our group developed a new 3-component coupling reaction involving the coupling of a primary amine, alkyne, and isonitrile in a single synthetic step catalyzed by a titanium pyrrolyl complex. The result is the formal iminoamination of an alkyne, which is not readily achievable using current carbonyl methodologies. The mechanism for the coupling is shown in Scheme 1.7.

Scheme 1.7 Proposed 3-component coupling reaction mechanism involving a primary amine, alkyne, and isonitrile.

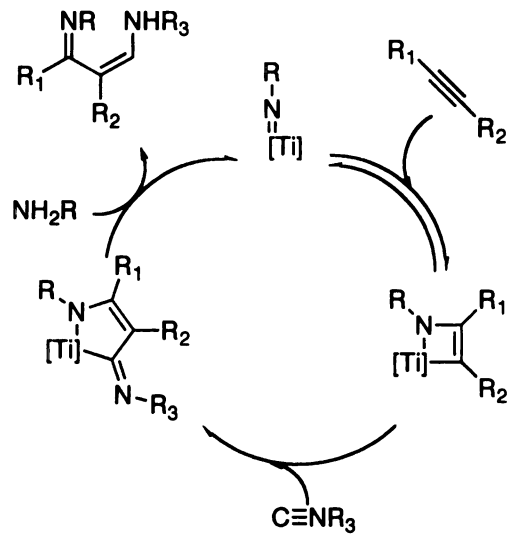

$Ti(NMe_2)_2(dpma)$ (**8**) catalyzes the coupling effectively allowing for the production of α,β-unsaturated β-iminoamines (Table 1.5).[23] One of the two identifiable by-products is an imine product from hydroamination of the alkyne by the primary amine. The other by-product is an *N,N*-disubstituted-formamidine, which results from the coupling of the primary amine with isonitrile. Altogether, the by-products are typically

found in less than 15% yield.

The regioselectivities of the 3-component coupling reaction with catalyst **8** are similar to the reported regioselectivies of the hydroamination reaction.[5] It is worthy to note that the coupling does not take place in the absence of the catalyst and even the by-products are not observed. Also, simple treatment of the hydroamination product with isonitrile in the presence of the catalyst results in no formation of the 3-component coupling product, therefore the azametallacyclobutene must be present to result in the formation of desired coupling product.

Table 1.5 Results of 3-component coupling with $Ti(NMe_2)_2(dpma)$ (**8**) at 10 mol% catalyst loading at 100 °C in toluene.

Amine	Alkyne	Isonitrile	% Yield	Product
$PhNH_2$	Bu^n—≡	C≡N–Bu^t	77	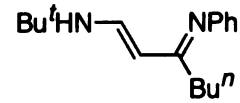
	Me—≡—Ph	C≡N–Bu^t	72	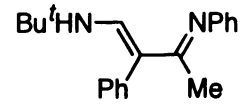
$CyNH_2$	Bu^n—≡	C≡N–Bu^t	66	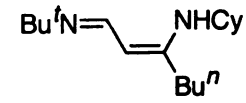 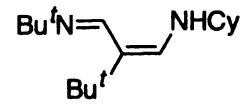 (1.2 : 1)

Catalyst **9** is also a very good 3-component coupling catalyst and works with a variety of alkynes and aniline derivatives. Moreover, our group has expanded the applications of the 3-component coupling reaction and developed new syntheses for quinolines, pyrimidines, and pyrazoles from the 3-component coupling product.[24]

1.7 Conclusion

The field of titanium-catalyzed hydroamination has seen an explosion of research since the first reported example of a titanium catalyst carrying out the hydroamination of an alkyne and a primary amine.[16] The development of well-defined pyrrolyl-based titanium catalysts has led to new methodologies in C–N bond forming reactions. Because so many of the applications listed are based on the hydroamination catalytic cycle, the hydroamination of alkynes can be used as a method for evaluating the efficacy of new catalyst designs. The following chapters discuss the investigation of elaborating the pyrrolyl framework in order to produce more reactive hydroamination catalysts with potential applications in multi-component coupling reactions.

1.8 References

1. Walsh, P. J.; Baranger, A. M.; Bergman, R. G. *J. Am. Chem. Soc.* **1992**, *114*, 1708.

2. (a)Baranger, A.M.; Walsh, P. J.; Bergman, R. G. *J. Am. Chem. Soc.* **1993**, *115*, 2753. (b) Walsh, P. J.; Baranger, A. M.; Bergman, R. G. *J. Am. Chem. Soc.* **1992**, *114*, 1708. (c) Duncan, A. P.; Bergman, R. G. *Chem. Rec.* **2002**, *2*, 431. (d) Le, S. Y.; Bergman, R. G. *Tetrahedron* **1995**, *51*, 4255. (e) Polse, J. L.; Andersen, R. A.; Bergman, R. G. *J. Am. Chem. Soc.* **1998**, *120*, 13405.

3. Johnson, J. S.; Bergman, R.G. *J. Am. Chem. Soc.*, **2001**, *123*, 2923.

4. Heutling, A.; Pohlki, F.; Doye, S. *Chem. Eur. J.* **2004**, *10*, 3059.

5. Shi, Y.; Ciszewski, J. T.; Odom, A. L. *Organometallics*, **2001**, *20*, 3967.

6. Ackerman, L.; Bergman, R. G. Loy, R. N. *J. Am. Chem. Soc.* **2003**, *125*, 11956.

8. Watson, D. A.; Chieu, M.; Bergman, R. G. *Organometallics*, **2006**, *25*, 4731.

8. Heutling, A.; Frauke Pohlki, F.; Igor Bytschkov, I.; Doye, S. *Angew. Chem. Int. Ed.* **2005**, *44*, 2951.

9. (a) Zhang, Z.; Schafer, L. L. *Org. Lett*, **2003**, *5*, 4733. (b) Li, C.; Thomson, R. K.; Gillon, B.; Patrick, B. O.; Schafer, L. L. *Chem. Commun.* **2003**, 2462 (c) Thomson, R. K.; Zahariev, F. E.; Zhang, Z.; Patrick, B. O.; Wang, Y.A.; Schafer, L. L. *Inorg. Chem.*, **2005**, *44*, 8680.

10. Bexrud, J. A.; Li. C.; Schafer, L. L. *Organometallics,* **2007,** *26,* 6366.

11. March, J. Advanced Organic Chemistry, Wiley-Interscience, New York, 4th ed., 1996, 45.

12. (a) Saeed, I.; Katao, S.; Nomura, K. *Organometallics*, **2009**, *28*, 111. (b) Hock A. S.; Schrock, R. R.; Hoveyda, A. H. *J. Am. Chem. Soc.*, **2006**, *128*, 16373. (c) Mazet, C.; Gade, L. H. *Organometallics*, **2001**, *20*, 4144. (d) Odom, A. L. *Dalton Trans.*, **2005**, 225 and references therein. (e) Schouteeten, S.; Allen, O. R.; Haley, A. D. ;. Ong, G. L.; Jones, G. D.; Vicic, D. A. *J. Organ. Chem.* **2006**, 4975.

13. Schrock, R. R.; Murdzek, J. S.; Bazan, G. C.; Robbins, J.; DiMare, M.; O'Regan, M. *J. Am. Chem. Soc.* **1990**, *112*, 3875.

14. Fulton, J. R.; Sklenak, S.; Bouwkamp, M. W.; Bergman, R. G. *J. Am. Chem. Soc.* **2002**, *124*, 4722.

15. Harris, S.A.; Ciszewski, J. T.; Odom, A.L. *Inorg. Chem.*, **2001**, *40*, 1987.

16. Cao, C.; Ciszewski, J. T.; Odom, A.L. *Organometallics*, **2001**, *20*, 5011.

17. (a) Littler, B. J.; Miller, M. A.; Hung, C. H.; Wagner, R. W.; O'Shea, D. F.; Boyle, P. D.; Lindsey, J. S. *J. Org. Chem.* **1999**, *64*, 1391. (b) Patchanita T. P.; Bhise, A. D.; Taniguchi, M.; Lindsey J. S. *J. Org. Chem.*, **2006**, *71*, 903.

18. Shi, Y.; Hall, C.; Ciszewski, J. T.; Cao, C.; Odom, A. L. *Chem. Commun.* **2003**, 586.

19. Swartz, D.L.; Odom, *Dalton Trans*. **2008**, 4254.

20. Cao, C.; Li, Y.; Shi, Y.; Odom, A. L. *Chem. Comm*. **2004**, 2002.

21. For $Ti(NMe_2)_2(dap)_2$ as a hydrohydrazination catalyst see (a) Cao, C. Shi, Y.; Odom, A.L. *Org. Lett*, **2002**, *4*, 2853. (b) Banerjee, S.; Shi, Y.; Cao, C.; Odom, A.L. *J. Organo. Chem*. **2005**, 5066.

22. Ramanathan, B.; Keith, A. J.; D. Armstrong D.; Odom, A.L. *Org. Lett.*, **2004**, 6, 2957.

23. Cao, C.; Shi, Y.; Odom, A. L. *J. Am. Chem. Soc.* **2002**, *125*, 2880.

24. Majumder, S.: Odom, A. L.; *manuscripts in preparation.*

CHAPTER 2

Synthesis, structure, and hydroamination kinetics of 2,2'-diaryldipyrrolylmethane and bis(2-arylpyrrolyl)titanium complexes

2.1 Introduction

The generation of new carbon-nitrogen bonds is a significant process in organic chemistry. The most atom economical process for the generation of amines and imines is through hydroamination, which is the formal addition of an N–H bond across an unsaturated C–C bond. Many natural products and pharmaceutical drugs contain C–N bonds; therefore these heteroatom molecules offer pharmaceutical applications as well as other industrial applications in the way of dyes, detergents, and fungicides.[1] Pyrrolyl-ligated titanium complexes provide very reactive catalysts for hydroamination. This chapter discusses 2,2'-diaryldipyrrolylmethane and bis(2-arylpyrrolyl)titanium complexes as competent hydroamination catalysts and gauges the efficacy of their design through kinetic studies.

2.2 Titanium Pyrrolyl Hydroamination

Titanium-catalyzed intermolecular hydroamination has been widely studied and has led to new methodologies in the synthesis of imines,[2] hydrazones,[3] indoles,[2] pyrroles,[4] unsaturated imines,[5] tautomers of 1,3-dimines,[6] and tautomers of 1,3-iminohydrazones.[7] In addition, a variety of nitrogen containing heterocycles have been synthesized by intramolecular cyclization.[8] There are many ancillary ligands on titanium known to mediate these types of transformations. The ligands employed include alkoxides,[9] amides,[10] amidates,[11] and pyrroles.[12] Pyrrolyl-ligated titanium complexes provide very reactive catalysts capable of extremely fast hydroamination.

Perhaps the most active precatalyst known for simple alkyne hydroamination as of 2008 was a dipyrrolylmethane-ligated titanium complex $Ti(NMe_2)_2(dpm)$ (**9**), where dpm is 5,5-dimethyldipyrrolylmethane. The dipyrrolylmethane ligand is readily prepared from acetone and pyrrole in the presence of trifluoroacetic acid (TFA). The ligand can then be placed on titanium by transamination with $Ti(NMe_2)_4$ (**3**) to yield the precatalyst in good yields (Scheme 2.1).[13]

Scheme 2.1. Synthesis of H_2dpm and $Ti(NMe_2)_2(dpm)$ (**9**).

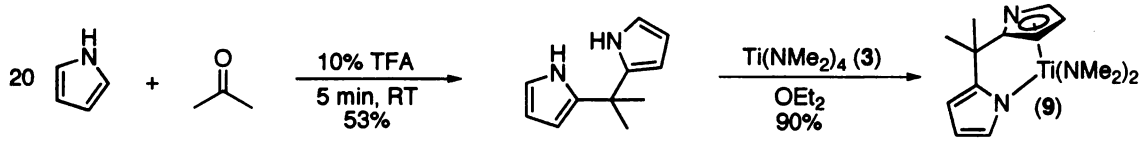

The use of pyrrole-based ancillary ligands offers several advantages compared to other architectures. First, pyrroles can be easily manipulated into multidenate ligands by a standard set of condensation reactions that take advantage of the nucleophilic nature of the pyrrole ring. Therefore, several classes of ligands can be synthesized in a small

number of steps (e.g. Mannich reaction) with a vast degree of steric and electronic variance. Secondly, pyrroles are relatively weak π donors compared to their alkoxide or amide counterparts due to the nitrogen lone pair delocalization by its participation in the ring's aromaticity. This decreased donation to titanium results in a more Lewis acidic metal center.

Titanium-catalyzed hydroamination is believed to operate through a smiliar mechanism as the Bergman mechanism for hydroamination elucidated by Bergman and co-workers using a zirconocene-based system (Scheme 2.2).[14] The first step in the catalytic cycle is the generation of a reactive titanium imido species (**A**). Introduction of an alkyne coordinates to **A** which undergoes a [2 + 2]-cylcoaddition to yield a azametallacyclobutene intermediate (**B**). Coordination of free primary amine to **B** in undergoes prontonlysis of the Ti–C bond to give bis(amido) titanium complex **C**. Further protonation from the amide regenerates the active catalyst **A** and yields the imine product.

Applying the steady-state approximation to the intermediates in the mechanism shown in Scheme 2.2, the following rate law can be derived (Equation 2.1).

$$v = \frac{k_1 k_2 k_3 [\text{alkyne}][\text{catalyst}]}{k_{-1}(k_2 + k_3 [\text{amine}])} \quad (2.1)$$

Scheme 2.2 Proposed mechanism for titanium-catalyzed alkyne hydroamination

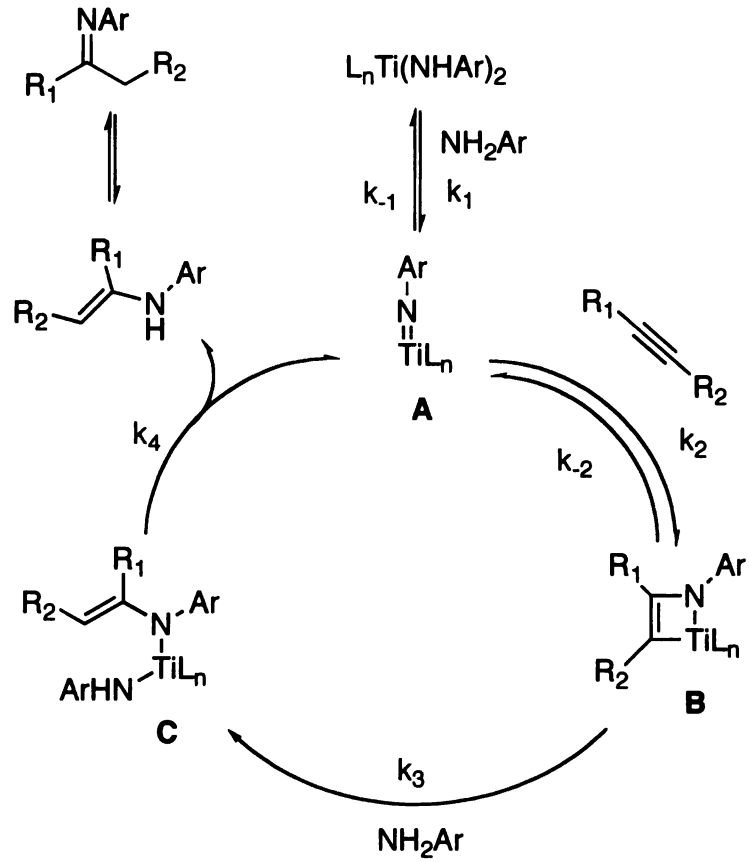

One can easily draw connections between the Group-4 Hydroamination Mechanism for alkyne hydroamination and the Chauvin mechanism for olefin metathesis (Scheme 2.3).

Scheme 2.3. Chauvin mechanism for olefin metathesis

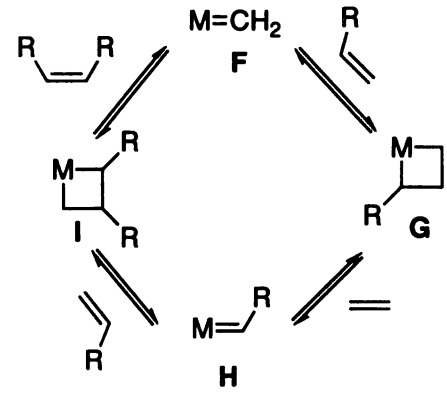

Both mechanisms are known to include metal-ligand multiple bond intermediates (**A** and **F**). Another key step is the [2 + 2]-cyclization between the C–C unsaturated bond

and the metal ligand multiple bond (**B** and **G**). Detailed olefin metathesis studies done by Schrock and co-workers found that increasing the Lewis acidity of d^0 metal centers led to an increase in catalysis rates.[15]

Given the similarities in mechanism and the known improvement in catalyst activity in d^0 Schrock carbenes bearing electron deficient alkoxides on Lewis acidic metal centers, it is expected that decreasing the donor ability of the pyrrole ligands could have a positive effect on catalyst reactivity. This chapter describes the effects on structure and catalysis 2-aryl substituents have on the dpm framework. Complexes containing 2-aryl bis(pyrrolyl) ligands were also synthesized to evaluate the effect the linker in the dpm framework has on structure and catalysis.

2.3 Hydroamination kinetics with titanium dipyrrolylmethane derivatives

The selective generation of 2-arylpyrroles can be achieved by the seminal methodology established by Sadighi and co-workers (Equation 2.1).[16] This technique allows for the production of 2-arylpyrroles on multigram scales. For this study, I wanted to investigate pyrroles of varying electronic and steric profiles.

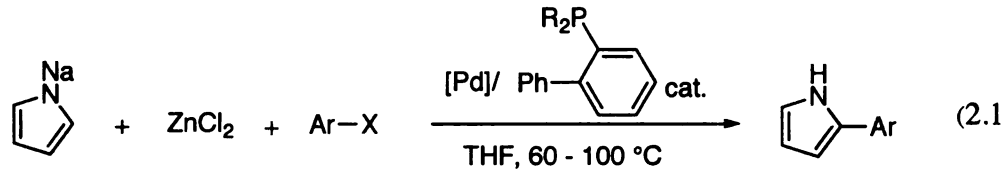

(2.1)

For this study, I prepared 2-Ar-pyrroles where Ar = 4-$(CF_3)C_6H_4$, 4-$(CH_3)C_6H_4$, 3,5-$(CF_3)_2C_6H_3$, and 2,4,6-$(CH_3)_3C_6H_2$. The typical procedure for the synthesis of dipyrrolylmethanes involves the use of a large excess of pyrrole with respect to the aldehyde or ketone (Scheme 2.1). However, in the preparation of 2-substituted dpm derivatives, pyrrole is the limiting reactant with excess acetone as the electrophile. The reaction is smoothly catalyzed by TFA to produce the ligands in good yield. The initial 5,5-dimethyldipyrrolylmethane derivatives prepared were 2,9-[3,5-$(CF_3)_2C_6H_3$]-5,5-dimethyldipyrrolylmethane ($H_2dpm^{3,5\text{-}CF3}$) and 2,9-[2,4,6-$(CH_3)_3C_6H_2$]-5,5-dimethyldipyrrolylmethane (H_2dpm^{mes}). These complexes were then reacted with $Ti(NMe_2)_4$ (**3**) to yield the corresponding dipyrrolylmethane metal complexes, $Ti(NMe_2)_2(dpm^{mes})$ (**12**) and $Ti(NMe_2)_2(dpm^{3,5\text{–}CF3})$ (**13**) (Scheme 2.4).

Scheme 2.4 Synthesis of H_2dpm^{mes}, $H_2dpm^{3,5-CF3}$, $Ti(NMe_2)_2(dpm^{mes})$ (**12**), and $Ti(NMe_2)_2(dpm^{3,5\text{-}CF3})$ (**13**).

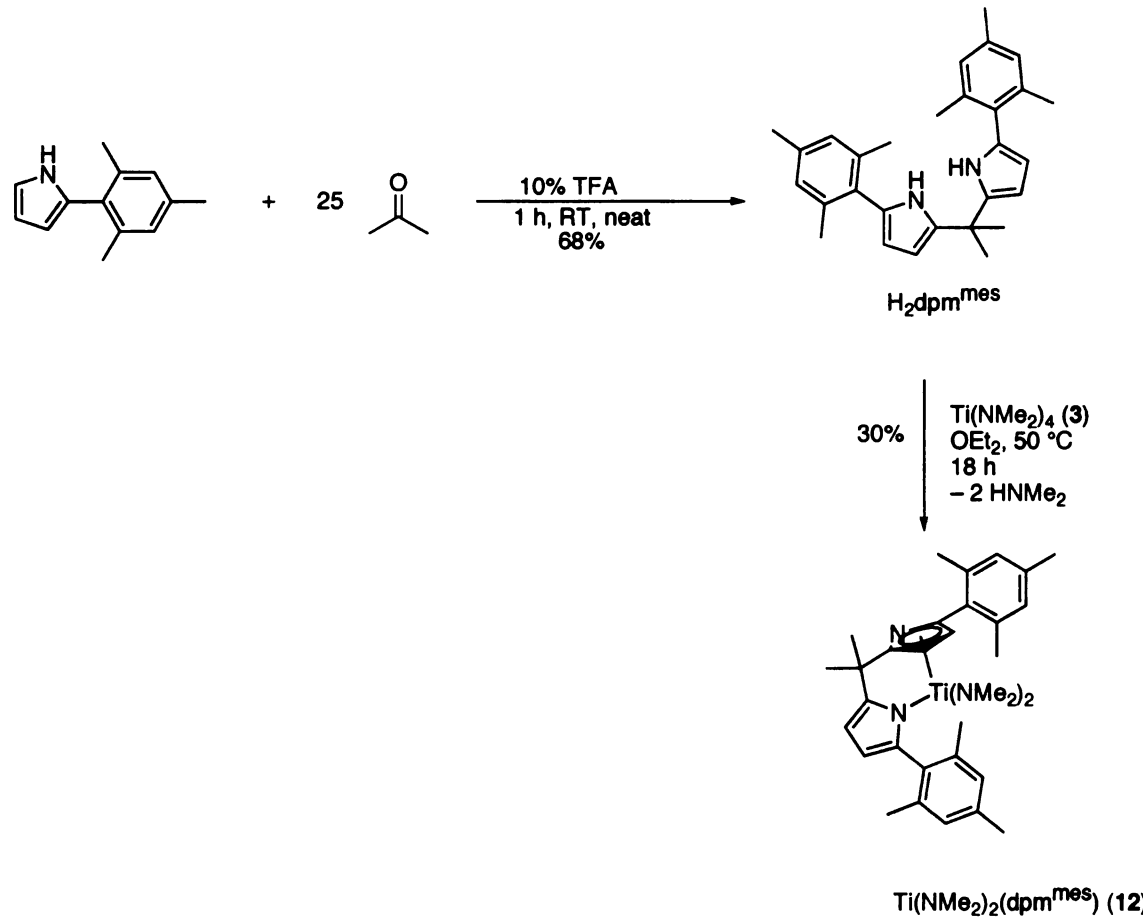

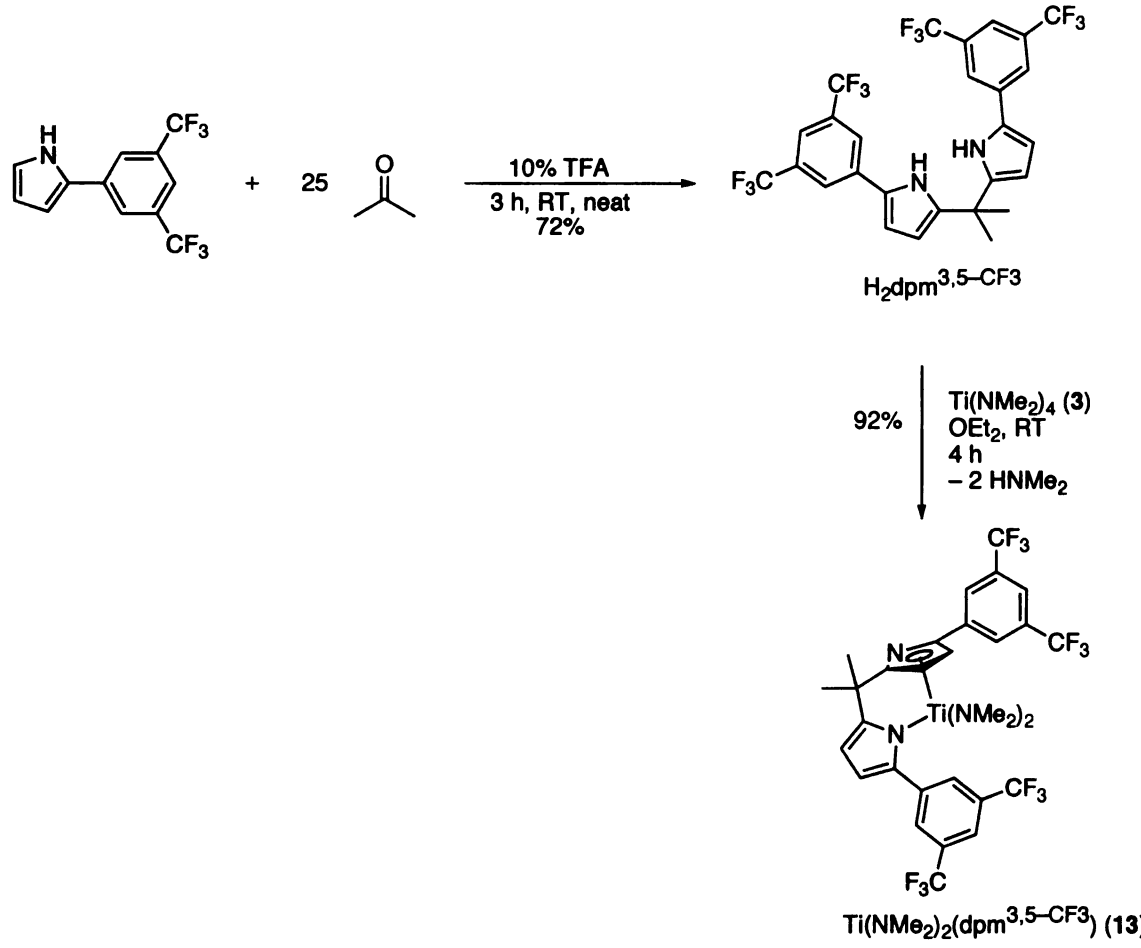

Single crystal X-ray diffraction shows that the pyrrole rings are in a η^1,η^5 conformation in the solid state for both $Ti(NMe_2)_2(dpm^{mes})$ (**12**) and $Ti(NMe_2)_2(dpm^{3,5-CF3})$ (**13**). The crystal structure of **13** is shown in Figure 2.1. This is similar to previous studies carried out by our group and the Love group on $Ti(NMe_2)_2(dpm)$ (**1**).[17] The pyrrole rings in $Ti(NMe_2)_2(dpm)$ (**9**) are in an η^1,η^5-conformation in the solid state as well. In cold solutions on the NMR timescale, resonances consistent with the solid state structure are observed. As the solution warms, resonances for the η^1-pyrrolyl and η^5-pyrrolyl coalesce, and the fast exchange limit is reached well before room temperature. The barrier for pyrrolyl ligand exchange was measured at 10 kcal/mol using line shape analysis.[4] It is believed that the pyrrolyl exchange occurs through a η^1,η^1-isomer.[18] The

magnitude for the barrier of pyrrolyl ligand exchange and the mechanism for isomerization are consistent with other known pyrrolyl isomerizations in the literature.[19]

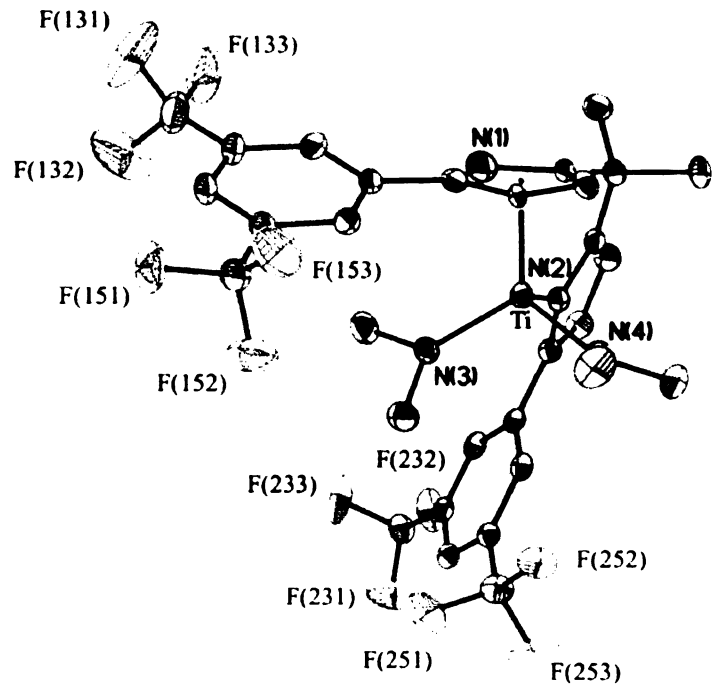

Figure 2.1 ORTEP structure from single-crystal X-ray diffraction of $Ti(NMe_2)_2(dpm^{3,5\text{-}CF3})$ (**13**). Selected bond distances (Å) and angles (deg): Ti-N(3) 1.875(5), Ti-N(4) 1.892(5), Ti-N(2) 2.048(5), Ti-N(1) 2.400(6); N(4)-Ti-N(3) 107.1(2), N(4)-Ti-N(2) 102.6(2), N(3)-Ti-N(2) 104.8(2).

Detailed NMR studies were carried out on **12** and **13** to investigate pyrrolyl exchange. Consistent with previous results, **12** and **13** show resonances for equivalent pyrrolyls at room temperature, indicative of rapid η^1,η^5-isomerization. Cooling the solutions to –60 °C showed no difference in the ^1H NMR spectrum. Parkin and Tanski have reported that increased sterics lower the barrier for pyrrolyl exchange.[18] These results are consistent with their findings, and assuming a pyrrolyl isomerization is taking place, one can place a maximum on the pyrrolyl exchange barrier of 5 kcal/mol.

To investigate the effect of removing the methylene linker in the dpm architecture on catalysis, I synthesized two bis(pyrrolyl) derivatives bearing the same aryl substituents. $Ti(NMe_2)_2(pyrr^{3,5\text{-}CF3})$ (**14**) and $Ti(NMe_2)_2(pyrr^{mes})_2$ (**15**) were prepared by reacting two equivalents of $Hpyrr^{mes}$ and $Hpyrr^{3,5\text{-}CF3}$ with $Ti(NMe_2)_4$ (**3**) to give the corresponding metal complexes (Scheme 2.5).

The solid-state structures for **14** and **15** are shown in Figures 2.2 and 2.3. Both structures show both pyrroles in an η^1:η^1-binding mode. Cooling solutions to –60 °C in the NMR probe showed no new resonances in the baseline.

Scheme 2.5 Synthesis of $Ti(NMe_2)_2(pyrr^{mes})_2$ (**15**) and $Ti(NMe_2)_2(pyrr^{3,5\text{-}CF3})_2$ (**14**).

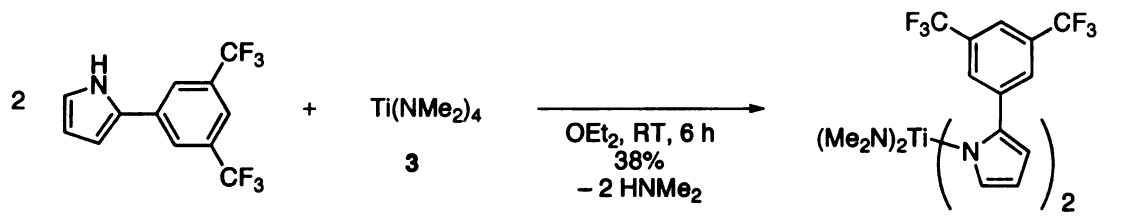

$Ti(NMe_2)_2(pyr^{3,5\text{-}CF3})_2$ (**14**)

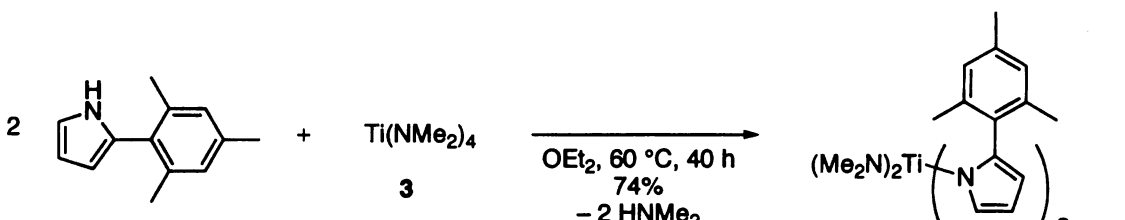

$Ti(NMe_2)_2(pyr^{mes})_2$ (**15**)

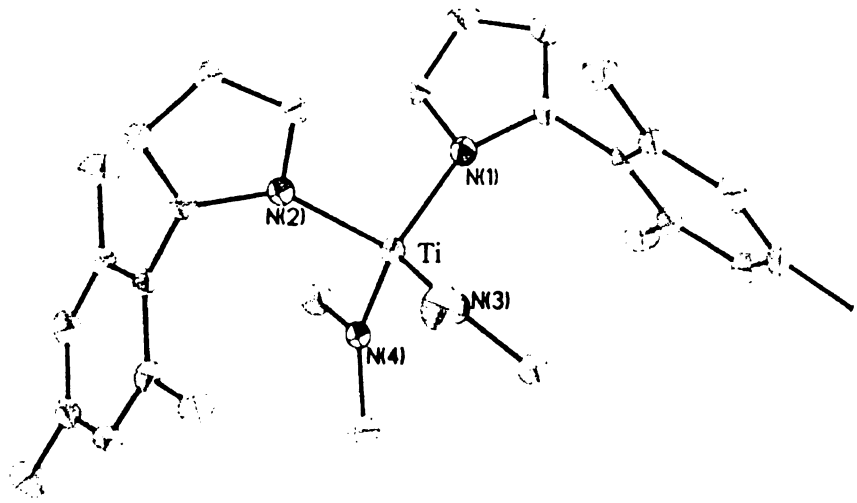

Figure 2.2 ORTEP structure from single-crystal X-ray diffraction on $Ti(NMe_2)_2(pyrr^{mes})_2$ (**15**). Selected bond distance (Å) and angles (deg): Ti-N(3) 1.844(4), Ti-N(4) = 1.865(4), Ti-N(2) 1.971(4), Ti-N(1) 2.007(4); N(3)-Ti-N(4) 109.3(2), N(3)-Ti-N(2) 107.5(2), N(4)-Ti-N(4) 109.3(2), N(3)-Ti-N(1) 112.0(2), N(4)-Ti-N(1) 114.1(2), N(2)-Ti-N(1) 105.2(2).

With these complexes in hand, I set out to answer several questions. First, how would sterics in the 2-position affect the catalysis rate? Second, how does the linker affect the catalysis rate? Third, can it be shown experimentally that electron-withdrawing substituents increase the catalytic activity as proposed in the Introduction?

To test the kinetic viability of these complexes, I chose a standard set of reaction conditions (Scheme 2.6). The reactions were run pseudo-first order in aniline. Aniline was chosen because it has a large catalyst scope and runs at a reasonable rate compared to other amines. The limiting reagent was 1-phenylpropyne. This alkyne was chosen for a couple of reasons.

First, it has good regioselectivity with most catalysts and runs at a reasonable rate. Second, an internal alkyne was required due to the rapidity of hydroamination with terminal alkynes with catalysts like $Ti(NMe_2)_2(dpm)$ (**9**). In addition to testing the kinetics of the titanium dpm derivatives, I also wanted to compare $Ti(NMe_2)_4$ (**3**), which serves as a very reasonable hydroamination catalyst as well, but is generally limited in substrate scope to aryl amines and can oligomerize terminal alkynes.

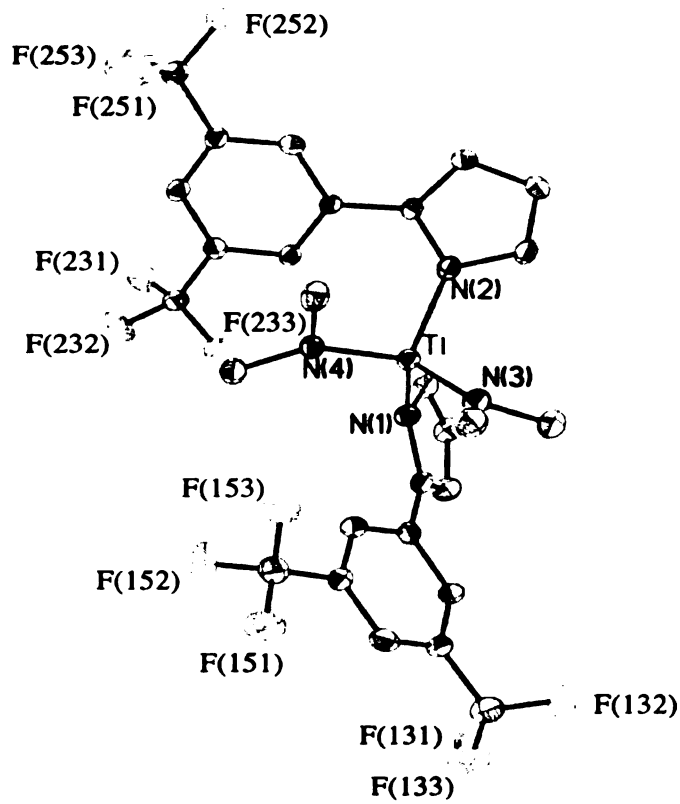

Figure 2.3 ORTEP structure from single-crystal X-ray diffraction on $Ti(NMe_2)_2(pyrr^{3,5\text{-}CF3})_2$ (**14**). Selected bond distances (Å) and angles (deg): Ti-N(1) 1.989(4), Ti-N(2) 2.011(4), Ti-N(3) 1.855(4), Ti-N(4) 1.848(4), N(4)-Ti-N(3) 108.88(17), N(4)-Ti-N(1) 114.72(16), N(3)-Ti-N(1) 107.32(16), N(4)-Ti-N(2) 107.97(16), N(3)-Ti-N(2) 1100.69(16), N(1)-Ti-N(2) 107.36(15).

These complexes were evaluated based on $Ti(NMe_2)_2(dpm)$ (**9**). Complex **9** catalyzes the reaction to completion efficiently in less than 4 hours at 75 °C with a rate constant of 1976 ± 130 $\times 10^{-7}$ s^{-1}. Often, catalytic reactions show a first-order dependence in catalyst concentration, which is true in this case. Changes in catalyst concentration track linearly with the rate constant (Figure 2.4).

Scheme 2.6 Reaction conditions for kinetic studies

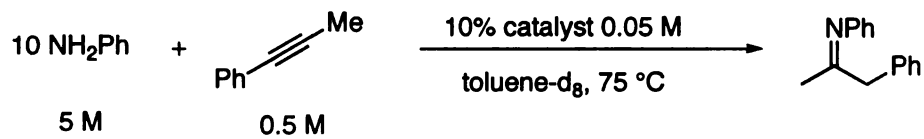

$$-\frac{d[\text{1-phenylpropyne}]}{dt} = k_{obs}t$$

Figure 2.4 Plot of catalyst concentration of **9** versus pseudo first-order rate constant for kinetic reaction conditions.

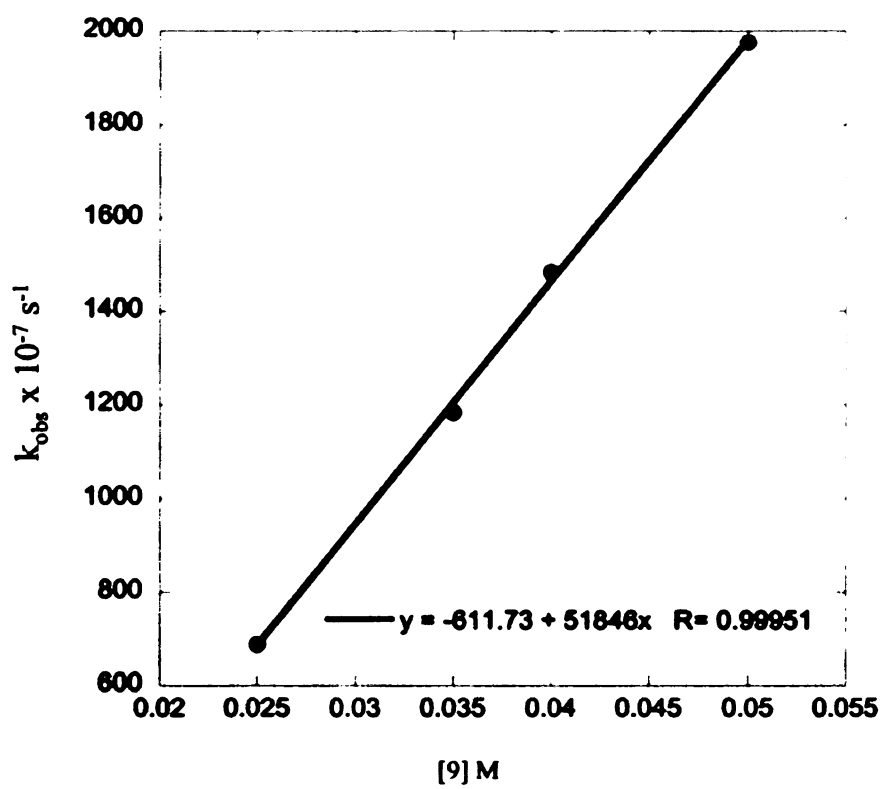

While most of the catalysts were quite regioselective, monitoring the reaction by disappearance of 1-phenylpropyne was preferential due to possible rate inconsistencies by measuring the formation of products which may include the other regioisomer. The comparison of these catalysts by relative reaction rate was measured by k_{obs}. A representative plot of the disappearance of ln[1-phenylpropyne] versus time with $Ti(NMe_2)_2(dpm)$ (**9**) as the catalyst is shown in Figure 2.5.

Figure 2.5 Representative plot of ln[1-phenylpropyne] vs time with complex **9** as the hydroamination catalyst.

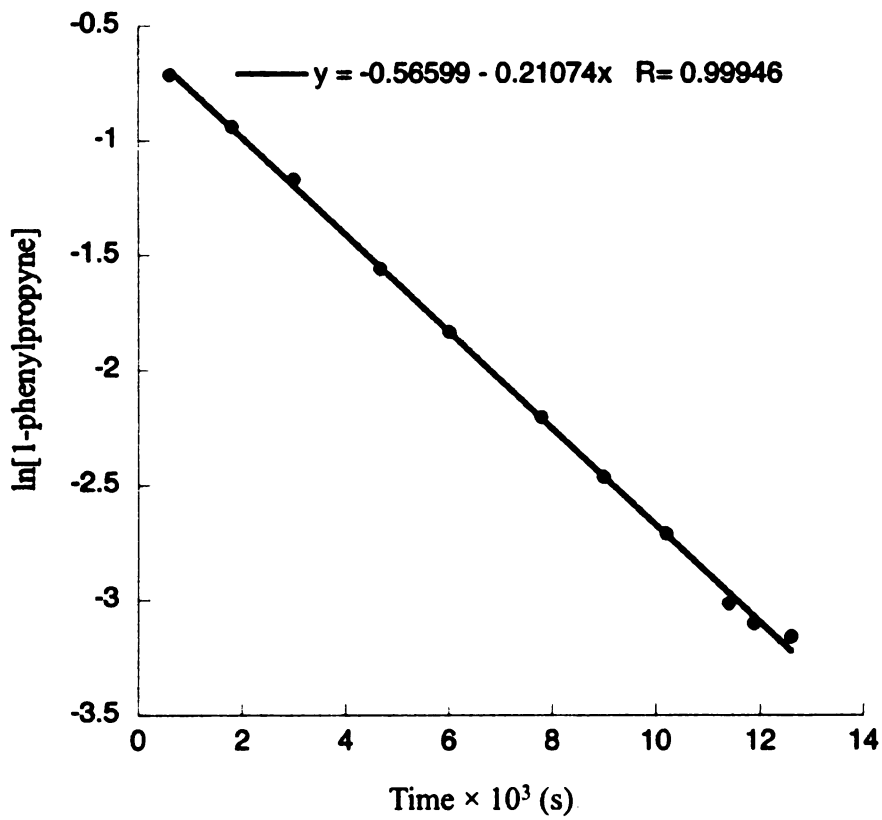

The results of this kinetic study are shown in Table 2.1 for catalysts **9** and **12** - **15**. The errors are based on 99% confidence level, with at least three repeated runs. The average error in rate constants was ~10% and varied from as little as 4% to as much as 20%.

Table 2.1 Observed rate constants for catalysts $Ti(NMe_2)_2(dpm)$ (**9**), $Ti(NMe_2)_2(dpm^{mes})$ (**12**), $Ti(NMe_2)_2(dpm^{3,5\text{-}CF3})$ (**13**), $Ti(NMe_2)_2(pyrr^{3,5\text{-}CF3})_2$ (**14**), $Ti(NMe_2)_2(pyrr^{mes})_2$ (**15**).

Entry	Catalyst[a]	k_{obs} ($\times 10^{-7}$ s^{-1})[b]
1	$Ti(NMe_2)_2(dpm)$ **9**	1976 ± 130
2	$Ti(NMe_2)_2(dpm^{3,5\text{–}CF3})$ **13**	780 ± 30
3	$Ti(NMe_2)_2(dpm^{mes})$ **12**	403 ± 80
4	$Ti(NMe_2)_2(pyrr^{3,5\text{–}CF3})_2$ **14**	1275 ± 72
5	$Ti(NMe_2)_2(pyrr^{mes})$ **15**	769 ± 30

[a] Conditions are shown in Scheme 2.6. [b] All errors are at the 99% confidence limit with at least three repeated runs.

It is quite clear to see from Table 2.1 that substitution on the 2-position of the dpm architecture results in a significant decrease in reaction rate. This decrease in rate can be attributed to increased sterics of the dpm framework near the substrate binding site. Comparatively, the unlinked bis(pyrrolyl) complexes still had a slower rate than $Ti(NMe_2)_2(dpm)$ (**9**), but showed a faster rate than their linked dpm derivaties by ~1.5 times. A possible explanation for the increase in hydroamination reaction rate for the unlinked pyrrolyl catalysts is their ability to rotate their bulky substiuents away from the substrate binding site unlike the dpm derivatives, leading to a more open metal center. While each of the dpm derivatives and bis(pyrrolyl) catalysts bearing an electron withdrawing substituent resulted in faster rates, these examples do not allow the separation of steric and electronic factors.

As a result, two additional catalysts were prepared $Ti(NMe_2)_2(pyrr^{4\text{-}CF3})$ (**16**) and $Ti(NMe_2)_2(pyrr^{tol})_2$ (**17**) that differ only in the donor ability of the substituent in the 4-position of the aromatic group. The pyrroles, 2-(4-(trifluoromethyl)phenyl)pyrrole ($Hpyrr^{4\text{-}CF3}$) and 2-(4-tolyl)pyrrole ($Hpyrr^{tol}$), were synthesized using Sadighi's protocol (Equation 2.1). The pyrroles were then placed on titanium by transamination with $Ti(NMe_2)_4$ (**3**) to give the corresponding metal complexes (Scheme 2.7).

Scheme 2.7 Synthesis of $Ti(NMe_2)_2(pyrr^{4\text{-}CF3})_2$ (**16**) and $Ti(NMe_2)_2(pyrr^{tol})_2$ (**17**).

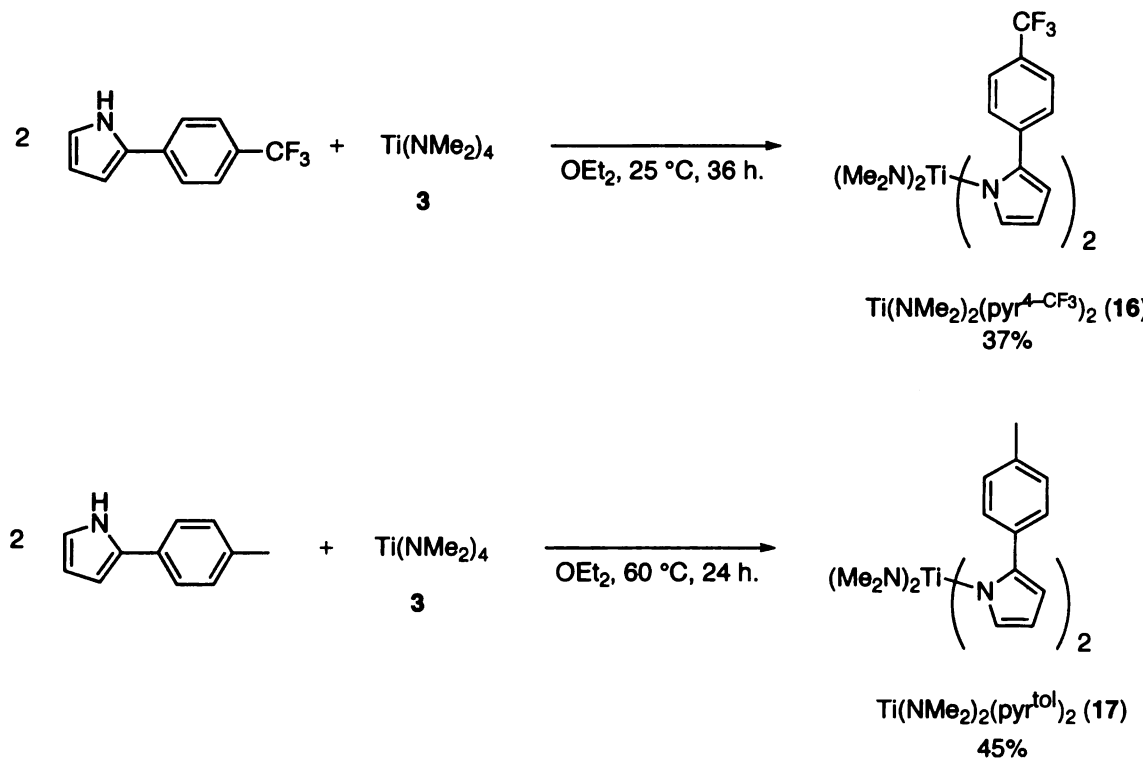

Catalysts **16** and **17** were tested under the same kinetic conditions as shown in Scheme 2.6. Table 2.2 shows the comparison of the bis(pyrrolyl) catalysts. $Ti(NMe_2)_2(pyrr^{tol})_2$ (**17**) had a rate constant of 880 ± 20 × 10^{-7} s^{-1}, while $Ti(NMe_2)_2(pyrr^{4\text{-}CF3})_2$ (**16**) gave a rate constant of 1255 ± 145 × 10^{-7} s^{-1}. It is clear to see that there is a dramatic difference in rate with the donor ability in the *para* position on the arene. $Ti(NMe_2)_2(pyrr^{3,5\text{-}CF3})_2$ (**14**) had a rate constant of 1275 ± 72 × 10^{-7} s^{-1}, similar to that of $Ti(NMe_2)_2(pyrr^{4\text{-}CF3})_2$ (**16**). The position of the electron-withdrawing substituent on the arene may have a significant effect on rate. While one may expect $Ti(NMe_2)_2(pyrr^{3,5\text{-}CF3})_2$ (**14**) to have a significantly higher rate than $Ti(NMe_2)_2(pyrr^{4\text{-}}$

$^{CF3})_2$ **(16)** due to the increase of electron-withdrawing substituents, it seems to be offset by the position of the substitution.

Table 2.2 Comparison of rate constants for hydroamination of the bis(pyrrolyl) catalysts. Errors are at the 99% confidence limit.

Entry	Catalyst[a]	k_{obs} ($\times 10^{-7}$ s^{-1})[b]
1	$Ti(NMe_2)_2(pyrr^{3,5\text{–}CF3})_2$ **14**	1275 ± 72
2	$Ti(NMe_2)_2(pyrr^{mes})_2$ **15**	769 ± 30
3	$Ti(NMe_2)_2(pyrr^{4\text{–}CF3})_2$ **16**	1255 ± 145
4	$Ti(NMe_2)_2(pyrr^{tol})_2$ **17**	880 ± 20

[a] Conditions are shown in Scheme 2.6. [b] All errors are at the 99% confidence limit with at least three repeated runs.

One possible complication with the bis(pyrrolyl) catalysts is disproportionation reactions to generate a mixture of mono(pyrrolyl) and tris(pyrrolyl) catalysts. This raises the question as to whether the mono(pyrrolyl) or the bis(pyrrolyl) complexes are the actual catalysts carrying out the reaction. There were many attempts to prepare and isolate mono(pyrrolyl) precatalysts, but these lead to impure mixtures. I attempted to study the kinetics of the mono(pyrrolyl) species by generating the complex in situ from $Ti(NMe_2)_4$ (**3**) and Hpyrr derivatives, but large variations in rate constant rendered these results unreliable. To investigate the possibility of crossover of the pyrrolyl ligands an experiment was carried out in a C_6D_6 solution of $Ti(NMe_2)_2(pyrr^{3,5\text{–}CF3})_2$ (**14**) and $Ti(NMe_2)_2(pyrr^{mes})_2$ (**15**) in a 1:1 ratio at 75 °C in the NMR probe. After several hours new resonances in the ^1H NMR spectrum could be observed, which are presumably due to pyrrolyl crossover (Equation 2.2).

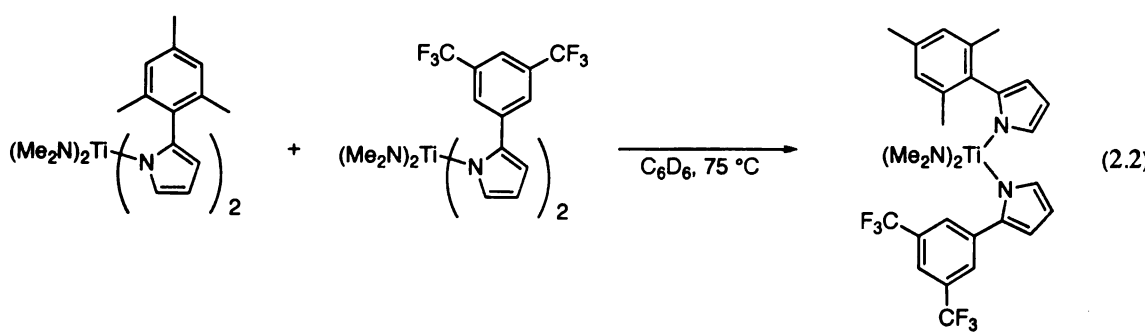

(2.2)

While there is no definitive answer as to whether the mono(pyrrolyl) or bis(pyrrolyl) or a mixture of both are carrying out the catalysis, it can be said that the active species is not $Ti(NMe_2)_4$ (**3**) or a species not containing the pyrrolyl ligand. Throughout all the catalyses no free Hpyrr resonances were observed in the ^1H NMR spectrum, therefore the maximum amount of $Ti(NMe_2)_4$ (**3**) that can be generated is half the amount of the concentration in our kinetic studies. Because the rate scales linearly with catalyst concentration, full disproportionation to $Ti(NMe_2)_4$ (**3**) and $Ti(pyrr)_4$ would

give a rate constant of 433 × 10^{-7} s^{-1}, half the $Ti(NMe_2)_4$ (**3**) rate under our standard conditions. Since all of the catalysts are faster than this, it can be said definitively that $Ti(NMe_2)_4$ (**3**) is not the active species.

2.4 Conclusion

Using readily available 2-substituted pyrroles, a route to 2,9-diaryldipyrrolylmethanes has been developed where the synthesized pyrroles can be used as the limiting reagent in condensation with acetone. Placing these new ligands on titanium is readily accomplished by reaction with $Ti(NMe_2)_4$ (**3**), and the resulting complexes show η^5,η^1-coordination of the dipyrrolylmethane in the solid state. However, the barrier for pyrrolyl exchange in these substituted dipyrrolylmethanes is quite low and is below what could be measured by variable temperature ^1H NMR spectroscopy.

Catalysis with these new dpm complexes was slower than with unsubstituted **9**, which are assigned to steric inhibition by the bulky groups near the substrate-binding site. Consistent with this, simple bis(pyrrolyl) complexes without the methylene linker and with the same substituents show faster catalysis rates, which is likely due to free rotation of the steric bulk away from the substrate binding site in the bis(pyrrolyl) derivatives. Using these bis(pyrrolyl) catalysts, I were able to show experimentally that hydroamination activity can be increased by adding electron-withdrawing groups to pyrrolyl substituents.

Comparison of various catalyst architectures shows that the pyrrolyl catalysts are quite rapid. It should be noted that this does not necessarily imply that these catalysts are superior for any particular application. The "best" catalyst for any particular application is a function of availability, selectivity, and activity with a particular set of substrates. For example, the fastest catalyst studied here, **9**, is a poor catalyst for some applications, e.g. hydrohydrazination,[20] and the only catalyst studied that leads to any product for others, e.g. the synthesis of 1-phenyl-2,5-dibenzylpyrrolyl from 1,6-diphenyl-1,5-hexadiyne and

aniline.[8] The aim is to optimize the activity of the most promising catalysts for these reactions, which my current results suggest are the dipyrrolylmethane complexes of titanium, especially $Ti(NMe_2)_2$(dpm) (**9**). From these experiments, I am discovering what electronic features and steric profiles encourage these useful C–N bond forming reactions.

2.4 Experimental

General Considerations. All manipulations of air sensitive compounds were carried out in an MBraun drybox under a purified nitrogen atmosphere. Anhydrous ether was purchased from Columbus Chemical Industries Inc., and pentane and toluene was purchased from Spectrum Chemical Mfg. Corp., were purified by sparging with dry N_2, then water was removed by running through activated alumina systems purchased from Solv-Tek. Hexanes and ethyl acetate were purchased from Mallinckodt-Baker Inc., and reagent grade acetone was purchased from Fisher Scientific and distilled from $CaSO_4$ under N_2 and stored over 4A molecular sieves. Trifluoroacetic acid was purchased from Aldrich and used as received. Aniline was purchased from Matheson, Coleman and Bell Mfg. and was distilled twice from calcium hydride under vacuum. 1-phenylpropyne was purchased from GFS Chemical, vacuum distilled, and then passed over two columns of neutral alumina. $Ti(NMe_2)_4$ (**3**)[21] was prepared using the literature procedures. 2-(2,4,6-trimethylphenyl)-1H-pyrrole ($Hpyrr^{mes}$) and 2-[3,5-bis(trifluoromethyl)phenyl]-1H-pyrrole ($Hpyrr^{3,5\text{-}CF3}$) were synthesized according to literature methods.[23] Deuterated solvents were dried over purple sodium benzophenone ketyl (C_6D_6) or phosphoric anhydride ($CDCl_3$) and distilled under a nitrogen atmosphere. Deuterated toluene was dried by passing it over two columns of neutral alumina. ^1H and ^{13}C spectra were recorded on Inova-300 or VXR-500 spectrometers. All spectra were referenced internally to residual protiosolvent (^1H) or solvent (^{13}C) resonances. ^1H and ^{13}C assignments were confirmed when necessary using two-dimensional ^1H–^1H and ^1H–^{13}C correlation NMR experiments. Chemical shifts are reported in ppm and coupling constants reported in Hz.

General Considerations for X-Ray Diffraction. Crystals grown from concentrated solutions at –35 °C quickly were moved from a scintillation vial to a microscope slide containing Paratone N. Samples were selected and mounted on a glass fiber in wax and Paratone. The data collections were carried out at a sample temperature of 173 K on a Bruker AXS platform three-circle goniometer with a CCD detector. The data were processed and reduced utilizing the program SAINTPLUS supplied by Bruker AXS. The structures were solved by direct methods (SHELXTL v5.1, Bruker AXS) in conjunction with standard difference Fourier techniques.

General Procedure for Kinetics. All manipulations were done in an inert atmosphere drybox. In a 2 mL volumetric flask was loaded the catalyst (10 mol %, 0.1 mmol), aniline (0.931 g, 911 μL, 10 mmol), 1-phenylpropyne (0.116 g, 125 μL, 1 mmol), and ferrocene (0.056 g, 0.3 mmol) as an internal standard. The solution was then diluted to 2 mL with deuterated toluene. An ample amount of solution (~0.75 mL) was put into a threaded J. Young NMR tube that was sealed with a cap and then wrapped with Teflon tape. The tube was then removed from the drybox and heated at 75 °C in the NMR spectrometer. The relative 1-phenylpropyne versus ferrocene concentration was monitored as a function of time. The fits are to the exponential decay of the starting material using the scientific graphing programs Origin or KaleidaGraph. The exact expression used to fit the data was $Y_t = Y_\infty + (Y_0 - Y_\infty) \exp^{-k_{obs}t}$ where Y = [1-phenylpropyne] at time = t (Y_t), infinity (Y_∞), or initial (Y_0). The variables Y_∞, Y_0, and k_{obs} were optimized in the fits.[22]

Synthesis of 2-(4-methylphenyl)-1H-pyrrole ($Hpyrr^{tol}$)

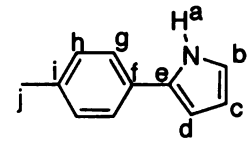

Under an atmosphere of dry nitrogen a threaded Schlenk tube was loaded with sodium pyrrole (4.69 g, 52.6 mmol), $ZnCl_2$ (7.17 g, 52.6 mmol) and a stirbar. To that same vessel was added of THF (40 mL) slowly (caution: exothermic). After 10 min, $Pd(OAc)_2$ (20 mg, 0.5 mol%) and 2-(di-*tert*-butylphosphino)biphenyl (26 mg, 0.5 mol%) were added to the Schlenk tube. The tube was then capped, taken from the dry box, and connected to a Schlenk line. Under a continuous flow of nitrogen the screw cap was removed, and 4-bromotoluene quickly was added. The screw cap was replaced after addition. The headspace in the Schlenk tube was evacuated and then placed in a 100 °C oil bath for 24 h. After 24 h, the tube was removed from the oil bath and allowed to cool to room temperature. The cap was removed, and the solution was transferred to a separatory funnel. The tube was rinsed with OEt_2 (30 mL) and of H_2O (30 mL), which were then added to the separatory funnel. The aqueous layer was extracted with OEt_2 (3 × 50 mL); the combined organic layers were collected and dried over $MgSO_4$. The solution was then filtered and concentrated in vacuo. Purification of the crude product was accomplished by column chromatography on silica gel using an eluting solution of hexanes:ethyl acetate (9:1) to yield an white solid (1.44 g, 54%). m.p. 145 °C. ^{1}H NMR (500 MHz, $CDCl_3$): 8.2 (br s, 1 H, H^a), 7.37 (d, J_{HH} = 8.46 Hz, 2 H, H^g or H^h), 7.18 (d, J_{HH} = 8.07 Hz, 2 H, H^g or H^h), 6.82 (m,1 H, H^c, H^b or H^d), 6.50 (m, 1 H, H^c, H^b or H^d), 6.31 (m, 1 H, H^c, H^d, or H^b), 2.39 (s, 3 H, H^j). ^{13}C {^{1}H}NMR (125 MHz, $CDCl_3$): 135.85 (C^i or C^f), 132.19 (C^i or C^f), 129.97 (C^e), 129.50 (C^h or C^g), 123.77 (C^h or C^g), 118.42

(C^c, C^d or C^b), 109.90 (C^d, C^c or C^b), 105.31 (C^c, C^d, or C^b), 21.38 (C^j). Elemental Analysis (Experimental) Calc. C: (84.10) 84.04, H: (7.02) 7.05, N:(8.66) 8.91.

Synthesis of 2-(4-trifluoromethylphenyl)-1H-pyrrole ($Hpyrr^{4\text{-}CF3}$)

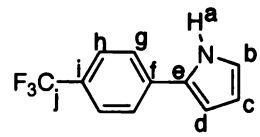

Under an atmosphere of dry nitrogen, a threaded Schlenk tube was loaded with sodium pyrrole (3.6 g, 40.4 mmol), $ZnCl_2$ (5.5 g, 40.4 mmol) and a stirbar. To that vessel was added 32 mL of THF slowly (caution: exothermic). After 10 min, $Pd(OAc)_2$ (15 mg, 0.5 mol%) and 2-(dicyclohexylphosphino)biphenyl (24 mg, 0.5 mol%) were added to the Schlenk tube. The screwcap was replaced, and the tube was removed from the dry box and connected to a Schlenk line. Under a continuous flow of nitrogen the screwcap was removed and 4-bromobenzotrifluoride (3 g, 13 mmol) quickly was added. The screwcap was replaced, and the headspace in the tube was evacuated. The tube was then placed in a 80 °C oil bath where it was allowed to react for 20 h. After the reaction was complete, the tube was removed from the oil bath and allowed to cool to room temperature. The cap was removed, and the solution was transferred to a separatory funnel. The tube was rinsed OEt_2 (30 mL) and H_2O (30 mL), which were then added to the separatory funnel. The aqueous layer was extracted with OEt_2 (3 × 50 mL); the combined organic layers were collected and dried over $MgSO_4$. The solution was then filtered and concentrated in vacuo. Purification of the crude product was accomplished by column chromatography on silica gel using an eluting solution of hexanes:ethyl acetate (9:1) to yield a white solid (2.53 g, 90%). m.p. 158 °C. ^{1}H NMR (500 MHz, $CDCl_3$): 8.46 (br s, 1 H, H^a), 7.59 (d, J_{HH} = 7.73 Hz, 2 H, H^h), 7.53 (d, J_{HH} = 7.73 Hz, 2 H, H^g), 6.91 (m, 1 H, H^d, H^b, or H^c), 6.62 (m, 1 H, H^d, H^c, or H^b), 6.33 (m, 1 H, H^b, H^d, or H^c). ^{13}C {^{1}H} NMR (125 MHz, $CDCl_3$): 135.91 (C^f), 130.6 (C^e), 127.85 (q, J_{CF} = 33 Hz, C^i), 125.92 (q, J_{CF} = 33 Hz, C^h),

124.29 (q, J_{CF} = 272 Hz, C^j), 123.58 (C^g) , 120.1 (C^b, C^c, or C^d), 110.65 (C^b, C^d, or C^c), 107.7 (C^c, C^d, or C^b). Elemental Analysis (Experimental) Calc. C: (62.22) 62.56, H: (3.54) 3.82, N: (6.51) 6.67.

Caution! The lithium pyrrolide of 2-(4-(trifluoromethyl)phenyl)pyrrole (Hpyrr4-CF_3) was recently prepared in our laboratory by addition of *n*-butyllithium to Hpyrr4-CF_3, which allowed apparent production of the desired lithium salt. This compound, Li(pyrrCF_3), was found to be explosive in the solid state under an inert atmosphere. It is likely that *o*-CF_3-aryl pyrrolides can undergo a similar decomposition. *Consequently, extreme caution should be used if alkali-metal salts are produced of aryl-substituted pyrroles containing CF_3 groups in the ortho or para positions of the arene.*[23] It is unknown if the same decomposition can occur in an explosive manner in solution as well, but we also urge caution with solutions of such compounds. We have produced the lithium salts of pyrroles containing *m*-CF_3-aryl groups on numerous occasions, and, thus far, these have not undergone the same explosive decomposition.

Synthesis of 2,9-bis[3,5-bis(trifluoromethyl)phenyl]-5,5-dimethyldipyrrolylmethane ($H_2dpm^{3,5\text{-}CF3}$)

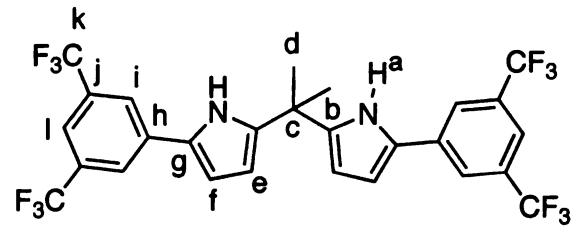

A 1-neck 14/20 25 mL round-bottom flask was charged with 2-[3,5-bis(trifluoromethyl)phenyl]-1H-pyrrole (0.4 g, 1.4 mmol) and acetone (2.08 g, 36 mmol). The flask then was sealed with a septum. The solution was stirred at room temperature while degassed under a flow of argon. After 15 min, trifluoroacetic acid (0.4 g, 3.6 mmol) was added via syringe. The solution was allowed to stir for 3 h under an argon atmosphere. The reaction was quenched with ~15 mL of 0.1 M NaOH solution. The resulting mixture was transferred to a separatory funnel where the aqueous layer was extracted with Et_2O (2 × 15 mL). The combined organic layers were dried over $MgSO_4$ and filtered. The solvent was removed in vacuo to give a purple oil. The oil was then tritrated with pentane to yield a pink solid (0.311 g, 72%). m.p. 130 °C. ^{1}H NMR (500 MHz, $CDCl_3$): 8.11 (br s, 2 H, H^a), 7.73 (s, 4 H, H^i), 7.6 (s, 2 H, H^l), 6.6 (m, 2 H, H^e or H^f), 6.2 (m, 2H, H^e or H^f), 1.76 (s, 6 H, H^d). ^{13}C {^{1}H}NMR (125 MHz, $CDCl_3$): 141.64 (C^h or C^g), 134.4 (C^h or C^g), 132.18 (q, J_{CF} = 31.94 Hz, C^j), 129.03 (C^b), 123.28 (q, J_{CF} = 272 Hz, C^k), 123.15 (q, J_{CF} = 2.54 Hz, C^i), 119.1 (q, J_{CF} = 3.91 Hz, C^l), 108.64 (C^e or C^f), 107.09 (C^e or C^f), 35.83 (C^c), 29.09 (C^d). Elemental Analysis (Experimental) Calc. C: (54.63) 54.19, H: (3.14) 3.03, N: (4.52) 4.68.

Synthesis of 2,9-bis(2,4,6,-trimethylphenyl)-5,5-dimethyldipyrrolylmethane (H_2dpm^{mes})

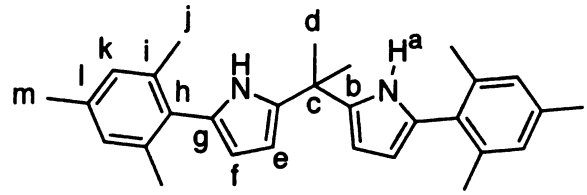

A 1-neck 14/20 25 mL round-bottom flask was charged with 2-(2,4,6–trimethylphenyl)-1H-pyrrole (0.25 g, 1.3 mmol) and acetone (1.96 g, 33 mmol) then sealed with a septum. The solution was stirred at room temperature while degassed under a flow of argon. After 15 min, trifluoroacetic acid (0.384 g, 3.3 mmol) was added via syringe. The solution was allowed to stir for 1 h. The reaction was quenched with ~15 mL of 0.1 M NaOH solution. The resulting mixture was transferred to a separatory funnel where the aqueous layer was extracted with Et_2O (2 × 15 mL). The combined organic layers were dried over $MgSO_4$ and filtered. The solvent was removed in vacuo to give an orange oil. The oil was then tritrated with pentane to yield an orange solid. (0.187 g, 68%). m.p. 115 °C. ^{1}H NMR (500 MHz, $CDCl_3$): 7.57 (br s, 2 H, H^a), 6.89 (s, 4 H, H^k), 6.09 (app t, J_{HH} = 2.87 Hz, 2 H, H^e or H^f), 5.88 (app t, J_{HH} = 5.86 Hz, 2 H, H^e or H^f), 2.2 (s, 6 H, H^m), 2.0 (s, 12 H, H^j), 1.6 (s, 6 H, H^d). ^{13}C {^{1}H}NMR (125 MHz, $CDCl_3$): 138.54 (C^l, C^i, or C^h), 138.31 (C^l, C^i, or C^h), 137.38 (C^l, C^i, or C^h), 130.83 (C^b or C^g), 128.76, 127.98 (C^k), 107.5 (C^e or C^f), 103.4(C^e or C^f), 35.30 (C^c), 28.95 (C^d), 20.99 (C^m), 20.52 (C^j). Elemental Analysis (Experimental) Calc: C, (84.85) 84.83, H: (8.37) 8.35, N: (6.78) 6.82.

Synthesis of $Ti(NMe_2)_2(dpm^{mes})$ (12):

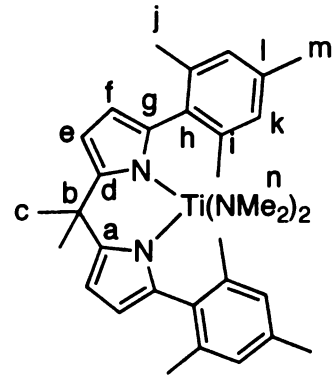

Under an atmosphere of dry nitrogen, a threaded pressure tube was loaded with $Ti(NMe_2)_4$ (**3**) (0.316 g, 1.4 mmol), H_2dpm^{mes} (0.578 g, 1.4 mmol), and Et_2O (8 mL). The pressure tube was sealed with a Teflon screw cap, taken out of the dry box, and put in a 50 °C oil bath, where it was left to react for 18 h. The pressure tube was then removed from the oil bath and taken back into an atmosphere of dry nitrogen, where the volatiles were removed in vacuo to yield an orange oily solid. Crystallization from pentane yielded an orange solid (0.225 g, 30%). m.p. 155 °C (dec). ^1H NMR (500 MHz, $CDCl_3$): 6.80 (s, 4 H, H^k), 6.37 (d, J_{HH} = 2.80 Hz, 2 H, H^f or H^e), 6.28 (d, J_{HH} = 2.77 Hz, 2 H, H^f or H^e), 2.59 (s, 12 H, H^n), 2.23 (s, 6 H, H^m), 2.18 (s, 12 H, H^j), 1.94 (s, 6H, H^c). ^{13}C {^1H} NMR (125 MHz, $CDCl_3$) 159.15 (C^h), 138.38 (C^i or C^l), 138.26 (C^i or C^l), 136.27 (C^d or C^g), 132.54 (C^g or C^d), 128.52 (C^k), 113.70 (C^e or C^f), 107.01 (C^e or C^f), 47.45 (C^n), 39.26 (C^b), 30.15 (C^m), 21.67 (C^j), 20.92 (C^c). After many attempts at elemental analysis, satisfactory results were not obtained. ^1H and ^{13}C NMR spectra are included in the Appendix to demonstrate purity.

Synthesis of $Ti(NMe_2)_2(dpm^{3,5\text{-}CF3})$ (13):

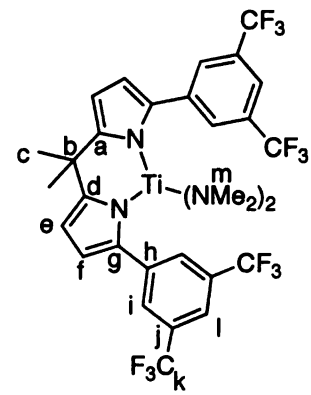

Under an atmosphere of dry nitrogen a vial was loaded with $Ti(NMe_2)_4$ (**3**) (0.131 g, 0.584 mmol) in Et_2O (3 mL). In a 20 mL scintillation vial was loaded 2,9-bis[3,5-bis(trifluoromethyl)phenyl]-5,5-dimethyldipyrrolylmethane (0.350 g, 0.584 mmol) in OEt_2 (3 mL). The solutions were put into a cold well where they sat until nearly frozen. To a thawing solution of $H_2dpm^{3,5\text{-}CF_3}$ was added to the cold solution of **3**. The solution was stirred at room temperature for 4 h. Volatiles were removed in vacuo to yield an orange solid (0.395 g, 92%). m.p. 150 °C (dec). ^1H NMR (300 MHz, $CDCl_3$): 7.96 (s, 4 H, H^i), 7.63 (s, 2 H, H^l), 6.55 (d, J_{HH} = 3.19 Hz, 2 H), 6.44 (d, J_{HH} = 3.18 Hz, 2 H), 2.6 (s, 12 H, H^m), 1.8 (s, 6 H, H^c). ^{13}C {^1H} NMR (125 MHz, $CDCl_3$): 162.84 (C^h), 138.18 (C^a or C^g), 138.04 (C^a or C^g), 131.17 (q, J_{CF} = 33.6 Hz, C^j), 126.26 (q, C^i), 119.55 (q, J_{CF} = 3.7 Hz, C^l), 110.22 (C^e or C^f), 109.53 (C^e or C^f), 45.88 (C^m), 39.67 (C^b)29.33 (C^c). Elemental Analysis (Experimental) Calc. C: (50.45) 50.84, H: (3.75) 3.85, N: (7.48) 7.65.

Synthesis of $Ti(NMe_2)_2(pyrr^{mes})_2$ (15):

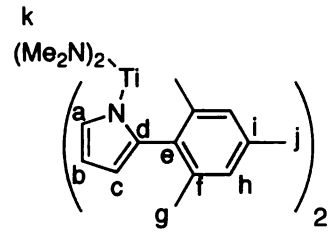

Under an atmosphere of dry nitrogen a threaded pressure tube was loaded with $Ti(NMe_2)_4$ (**3**) (0.075 g, 0.334 mmol), $Hpyrr^{mes}$ (0.124 g, 0.667 mmol), and Et_2O (5 mL). The pressure tube was then sealed with a Teflon screwcap and wrapped with Teflon tape. The pressure tube was then taken out of the dry box and put into a 60 °C oil bath for 40 h. After 40 h, the pressure tube was taken back into an atmosphere of dry nitrogen, and the volatiles were removed in vacuo to yield a yellow solid (0.125 g, 74%). m.p. 160 °C (dec). ^1H NMR (500 MHz, $CDCl_3$): 6.83 (s, 4 H, H^h), 6.81 (m, 2 H, H^a, H^b, or H^c), 6.19 (m, 2 H, H^b, H^a or H^c), 5.91 (m, 2 H, H^a ,H^b, or H^c), 2.77 (s, 12 H, H^k), 2.28 (s, 6H, H^j), 2.1 (s, 12 H, H^g). ^{13}C {^1H} NMR (125 MHz, $CDCl_3$): 139.2 (C^f), 137.54 (C^i, C^e, or C^d), 136.85 (C^i, C^e, or C^d), 134.65 (C^i, C^e, or C^d), 127.6 (C^h), 123.09 (C^a, C^c, or C^b), 108.6 (C^a C^b or C^c), 108.3 (C^a, C^b, or C^c), 44.14 (C^k), 21.04 (C^j), 20.36 (C^g). Elemental Analysis (Experimental) Calc. C: (70.98) 71.42, H: (8.01) 7.99, N: (10.97) 11.10.

Synthesis of $Ti(NMe_2)_2(pyrr^{3,5\text{-}CF3})_2$ (14)

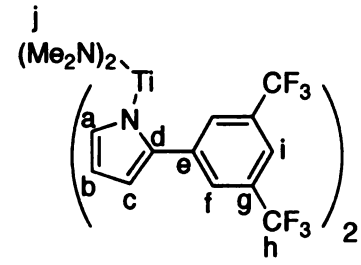

Under an atmosphere of dry nitrogen, a 20 mL scintillation vial was loaded with $Ti(NMe_2)_4$ (**3**) (0.150 g, 0.669 mmol) in OEt_2 (3 mL). A separate vial was loaded $Hpyrr^{3,5\text{–}CF3}$ (0.372 g, 1.33 mmol) in OEt_2 (5 mL). $Hpyrr^{3,5\text{–}CF_3}$ was then added to the vial containing **3** at room temperature. The solution was allowed to stir at room temperature for 6 h. Crystallization from pentane yielded the bis(pyrrolyl) as an orange solid (0.175 g, 38%). m.p. 86 °C (dec). ^1H NMR (500 MHz, $CDCl_3$): 7.74 (s, 4 H, H^f), 7.61 (s, 2 H, H^i), 6.89 (m, 2 H, H^a, H^b, or H^c), 6.48 (m, 2 H, H^a, H^b, or H^c), 6.25 (m, 2 H, H^a, H^b, or H^c), 3.0 (s, 12 H, H^j). ^{13}C {^1H} NMR (125 MHz, $CDCl_3$): 138.88 (C^e), 137.70 (C^d), 131.62 (q, J_{CF} = 33 Hz, C^g), 126.63 (C^a, C^b, or C^c), 125.96 (C^f), 123.35 (J_{CF} = 273 Hz, C^h), 119.1 (C^i), 111.86 (C^a, C^b, or C^c), 111.20 (C^a, C^b, or C^c), 44.53 (C^j). Elemental Analysis (Experimental) Calc. C: (48.48) 48.57, H: (3.53) 3.49, N: (7.78) 8.09.

Synthesis of $Ti(NMe_2)_2(pyrr^{4\text{-}CF3})_2$ (16)

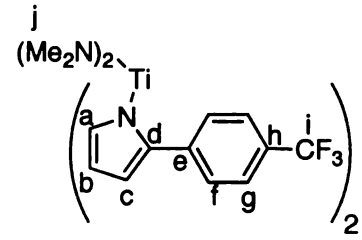

Under an atmosphere of dry nitrogen, a 20 mL scintillation vial was loaded with $Ti(NMe_2)_4$ (**3**) (0.061 g, 0.272 mmol), $Hpyrr^{4\text{-}CF3}$ (0.115 g, 0.544 mmol), OEt_2 (3 mL), and a stir bar. The vial was then capped and allowed to stir for 36 h at room temperature. The volatiles were removed in vacuo to yield an orange oil. Crystallization from pentane yielded an orange solid (0.069 g, 45%). m.p. 72 °C. ^1H NMR (500 MHz, $CDCl_3$): 7.47 (d, J_{HH} = 7.88 Hz, 4 H, H^g), 7.45 (d, J_{HH} = 7.89 Hz, 4 H, H^f), 7.00 (m, 2 H, H^c), 6.36 (m, 2 H, H^a , H^b, or H^c), 6.27 (m, 2 H, H^c, H^a or H^b), 3.16 (s, 12 H, H^j). ^{13}C {^1H} NMR (125 MHz, $CDCl_3$): 140.43 (C^e), 139.50 (C^d), 127.64 (q, J_{CF} = 33 Hz, C^h), 126.56 (C^f), 126.51 (C^b, C^a, or C^c), 125.12 (q, J_{CF} = 11.78 Hz, C^g), 124.31 (q, J_{CF} = 272 Hz, C^i), 111.07 (C^a, C^b, or C^c), 109.86 (C^a, C^b, or C^c), 44.68 (C^j). Elemental Analysis (Experimental) Calc. C: (55.83) 56.13, H: (5.11) 4.71, N: (10.29) 10.07

Synthesis of $Ti(NMe_2)_2(pyrr^{tol})_2$ (17):

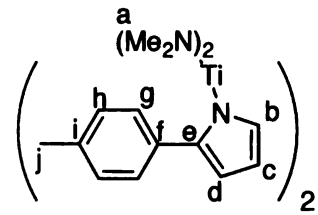

Under an atmosphere of dry nitrogen a threaded pressure tube was loaded with $Hpyrr^{tol}$ (0.115 g, 0.732 mmol), $Ti(NMe_2)_4$ (**2**) (0.082 g, 0.366 mmol), OEt_2 (3 mL), and a stirbar. The pressure tube was then sealed with a Teflon screwcap and then wrapped with Teflon tape. The tube was removed from the dry box and placed in a 60 °C oil bath, where it was left to react for 24 h. After the reaction was complete, it was taken back into an atmosphere of dry nitrogen. The reaction mixture was transferred to a 20 mL scintillation vial where the volatiles were concentrated in vacuo to yield an orange oil. Crystallization from pentane yielded an orange solid (0.060 g, 37%). m.p. 71 °C. ^1H NMR (500 MHz, $CDCl_3$): 7.18 (d, J_{HH} = 7.68 Hz, 4 H, H^h or H^g), 7.04 (d, J_{HH} = 7.77, 4 H, H^h or H^g), 6.90 (m, 2 H, H^b, H^c, or H^d), 6.27 (m, 2 H, (H^c, H^b, or H^d), 6.18 (m, 2 H, H^c ,H^b, H^d), 2.99 (s, 12 H, H^a), 2.29 (s, 6 H, H^j). ^{13}C {^1H} NMR (125 MHz, $CDCl_3$): 141.11 (C^i), 135.53 (C^f), 134.57 (C^e), 128.82 (C^h or C^g), 126.97 (C^h or C^g), 125.67 (C^d), 110.05 (C^b, C^c, or C^d), 107.68 (C^b ,C^d or C^c), 44.68 (C^a), 21.10 (C^j). Elemental Analysis (Experimental) Calc. C: (69.53) 69.94, H: (7.60) 7.19, N: (12.17) 12.49.

2.5 References

1. Chenier, P.J. *Survey of Industrial Chemistry,* John Wiley & Sons, New York, **1986**; 82.

2. (a) Zhang, Z.; Schafer, L. L. *Org. Lett.* **2003**, 5, 4733. (b) Cao, C.; Ciszewski, J. T.; Odom, A. L. *Organometallics*, **2001**, *20*, 5011.

3. (a) Cao, C.; Shi, Y.; Odom, A. L. *Org. Lett.* **2002**, *4*, 2853. (b) Khedkar, V.; Tillack, A.; Michalick, M.; Beller, M. *Tetrahedron Lett.* **2004**, *45*, 3123. (c) Ackerman, L.; Born, R. *Tetrahedron Lett.* **2004**, *45*, 9541. (d) Khedkar, V.; Tillack, A.; Michalik, M.; Beller, M. *Tetrahedron* **2005**, *61*, 7622.

4. Cao, C.; Shi, Y.; Odom, A. L. *J. Am. Chem. Soc.* **2003**, *125*, 2880.

5. Cao, C.; Li, Y.; Odom, A. L. *Chem. Commun.* **2004**, 2002.

6. Cao, C.; Shi, Y.; Odom, A. L. *J. Am. Chem. Soc.* **2003**, *125*, 2880.

7. Banerjee, S.; Shi, Y.; Cao, C.; Odom, A.L. *J. Organomet. Chem.* **2005**, *690*, 5066.

8. Majumder, S.; Odom. A. L. *Organometallics*, **2008**, *27*, 1174.

9. Khedkar, V.; Tillack, A.; Beller, M. *Org. Lett.* **2003**, *5*, 4767.

10. Shi, Y.; Ciszewski, J. T.; Odom, A. L. *Organometallics*, **2001**, *20*, 3967.

11. Bexrud, J. A.; Li, C.; Schafer, L. L.*Organometallics*, **2007**, *26*, 6366.

12. Swartz, D.L.; Odom. A.L. *Organometallics*, **2006**, *26*, 625.

13. Littler, B.J.; Miller, M.A.; Hung, C. H.; Wagner, R.W.; O'Shea, D.F.; Boyle, P.D.; Lindsey, J. S. *J. Org. Chem.* **1999**, *64*, 1391.

14. (a)Baranger, A.M.; Walsh, P. J.; Bergman, R. G. *J. Am. Chem. Soc.* **1993**, *115*, 2753. (b) Walsh, P. J.; Baranger, A. M.; Bergman, R. G. *J. Am. Chem. Soc.* **1992**, *114*, 1708. (c) Duncan, A.P.; Bergman, R. G. *Chem. Rec.* **2002**, *2*, 431. (d) Le, S. Y.; Bergman, R. G. *Tetrahedron* **1995**, *51*, 4255. (e) Polse, J. L.; Andersen, R. A.; Bergman, R. G. *J. Am. Chem. Soc.* **1998**, *120*, 13405.

15. Schrock, R. R.; Murdzek, J. S.; Bazan G. C.; Robbins, J.; DiMare, M.; O'Reagan, M. *J. Am. Chem. Soc.* **1990**, *112*, 3875.

16. Reith, R. D.; Mankad, N. P.; Calimano, E.; Sadighi, J. P. *Org. Lett.* **2004**, *6*, 3981.

17. A. Novak, A. J. Blake, C. Wilson and J. B. Love, *Chem. Commun.*, **2002**, 2796.

18. Shi, Y; Hall, C.; Ciszewski, J. T.; Cao, C.; Odom. A.L. *Chem. Commun.*, **2003**, 586.

19. Tanski, J. M.; Parkin, G. *Organometallics* **2002**, *21*, 587.

20. Banerjee, S.; Odom, A. L. unpublished results.

21. Bradley, D. C.; Thomas, I.M.; J. Chem. Soc., **1960**, 3859.

22. Espenson, J. H. *Chemical Kinetics and Reaction Mechanisms*; McGraw-Hill: New York, 1995.

23. A similar caution has been issued by Wigley and co-workers concerning Li-4-$CF_3C_6H_4$, which likely undergoes a similar decomposition: Weller, K. J.; Gray, S. D.; Briggs, P. M.; Wigley, D. E. *Organometallics* **1995**, *14*, 5588.

CHAPTER 3

Synthesis, structure, and hydroamination reactivity of electron deficient titanium complexes bearing bis- and mono(pyrrolyl) ligands

3.1 Introduction

Pyrrole-based ancillary ligands on titanium are a useful class of compounds known to participate in catalytic hydroamination,[1] iminoamination,[2] and hydrohydrazination.[3] In the previous chapter, I reported that placing aryl-substituents on the 2-position of the pyrrolyl provided effective catalysts for the hydroamination of primary amines and alkynes. Using these bis(2-arylpyrrolyl) titanium catalysts, I was able to show experimentally that hydroamination activity can be increased by adding electron-withdrawing groups to the pyrrolyl ligand, however the addition of sterically hindered groups in these positions inhibits access to the metal center negatively affecting catalysis rates.[4]

In an attempt to increase the hydroamination activity of these bis(pyrrolyl) titanium catalysts, moving electron-withdrawing substituents from the 2-position to the 3-position of the pyrrole may provide greater access to the binding site resulting in enhanced hydroamination activity. This chapter discusses the synthesis and hydroamination catalysis of 3-arylpyrrolyl titanium complexes.

3.2 Results and Discussions

The synthesis of 3-arylpyrroles can be achieved by the seminal methodology established by Smith and co-workers, which begins with an iridium-catalyzed reaction of N-*Boc*-pyrrole with 4,4,5,5-tetramethyl-1,3,2-dioxaborolane (HBpin) to generate 3-(pinacolboryl)-N-*Boc*-pyrrole. The aryl group is then installed by Suzuki cross-coupling to generate 3-aryl pyrroles on multi-gram scales (Scheme 3.1).[5]

Scheme 3.1 Smith borylation followed by Suzuki coupling to prepare 3-substituted pyrroles. (Cod = 1,5-cyclooctadiene, Bu^{t}bipy = 4,4'-di-*tert*-butyl-2,2'-bipyridine, Boc = *tert*-butyl-carboxylate).

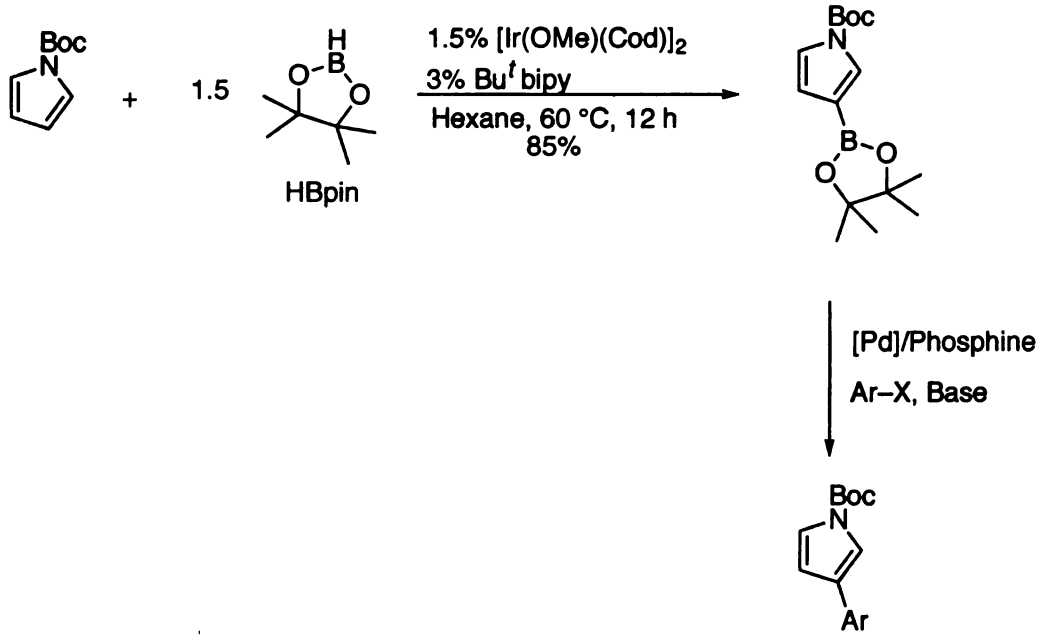

Using the above methodology I was able to synthesize 3-C_6F_5 (3-Hpyrr^{C6F5}) and 3,5–$(CF_3)C_6H_3$ (3-Hpyrr$^{3,5-CF3}$) pyrroles in 53% and 76% isolated yields (Scheme 3.2). Reacting 3-Hpyrr$^{3,5-CF3}$ with half an equivalent of $Ti(NMe_2)_4$ (**3**) yields

$Ti(NMe_2)_2(NHMe_2)(pyrr^{3,5\text{–}CF3})_2$ (**19**) in 76% yield (Equation 3.1). Single crystal X-Ray diffraction on **19** shows that the pyrrolyls are η^1:η^1-bound in the solid-state taking on a pseudo trigonal-bipyramidal geometry (tbp). A structure for **19** is shown in Figure 3.1.

Scheme 3.2 Synthesis of 3-Hpyrr$^{3,5\text{–}CF3}$ and 3-Hpyrr^{C6F5}.

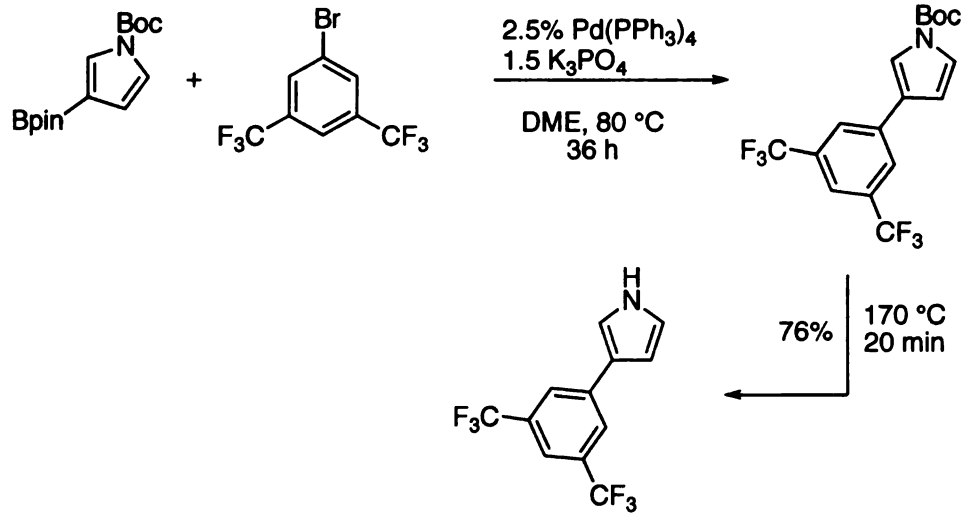

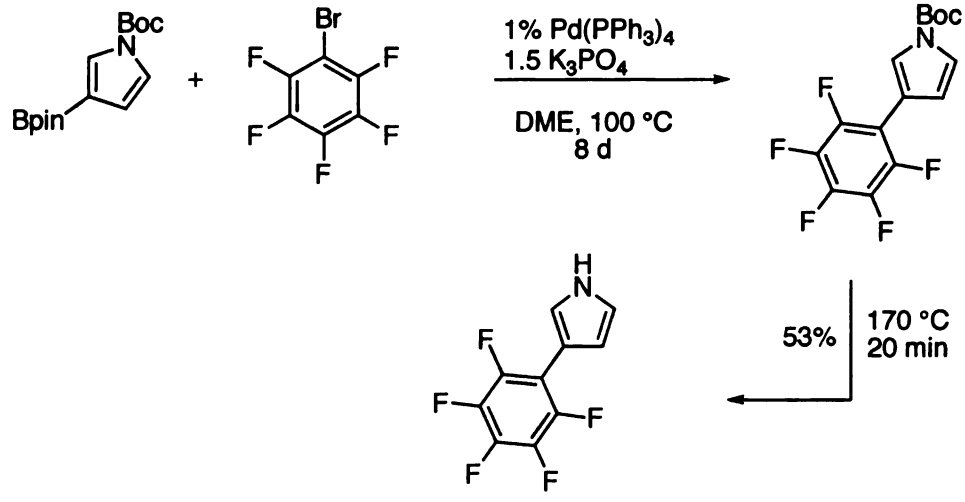

Consequently, moving the aryl groups from the 2-position to the 3-position on the pyrrole reduces sterics around the metal center allowing for the retention of dimethylamine. As expected the longest Ti–N bond distance is from the dimethylamine

ligand, 2.248(4) Å, which sits in the axial position *trans* to one of the pyrrolyl ligands. The average Ti–N(NMe_2) bond distance is 1.867 Å, while the average pyrrolyl Ti–N bond distance is 2.075 Å. These bond distances are quite similar to previously reported derivatives.[4]

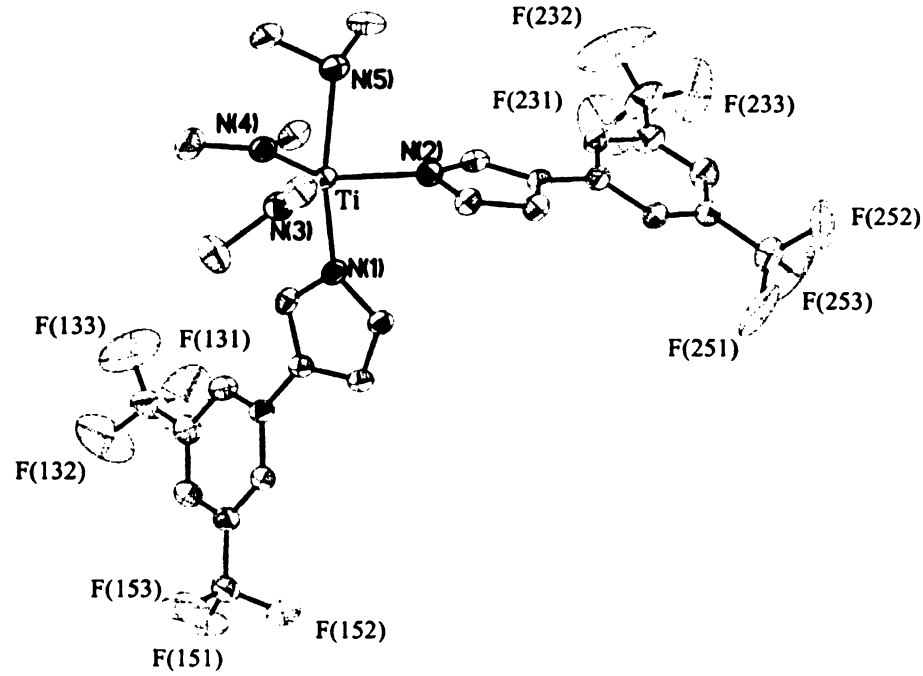

Figure 3.1 ORTEP structure from single crystal X-ray diffraction on $Ti(NMe_2)_2(NHMe_2)(3\text{-}pyr^{3,5\text{-}CF3})_2$ (**19**) with thermal ellipsoids at 50% probability level. Selected bond distances (Å) and angles (deg). Ti-N(1) 2.098(4), Ti-N(2) 2.053(5), Ti-N(3) 1.862(5), Ti-N(4) 1.873(5), Ti-N(5) 2.248(4), N(1)-Ti-N(2) 87.89(18), N(2)-Ti-N(3) 116.7(2), N(3)-Ti-N(4) 111.9(2), N(4)-Ti-N(5) 90.21(18), N(2)-Ti-N(4) 130.8(2), N(2)-Ti-N(5) 81.54(17), N(3)-Ti-N(5) 91.33(18), N(1)-Ti-N(3) 99.01(19), N(1)-Ti-N(4) 87.89(18), N(1)-Ti-N(5) 167.72(18).

The ^1H spectrum of **19** at room temperature is inconsistent with the solid-state structure showing equivalent pyrrolyls. This is indicative of a rapid isomerization on the

NMR timescale. Cooling solutions of **19** in $CDCl_3$ to –60 °C in the NMR probe produces a rather complex ^1H spectrum. Small peaks in the aromatic region present in the room temperature ^1H spectrum, which were presumed to be impurities, intensify at –60 °C in the ^1H spectrum and the aromatic peaks associated with the pyrrolyls of **19** split into new resonances. New peaks also appear in the methyl region and the methyl peaks associated with the dimethylamine ligand begin to split as well. Due to the complexity of the ^1H spectrum at –60 °C a definitive structural assignment of the peaks in the spectrum was not possible. One possible explanation for this behavior is that there could be additional isomers of **19** in solution causing the complexity of the ^1H spectrum at room temperature as well as at depressed temperatures.

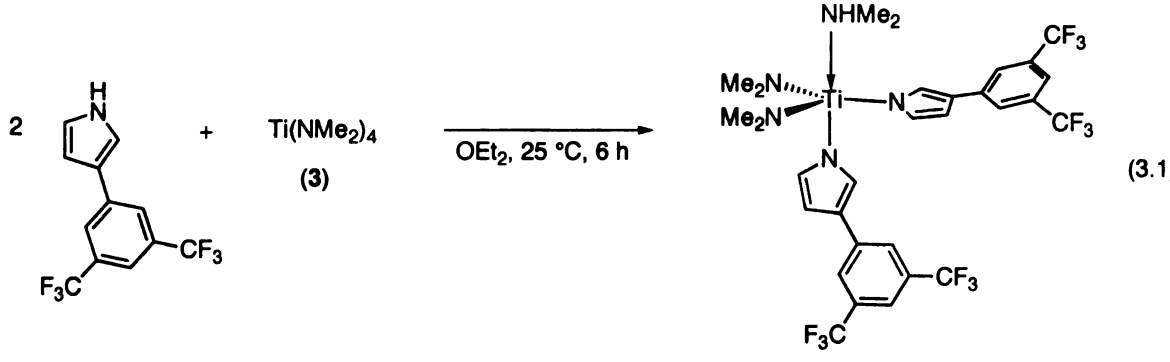

(3.1)

$Ti(NMe_2)_2(NHMe_2)(3\text{-}pyrr^{3,5\text{-}CF3})$ (**19**)

Surprisingly, reacting 2 equivalents of $3\text{-}Hpyrr^{C6F5}$ with $Ti(NMe_2)_4$ (**3**) does not seem to yield a single metal complex $Ti(NMe_2)_2(NHMe_2)(pyr^{C6F5})_2$ or $Ti(NMe_2)_2(NHMe_2)_2(pyr^{C6F5})_2$. The ^1H NMR spectrum of the orange solid obtained from the reaction mixture is rather perplexing. Integration of the peaks did not correspond to a single metal complex. Variable temperature ^1H NMR experiments were carried out in toluene-d_8 proved to be fairly informative. An increase in temperature in the NMR probe results in new resonances in the baseline of the ^1H spectrum as well as significant shifts

in the methyl groups assigned to NMe_2 groups. One possible explanation for this behavior is that upon formation of $Ti(NMe_2)_2(NHMe_2)_n(pyr^{C6F5})_2$, it disproportionates to yield a mixture of mono- and tris(pyrrolyl) complexes (Scheme 3.3) and pyrrolyl crossover is occurring at elevated temperatures. Attempts to isolate a single metal complex from the reaction of 3-$Hpyrr^{C6F5}$ and $Ti(NMe_2)_4$ (**3**) via crystallization were successful. Single crystals of $Ti(NMe_2)_2(NHMe_2)(pyrr^{C6F5})_2$ were grown from a OEt_2/pentane solution at –35 °C, proving that $Ti(NMe_2)_2(NHMe_2)(pyrr^{C6F5})_2$ is formed at low temperatures.

Scheme 3.3 Possible pyrrolyl crossover in the reaction of $Hpyrr^{C6F5}$ and $Ti(NMe_2)_4$ (**3**).

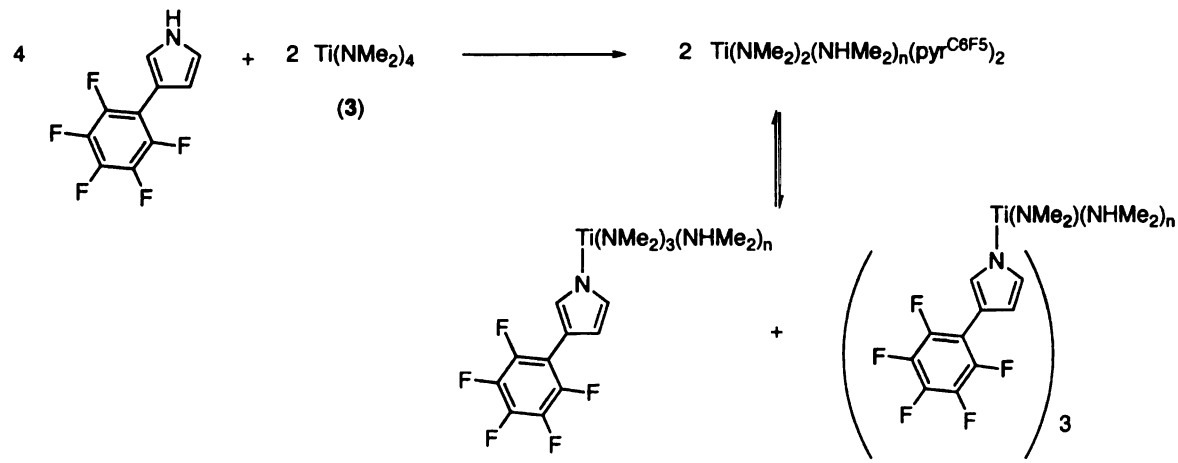

The reaction of aniline and 1-phenylpropyne under pseudo-first order reaction conditions at 75 °C with **19** as the catalyst, results in the reaction being ~10% complete after 10 h. One possible explanation for the slow catalysis may be that pyrrolyl crossover is occurring at elevated temperatures, similar to the process depicted in Scheme 3.3. This assertion warrants further investigation.

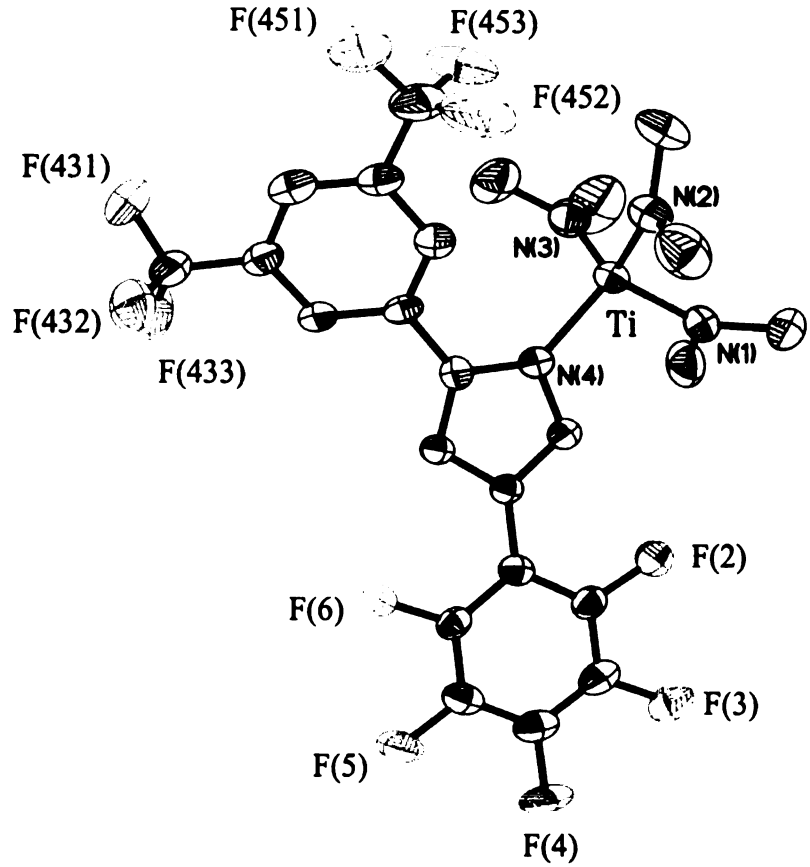

Figure 3.2 ORTEP structure from single crystal X-ray diffraction on $Ti(NMe_2)_3(pyr^{2\text{-}CF3\text{-}4C6F5})$ (**20**) with thermal ellipsoids at 50% probability level. Selected bond distances (Å) and angles (deg). Ti-N(1) 1.865(4), Ti-N(2) 1.861(5), Ti-N(3) 1.865(5), Ti-N(4) 2.074(5), N(1)-Ti-N(2) 106.7(2), N(2)-Ti-N(3) 108.3(2), N(3)-Ti-N(4) 117.09(19), N(2)-Ti-N(4) 110.2(2), N(1)-Ti-N(4) 106.35(19).

In an attempt to reduce amine coordination, pyrrolyl crossover and also to increase the hydroamination activity, I prepared 2-(3,5-bis(trifluoromethyl)phenyl)-4-(perfluorophenyl)pyrrole and the corresponding titanium complex (Scheme 3.4).

Scheme 3.4 Synthesis of 2-(3,5-bis(trifluoromethyl)phenyl)-4-(perfluorophenyl)pyrrole ($Hpyr^{2\text{-}CF3\text{-}4\text{-}C6F5}$) and $Ti(NMe_2)_3(pyr^{2\text{-}CF_3\text{-}4C_6F_5})$ (**20**).

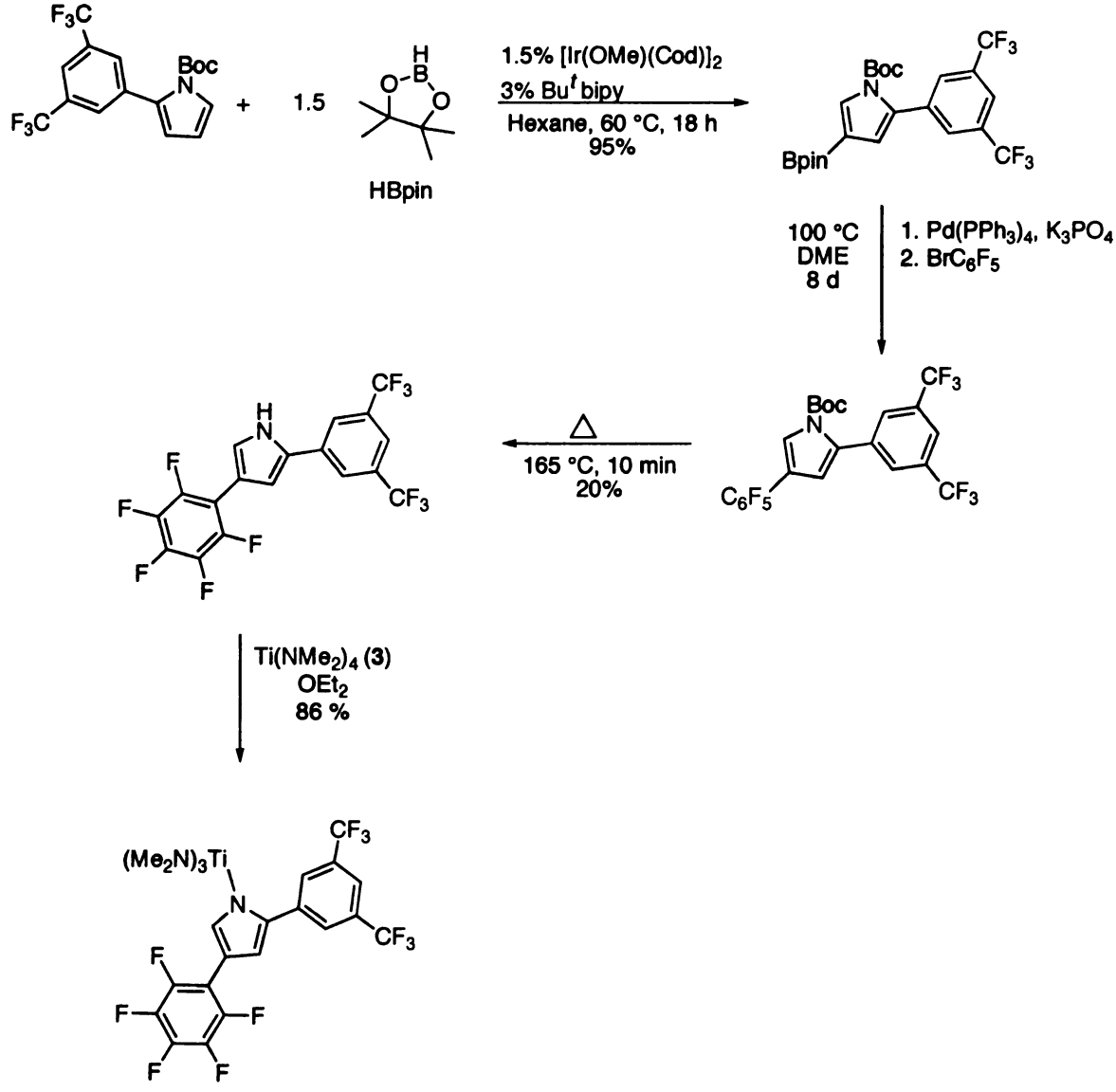

$Ti(NMe_2)_3(pyr^{2\text{-}CF3\text{-}4C6F5})$ (**20**)

Reacting 1 equivalent of $Hpyr^{2\text{-}CF3\text{-}4\text{-}C6F5}$ with $Ti(NMe_2)_4$ (**3**) generates $Ti(NMe_2)_3(pyr^{2\text{-}CF3\text{-}4C6F5})$ (**20**) in 86% yield. A structure of **20** is shown in Figure 3.2.

The synthesis of $Ti(NMe_2)_2(pyr^{2\text{-}CF3\text{-}4C6F5})_2$ would have been preferential, but reacting two equivalents of $Hpyr^{2\text{-}CF3\text{-}4C6F5}$ with $Ti(NMe_2)_4$ (**3**) produces only the

mono(pyrroyl) titanium complex. Attempts to prepare $Ti(NMe_2)_2(pyr^{2\text{-}CF3\text{-}4C6F5})_2$ by salt metathesis through the reaction of 2 equivalents of $Lipyr^{2\text{-}CF3\text{-}4C6F5}$ with $Ti(NMe_2)_2Cl_2$ yielded only the mono(pyrrolyl) complex as well.

Complex **20** is a very competent hydroamination catalyst carrying out the reaction of 1-phenylpropyne and aniline in less than 6 hours at 75 °C. Reintroducing sterics in the 2-position of the pyrrolyl in **20** proved advantageous in preparing a much more reactive catalyst compared to **19**.

Complex **20** was the first mono(pyrrolyl) titanium complex I had prepared and isolated since working with these pyrrolyl titanium complexes. I wanted to evaluate the hydroamination reactivity of **20** relative to $Ti(NMe_2)_2(pyr^{mes})_2$ (**13**), a bis(pyrrolyl) titanium catalyst from Chapter 2, as well as $Ti(indenyl)_2Me_2$ (**21**) which has been shown by Doye and co-workers to be a fairly general alkyne hydroamination catalyst, through kinetic studies.[6] The conditions for the kinetic study are shown in Scheme 3.5

Scheme 3.5 Conditions for kinetic study

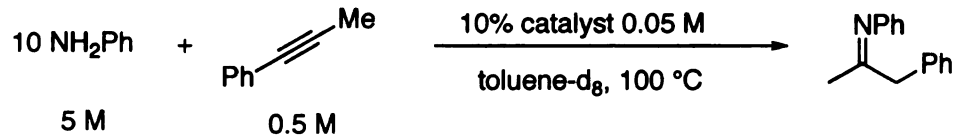

$$-\frac{d[\text{1-phenylpropyne}]}{dt} = k_{obs}t$$

Both **20** and $Ti(NMe_2)_2(pyr^{mes})_2$ (**13**) carry out the reaction of aniline and 1-phenylpropyne effectively at 75 °C. While $Ti(indenyl)_2Me_2$ (**21**) was active at 75 °C, the results were inconsistent at this temperature, which was apparently due to a catalyst activation period. Assuming that there was an activation problem, I incubated the catalyst

with the aniline portion at 100 °C prior to alkyne addition. However, this still did not result in good reproducibility of the kinetics under these conditions. Consequently, I ran the reactions with $Ti(indenyl)_2Me_2$ (**21**) at 100 °C, which afforded plots that reliably fit to first-order kinetics. The results of the kinetic study are shown in Table 3.1. The errors are at the 99% confidence limit and based off as least three repeated runs and range from as little as 7% to as much as 27%.

The results in Table 3.1 suggest that the pyrrolyl framework is quite effective relative to other catalyst architecture. Comparison of $Ti(indenyl)_2(Me)_2$ (**21**) with $Ti(NMe_2)_2(pyrr^{mes})_2$ (**13**) under identical conditions reveals that this pyrrolyl catalyst is about a factor of 4 times faster for these substrates. Complex **20** was significantly faster than $Ti(Indenyl)_2(Me)_2$ (**21**), which resulted in catalysis about 8 times faster, and was twice as fast as $Ti(NMe_2)_2(pyrr^{mes})$ (**13**).

Table 3.1 Comparison of $Ti(NMe_2)_2(pyr^{2\text{-}CF3\text{-}4C6F5})$ (**20**), $Ti(NMe_2)_2(pyr^{mes})_2$ (**13**), and $Ti(indenyl)_2Me_2$ (**21**).

Entry	Catalyst[a]	k_{obs} ($\times 10^{-7}$ s^{-1})
1	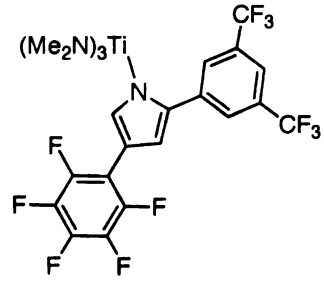 **20**	7366 ± 2002
2	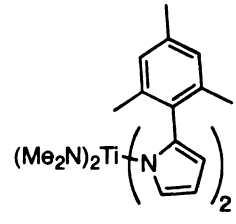 **13**	888 ± 61
3	$Ti(Indenyl)_2Me_2$ **21**	3888 ± 764

3.3 Conclusion

Using the seminal C–H activation/borylation work by Smith and co-workers followed by Suzuki coupling, two new 3-substituted pyrroles were synthesized as well as a 2,4-disubstituted pyrrole. Placing 3-Hpyrr$^{3,5\text{–}CF3}$ on titanium is readily accomplished by reaction with $Ti(NMe_2)_4$ (**3**). The decreased sterics of the 3-substituted pyrrole compared to the 2-substituted derivative results in an increased coordination number with retention of $HNMe_2$. However, subjecting $Ti(NMe_2)_2(pyrr^{3,5\text{–}CF3})_2(NHMe_2)$ (**19**) to the hydroamination of aniline and 1-phenylpropyne resulted in extremely slow catalysis.

The reaction of 2 equivalents of 3-Hpyrr^{C6F5} with $Ti(NMe_2)_4$ (**3**) does not yield the anticipated bis(pyrrolyl) complex. Variable temperature experiments on the orange solid from the reaction mixture suggest ligand exchange is occurring to give a mixture of titanium complexes that are relatively hydroamination inactive.

While the bis(3-arylpyrrolyl) titanium complex resulted in disappointing catalysis, fast hydroamination kinetics were achieved with $Ti(NMe_2)_3(pyrr^{2\text{-}CF3\text{-}4\text{-}C6F5})$ (**20**). The comparison of **20** relative to $Ti(NMe_2)_2(pyrr^{mes})_2$ (**13**) and Ti(indenyl)Me_2 (**21**) under identical reaction conditions shows that the **20** is significantly faster than the bis(pyrrolyl) complex **13** and the Cp-based system **21**. Whether the faster rates with **20** are due to electronic factors resulting from the different ligand architecture or steric constraints, or a combination of the two effects is currently unknown, which is subject of ongoing scrutiny.

The further optimization of these 3-aryl pyrroles towards the synthesis of more reactive titanium catalysts is addressed in the following chapter.

3.4 Experimental

General Considerations: All manipulations of air sensitive compounds were carried out in an MBraun drybox under a purified nitrogen atmosphere. Anhydrous ether was purchased from Columbus Chemical Industries Inc. Pentane and toluene were purchased from Spectrum Chemical Mfg. Corp. These were purified by sparging with dry N_2, then dried by running through activated alumina systems purchased from Solv-Tek. Hexanes and ethyl acetate were purchased from Mallinckodt Baker Inc. Pinacolborane was purchased from BASF and was used as received. N-Boc-pyrrole was vacuum distilled and stored under a purified nitrogen atmosphere over molecular sieves. Di-*tert*-butyl-dicarbonate (Boc anhydride) was purchased from Oakwood Chemical and was used as received. Aniline was purchased from Matheson Coleman and Bell Mfg. and was distilled twice from calcium hydride under vacuum. 1-phenylpropyne was purchased from GFS Chemical, distilled under vacuum, and then passed over two columns of neutral alumina. $Ti(NMe_2)_4$,[7] 2-[3,5-bis(trifluoromethyl)phenyl]-1H-pyrrole ($Hpyrr^{3,5\text{-}CF3}$),[9] and $Ti(indenyl)_2(Me)_2$[10] were synthesized according to literature methods. Deuterated solvents were dried over purple sodium benzophenone ketyl (C_6D_6) or phosphoric anhydride ($CDCl_3$) then distilled under a nitrogen atmosphere. Deuterated toluene was dried by passing it through two columns of neutral alumina. ^1H and ^{13}C spectra were recorded on Inova-300 or VXR-500 spectrometers. All spectra were referenced internally to residual protiosolvent (^1H) or solvent (^{13}C) resonances.

General Considerations for X-Ray Diffraction. Crystals grown from concentrated solutions at –35 °C quickly were moved from a scintillation vial to a microscope slide containing Paratone N. Samples were selected and mounted on a glass fiber in wax and

Paratone. The data collections were carried out at a sample temperature of 173 K on a Bruker AXS platform three-circle goniometer with a CCD detector. The data were processed and reduced utilizing the program SAINTPLUS supplied by Bruker AXS. The structures were solved by direct methods (SHELXTL v5.1, Bruker AXS) in conjunction with standard difference Fourier techniques.

General Procedure for Kinetics. All manipulations were done in an inert atmosphere drybox. In a 2 mL volumetric flask was loaded the catalyst (10 mol %, 0.1 mmol), aniline (0.931 g, 911 μL, 10 mmol), 1-phenylpropyne (0.116 g, 125 μL, 1 mmol), and ferrocene (0.056 g, 0.3 mmol) as an internal standard. The solution was then diluted to 2 mL with deuterated toluene. An ample amount of solution (~0.75 mL) was put into a threaded J. Young tube that was sealed with a cap and then wrapped with Teflon tape. The tube was then removed from the drybox and heated at 75 or 100 °C in the NMR spectrometer. The relative 1-phenylpropyne versus ferrocene concentration was monitored as a function of time. The fits are to the exponential decay of the starting material using the scientific graphing programs Origin or KaleidaGraph. The exact expression used to fit the data was $Y_t = Y_\infty + (Y_0 - Y_\infty)\ \exp^{-k_{obs}t}$ where Y = [1-phenylpropyne] at time = t (Y_t), infinity (Y_∞), or initial (Y_0).[8] The variables Y_∞, Y_0, and k_{obs} were optimized in the fits.

Synthesis of 3-(3,5-bis(trifluoromethyl)phenyl)-1*H*-pyrrole (3-Hpyrr$^{3,5-CF3}$)

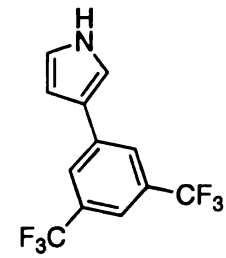

Under an atmosphere of dry N_2, tetrakis(triphenylphosphine)palladium (0.817 g, 0.07 mmol) was loaded into a 20 mL scintillation vial in DME (5 mL). To the same vial was added 3,5-bis(trifluoromethyl)bromobenzene (4 g, 13.69 mmol), and the two were stirred 10 min before being transferred to a Schlenk tube. To the Schlenk tube was added 3-(pinacolboryl)-N-*Boc*-pyrrole (3.9 g, 13.31 mmol) in DME (10 mL). Finally, K_3PO_4 (5.31 g, 19.97 mmol) was added. The tube was capped, taken out the dry box, and connected to a Schlenk line. The headspace of the Schlenk tube was removed, and the vessel was placed in a 100 °C oil bath for 24 h. When the reaction was complete as judged by GC-FID, the solution was transferred to a separatory funnel. The tube was rinsed with OEt_2 (30 mL) and H_2O (30 mL). The solution was extracted with OEt_2 (2 × 50 mL). The combined organic layers were collected and dried over $MgSO_4$. The solution was filtered and volatiles were removed in vacuo to yield a viscous oil. The oil was then transferred to a threaded Schlenk tube equipped with a stirbar. Then it was placed under a continuous flow of N_2. The reaction vessel was heated in an oil bath at 170 °C with stirring for ~ 20 min. The black solution was then run through a plug of silica gel with methylene chloride (500 mL). The volatiles were removed in vacuo to yield a white solid (2.81 g, 76%). M.p. 106-109 °C ^{1}H NMR ($CDCl_3$, 500 MHz): 8.37 (br s, 1 H), 7.90 (s, 2 H), 7.65 (s, 1 H), 7.18 (m, 1 H), 6.87 (q, 1 H), 6.58 (m, 1 H). ^{13}C {^{1}H}

NMR ($CDCl_3$, 125 MHz): 138.04, 131.81 (q, J_{CF} = 31.51 Hz), 124.85 (dd), 123.77 (q, J_{CF} = 277.72 Hz), 122.53, 119.78, 118.77 (sept., J_{CF} = 4.63 Hz), 115.74, 106.63. Anal. (Found) Calcd: C, (51.63) 51.29; H, (2.53) 2.33; N, (5.02) 5.03.

Synthesis of 3-(perfluorophenyl)-1*H*-pyrrole

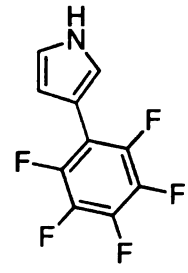

Under an atmosphere of dry N_2, tetrakis(triphenylphosphine)palladium (0.107 g, 0.092 mmol) was loaded into a 20 mL scintillation vial in DME (5 mL). To the same vial was added pentafluorobromobenzene (2.2 g, 8.9 mmol), and the two were stirred 10 min before being transferred to a Schlenk tube. To the tube was added 3-(pinacolboryl)-N-*Boc*-pyrrole (2.63 g, 8.98 mmol) in DME (10 mL). Finally, K_3PO_4 (3.58 g, 13.46 mmol) was added. The tube was capped, taken out the dry box, and connected to a Schlenk line. The headspace was removed, and the vessel was placed in a 100 °C oil bath for 8 d. When the reaction was complete as judged by GC-FID, the tube was rinsed with OEt_2 (30 mL) and H_2O (30 mL). The solution was transferred to a separatory funnel and extracted with OEt_2 (2 × 50 mL). The combined organic layers were collected and dried over $MgSO_4$. The solution was then filtered and the volatiles removed in vacuo to yield a viscous oil. The oil was then transferred to a threaded Schlenk tube equipped with a stirbar. Then it was placed under a continuous flow of N_2. The reaction vessel was heated in an oil bath at 170 °C with stirring for ~ 20 min. The black solution was then run through a plug of silica gel with methylene chloride (500 mL). The volatiles were removed in vacuo to yield a white solid (1.1 g, 53%). M.p 48-51 °C. ^1H NMR ($CDCl_3$, 500 MHz): 8.46 (s, 1 H), 7.29 (s, 1 H), 6.89 (app s, 1H), 6.68 (app s, 1 H). ^{13}C {^1H} NMR ($CDCl_3$, 125 MHz) δ 145.10-144.08 (m), 143.05-142.98 (m), 139.41-139.29 (m),

138.99-138.88 (m), 137.41-137.29 (m), 137.18-36.93 (m), 119.48 (t, J_{CF} = 6.81 Hz), 118.43, 111.23-110.01 (m), 109.34 (t, J_{CF} = 5.98 Hz). Anal. (Found) Calcd: C, (51.37) 51.52; H, (1.72) 1.73; N, (5.85) 6.01.

Synthesis of $Ti(NMe_2)_2(3\text{-}pyrr^{3,5\text{–}CF3})_2(NHMe_2)$ (19)

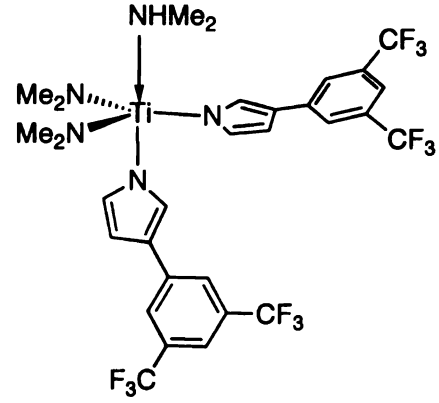

Under an atmosphere of dry N_2, 3-$Hpyr^{3,5\text{–}CF3}$ (0.283 g, 1.01 mmol) was loaded into a 20 mL scintillation vial in OEt_2 (3 mL). In a separate vial was loaded $Ti(NMe_2)_4$ (**3**) (0.113 g, 0.506 mmol) in OEt_2 (3 mL). The two vials were capped and put into a cold well, where they sat until frozen. 3-$Hpyrr^{3,5\text{–}CF3}$ was added to the vial containing **3** and the solution was allowed to warm to room temperature where it was left to stir for 6 h. After 6 h the solution was concentrated in vacuo to yield a red oil. The oil was then triturated with pentane to yield a red solid. The solid was crystallized from pentane to yield $Ti(NMe_2)_2(NHMe_2)(pyrr^{3,5\text{–}CF3})_2$ as a red solid (0.285 g). Due to probable isomerization of **19** in solution, the ^1H and ^{13}C spectra recorded were not consistent with the solid structure. See Appendix for ^1H and ^{13}C spectra for **19**.

Synthesis of 2-(bis(trifluoromethyl)phenyl)-4-pentafluorophenyl-pyrrole

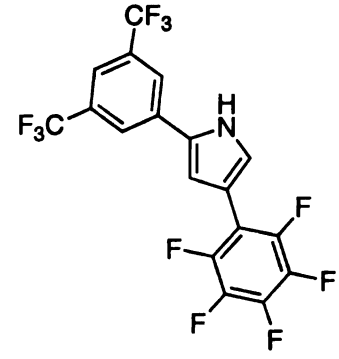

Under an atmosphere of dry N_2, $[Ir(OMe)(Cod)]_2$ (0.1g, 0.151 mmol) was loaded into a 20 mL scintillation vial with hexane (4 mL) and HBpin (1.92 g, 15 mmol) and stirred for 10 min prior to the addition of Bu^tbipy (0.081 g, 0.302 mmol) which was then stirred for another 10 min. To the same vial was added N-Boc-2-(3,5-(bistrifluoromethyl)phenyl)pyrrole (3.8 g, 10 mmol) in hexane (5 mL). The resulting reaction mixture was then transferred to a Schlenk tube, sealed, taken out of the dry box, and put in a 60 °C oil bath for 36 h. After the reaction was complete by GC-FID, the crude mixture was run through two plugs of silica gel with copious amounts methylene chloride. The volatiles were removed in vacuo to yield a clear oil. Trituration with pentane yielded and N-Boc-2-(3,5-(bistrifluoromethyl)phenyl)-4-pinacolboryl-pyrrole compound as a white solid. The product was used without any further purification. Under an atmosphere of dry N_2, a 20 mL scintillation vial was loaded with $Pd(PPh_3)_4$ (0.140 g, 0.120 mmol) in DME (5 mL), BrC_6F_5 (0.632 g., 2.57 mmol), and N-Boc-2-(3,5-(bistrifluoromethyl)phenyl)-4-pinacolboryl-pyrrole (1.18 g., 2.33 mmol). The solution was transferred to a Schlenk tube, sealed, removed from the dry box, and connected to a Schlenk line. Under a continuous flow of N_2, the cap was removed, K_3PO_4 was added to the vessel, and the vessel was quickly capped. The headspace in the Schlenk tube was

evacuated and the tube was heated in an oil bath at 100 °C for 8 d. After 8 d the reaction mixture was transferred to a separatory funnel. The tube was rinsed with H_2O (30 mL) and EtOAc (30 mL). The solution was extracted with EtOAc (3 × 30 mL). The combined organic layers were collected and dried over $MgSO_4$. The volatiles were removed in vacuo to yield a viscuous oil. The oil was transferred to a Schlenk tube and placed in a 165 °C oil bath for 10 min under a continuous flow of N_2. After 10 min the crude mixture was run through a plug of silica with methylene chloride (500 mL). The volatiles were removed in vacuo to yield a pale pink solid. Crystallization from pentane yielded the product as a pale pink solid (0.2, 19.2 %). M.p 146-149 °C. ^1H NMR (500 MHz, $CDCl_3$): 9.01 (br s, 1 H), 7.90 (s, 2 H), 7.72 (s, 1 H), 7.42 (s, 1 H), 7.06 (s, 1 H). ^{13}C $\{^1H\}$ NMR (125 MHz, $CDCl_3$): 133.75, 132.52 (q, J_{CF} = 33.9 Hz), 129.79, 123.18 (q, J_{CF} = 276 Hz), 123.8-123.58 (m), 122.12, 122.14-121.9 (m), 120.19-119.5 (m), 111.88, 110.9-110.05 (m), 109.1-108.85 (m). Anal. (Found) Calcd: C, (48.11) 48.56; H, (1.27) 1.36; N, (3.22) 3.15.

Synthesis of $Ti(NMe_2)_3(pyr^{2\text{-}CF3\text{-}4\text{-}C6F5})$ (20)

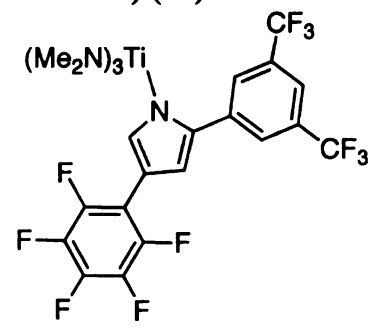

Under an atmosphere of dry N_2, $Ti(NMe_2)_4$ (**3**) (0.05 g, 0.223 mmol) was loaded into a 20 mL scintillation vial in OEt_2 (2 mL). In a separate vial was loaded 2-(3,5-(bistrifluoromethyl)phenyl)-4-pentafluoropheny pyrrole (0.1 g, 0.223 mmol) in OEt_2 (2 mL). The vials were placed in a cold well where that sat until frozen. While still cold, $Hpyrr^{2\text{-}CF3\text{-}4\text{-}C6F5}$ was added to the vial containing **3**. The solution was allowed to stir at room temperature for ~18 h. The following day the volatiles were removed in vacuo to yield a yellow solid. Crystallization from OEt_2/pentane yielded the title compound as a yellow solid (0.12 g 86%). M.p 76-79 °C. ^1H NMR (500 MHz, $CDCl_3$) 7.85 (2 H, s), 7.70 (1 H, s), 7.37 (1 H, s), 6.80 (1 H, s), 3.13 (18 H, s). ^{13}C $\{^1H\}$ NMR (125 MHz, $CDCl_3$): 145.1-144.80 (m), 142.98-142.5 (m), 138.45, 139.05-138.73 (m), 137.51- 136.97 (m), 131.46 (q, J_{CF} = 33 Hz), 131.47-131.25 (m), 126.88 (q, J_{CF} = 3.5 Hz), 126.75, 123.55 (q, J_{CF} = 273 Hz), 119.41-119.21 (m), 111.60-111.49 (m), 110.82-110.67 (m), 43.74. Anal. (Found) Calcd: C, (46.25) 46.17; H, (3.73) 3.71; N, (8.86) 8.97.

3.5 References

1. (a) Shi, Y.; Hall, C.; Ciszewski, J. T.; Cao, C.; Odom, A. L. *Chem. Commun.* **2003**, *5*, 586. (b) Cao, C.; Li, Y.; Shi, Y.; Odom, A.L. *Chem. Commun*, **2004**, *17*, 2002. For some recent reviews on hydroamination see: (a) Odom, A. L. Dalton Trans. **2005**, 225. (b) Muller, T. E.; Hultzsch, K. C.; Yus, M.; Foubelo, F.; Tada, M. *Chem Rev.*, **2008**, *108*, 3795.

2. Cao, C.; Shi, Y.; Odom, A. L. *J. Am. Chem. Soc.* **2003**, *125*, 2880.

3. Banerjee, S.; Barnea, E.; Odom, A. L. *Organometallics*, **2008**, *27*, 1005.

4. Swartz II, D. L.; Odom. A. L. *Organometallics*, **2006**, *25*, 6125.

5. For some additional reports on iridium catalyzed borylation/coupling reactions see. (a) Paul, S.; Chotana, G. A.; Holmes, D.; Reichle, R. C.; Maleczka, R. E.; Smith III, M.R. *J. Am. Chem. Soc.* **2006**, *128*, 15552. (b) Holmes, D.; Chotana, G. A.; Maleczka, R. E.; Smith III, M. R. *Org. Lett.* **2006**, *8*, 1407. (c) Chotana, G. A.; Rak, M. A.; Smith III, M. R. *J. Am. Chem. Soc.* **2005**, *127*, 10539. (d) Boebel, T.A.; Hartwig, J. F. *Organometallics*, **2008**, *27*, 6013. (e) Ishiyama, T.; Takagi, J.; Ishida, K.; Miyaura, N.; Anastasi, N. R.; Hartwig, J. F. *J. Am. Chem. Soc.*, **2002**, *124*, 390.

6. Heutling, A.; Pohlki, F.; Doye, S. *Chem. Eur. J.* **2004**, *10*, 3059.

7. Bradley, D. C.; Thomas, I. M. *J. Chem. Soc.* **1960**, 3859.

8. Espenson, J. H. *Chemical Kinetics and Reaction Mechanisms*; McGraw-Hill: New York, 1995.

9. Rieth, R. D.; Mankad, N. P.; Calimano, E.; Sadighi, J. P. *Org. Lett.* **2004**, *6*, 3981.

10. Balboni, D.; Camurati, I.; Prini, G.; Resconi, L. *Inorg. Chem.* **2001**, *40*, 6588.

CHAPTER 4

Synthesis, structure, and hydroamination kinetics of 3,3'-diaryldipyrrolylmethane titanium complexes

4.1 Introduction

Dipyrrolylmethane ligands on titanium are effective catalysts for the hydroamination of primary amines and alkynes as well as iminoamination.[1] The fastest hydroamination catalyst in the literature as of 2008 was $Ti(NMe_2)_2$(dpm) (**9**), where dpm is 5,5-dimethyldipyrrolylmethane (Figure 4.1).[2] The previous chapters have discussed the approaches taken to alter the dpm framework to improve catalyst reactivity with hopes of generating more reactive catalysts and applying them to multi-component coupling reactions. However, every attempt to prepare a catalyst more active than **9** has been unsuccessful.

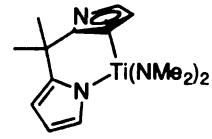

$Ti(NMe_2)_2$(dpm) (**9**)

Figure 4.1 Solid-state structure of $Ti(NMe_2)_2$(dpm) (**9**).

Putting sterics on the 2-position of the dpm framework results in decreased hydroamination reactivity, which is attributed to steric inhibition near the substrate binding site.[2] In the same report, it was shown experimentally with bis(pyrrolyl) titanium catalysts, that the hydroamination reactivity increases with electron-withdrawing substituents. Moving sterics from the 2-position to the 3-position on the dpm framework could result in faster catalysis than $Ti(NMe_2)_2$(dpm) (**9**). This chapter discusses the synthesis, structure, and hydroamination kinetics of 3,3'-diaryldipyrrolylmethane titanium complexes.

4.2 Results and discussions

The synthesis of 3-arylpyrrole complexes is greatly enabled by contributions from Smith and co-workers who demonstrated the selective generation of 3-(pinacolboryl)-N-Boc-pyrrole, which can then be coupled with aryl halides using a palladium catalyst. (Scheme 4.1).[3]

Scheme 4.1 Synthesis of 3-aryl pyrroles.

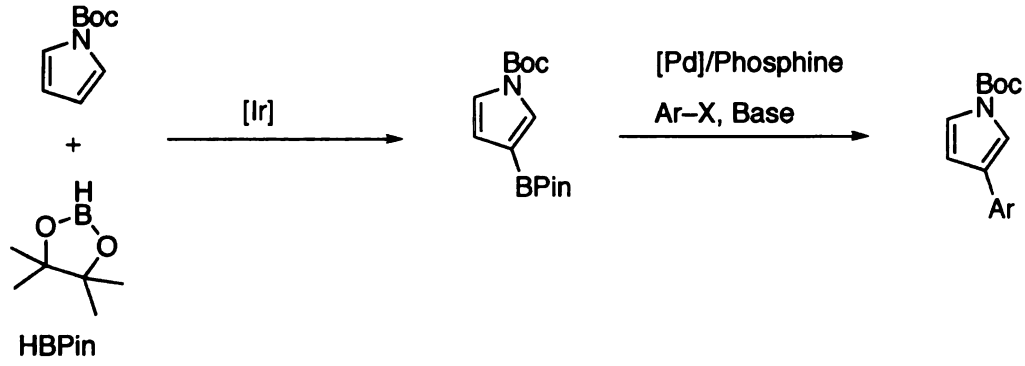

Using this synthetic procedure I prepared 3-(3,5-(CF_3)-C_6H_3) pyrrole (3-$Hpyrr^{3,5-CF3}$) and 3-(2,4,6-$(F)_3$-C_6H_2) pyrroles (3-$Hpyrr^{C6F3}$) to use as starting materials for 3-substituted dpm derivatives. The decision to use these two pyrroles was driven by a few initial results. First, it was shown experimentally that electron-withdrawing substituents on pyrrolyl ligands increase hydroamination catalysis rates. Therefore, the ligands should be electron deficient. Second, a comparison of $Ti(NMe_2)_2(pyrr^{3,5-CF3})$ (**14**), which has two CF_3 groups in the *meta* positions of the arene, and $Ti(NMe_2)_2(pyrr^{4-CF3})_2$ (**16**), which has one CF_3 group in the *para* position on the arene, had similar catalysis rates (Table 4.1). For that reason, I wanted to see what effect placing electron-withdrawing groups at the *ortho* and *para* positions had on the catalysis activity.

Table 4.1 Comparison of hydroamination catalysis rate constants $Ti(NMe_2)_2(pyrr^{3,5-CF3})_2$ (**14**) and $Ti(NMe_2)_2(pyrr^{4-CF3})_2$ (**16**) from Chapter 2. The reaction conditions are shown in Scheme 4.4. Rates are at the 99% confidence level with at least 3 repeated runs.

Entry	Catalyst	k_{obs} ($\times 10^{-7}$ s^{-1})
1	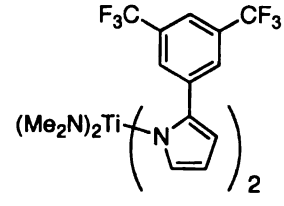 **14**	1275 ± 72
2	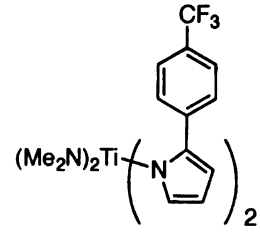 **16**	1255 ± 145

The usual procedure for the synthesis of 2,2'-diaryldipyrrolylmethanes involves the neat reaction of 2-aryl pyrroles in excess acetone with a catalytic amount of trifluoroacetic acid (TFA). However, using these reaction conditions with 3-aryl pyrroles did not yield the corresponding 3,3'-diaryldipyrrolylmethane derivatives. Switching to a Lewis acid, $InCl_3$, catalyzes the reaction of 3-aryl pyrroles and acetone to yield two new 3,3'-diaryldipyrrolylmethanes, $3\text{-}H_2dpm^{3,5-CF3}$ and $3\text{-}H_2dpm^{C6F3}$ in 76% and 14% isolated yields. These complexes react with $Ti(NMe_2)_4$ (**3**) to yield two new titanium

precatalysts, $Ti(NMe_2)_2(NHMe_2)(dpm^{3,5\text{–}CF3})$ (**22**) and $Ti(NMe_2)_2(NHMe_2)(dpm^{C6F3})$ (**23**) in 92% and 86% crystallized yields (Scheme 4.2).

Scheme 4.2 Synthesis of $3\text{-}H_2dpm^{3,5\text{–}CF3}$, $3\text{-}H_2dpm^{C6F3}$, $Ti(NMe_2)_2(NHMe_2)(dpm^{3,5\text{–}CF3})$ (**22**) and $Ti(NMe_2)_2(NHMe_2)(dpm^{C6F3})$ (**23**).

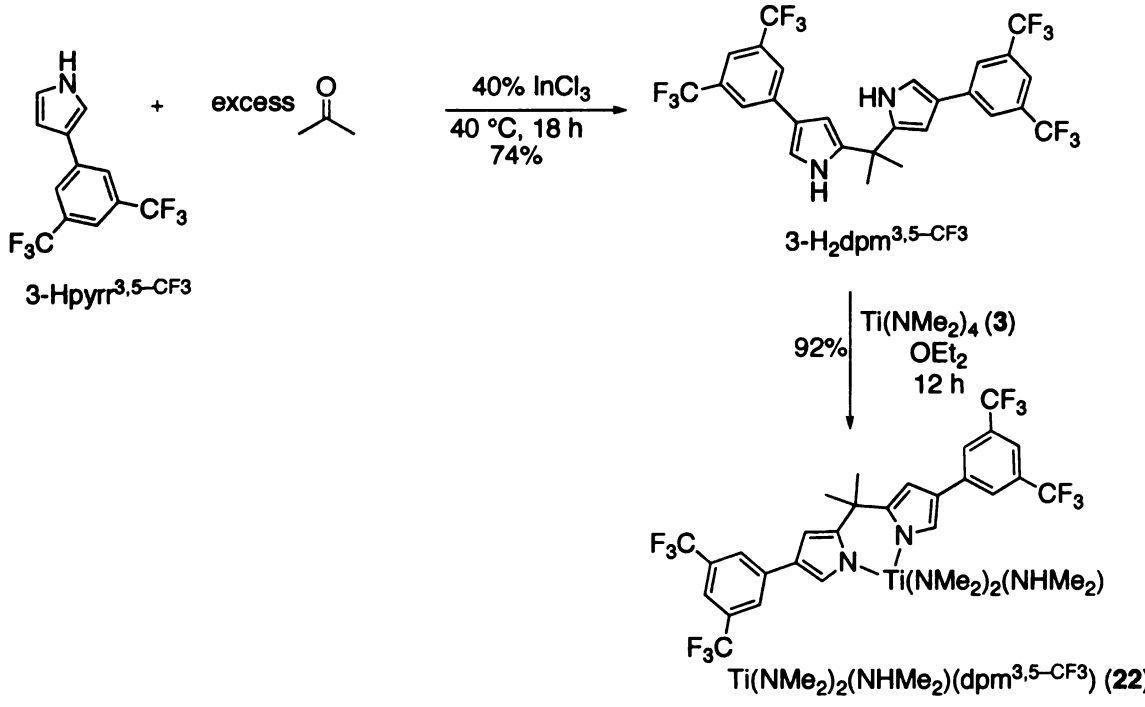

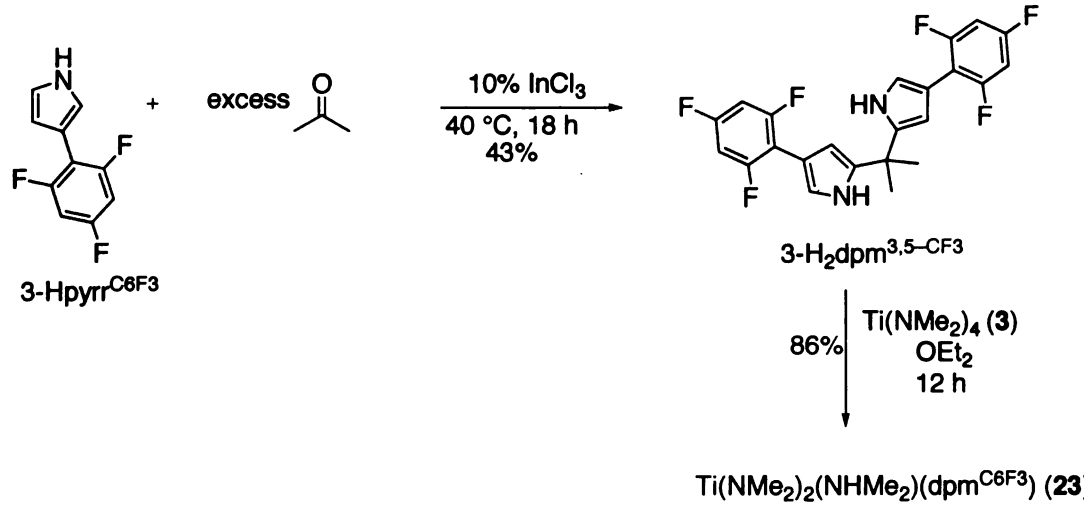

The solid-state structure of **22** has a pseudo trigonal bipyramidal (tbp) geometry with the pyrrolyls η^1,η^1-bound. The ^{1}H NMR spectrum is consistent with the solid-state structure showing equivalent pyrrolyls. There is a broad singlet at 2.61 ppm in the ^{1}H spectrum that integrates to 6 hydrogens, which are assigned to the methyl groups on dimethylamine. As expected, the longest Ti-N bond length is for the dimethylamine ligand at 2.135(17) Å, which sits in the equatorial plane.

Attempts to grow X-ray quality crystals of **23** are currently underway. The ^{1}H NMR spectrum of **23** is similar to **22,** showing equivalent pyrrolyls and a broad singlet at 2.49 ppm corresponding to 6 hydrogens, which are assigned to the methyl groups on a coordinated dimethylamine.

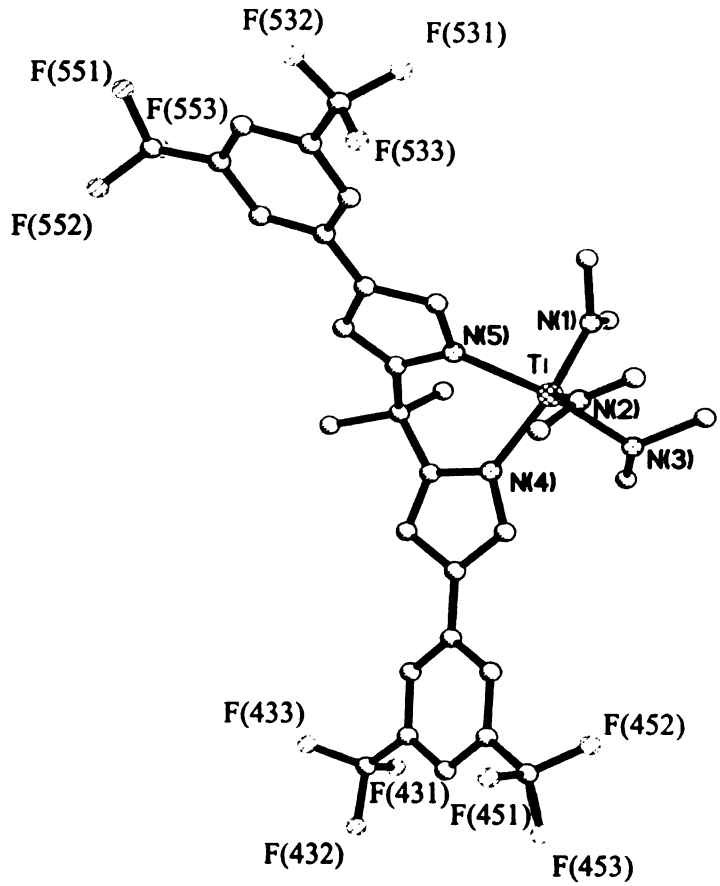

Figure 4.2 Solid-state structure of $Ti(NMe_2)_2(NHMe_2)(3\text{-}dpm^{3,5\text{-}CF3})$ (**22**) from single crystal X-ray diffraction. Selected bond distances (Å) and bond angles (deg): Ti-N(1) 1.931(18), Ti-N(2) 1.826(13), Ti-N(3) 2.135(17), Ti-N(4) 2.051(9), Ti-N(5) 2.067(9), N(1)-Ti-N(2) 109.6(9) N(2)-Ti-N(3) 97.7(7), N(3)-Ti-N(4) 84.8(5), N(4)-Ti-N(5) 82.3(4), N(2)-Ti-N(4) 108.8(6), N(2)-Ti-N(5) 102.8(5), N(3)-Ti-N(5) 158.4(6), N(1)-Ti-N(3) 87.2(7), N(1)-Ti-N(4) 141.4(8), N(1)-Ti-N(5) 92.2(6).

To test the kinetic ability of these catalysts compared to $Ti(NMe_2)_2(dpm)$ (**9**), precatalysts **22** and **23** were tested under the kinetic conditions reported in Chapter 2 (Scheme 4.3).[2] In addition to running the reactions at 75 °C in toluene-d_8 in the NMR probe, they were also run at 75 °C in a reaction calorimeter.[4,5] The disappearance of the

1-phenylpropyne starting material versus time was used to fit the first-order equations as measured by ^{1}H NMR spectroscopy. Alternatively, integrated heat flow versus time, *t*, divided by the total heat of reaction would be used to give the percent conversion, which also fit well to first order equations.[6] The methods were consistent with each other, producing the same rate for each catalyst. The results of the kinetic studies on compounds **9**, **22**, and **23** are shown in Table 4.2. The errors are based of at least three repeated runs and are at the 99% confidence level. The errors varied from as little as 7% to as much as 10%.

Scheme 4.3 Reaction conditions for kinetic study

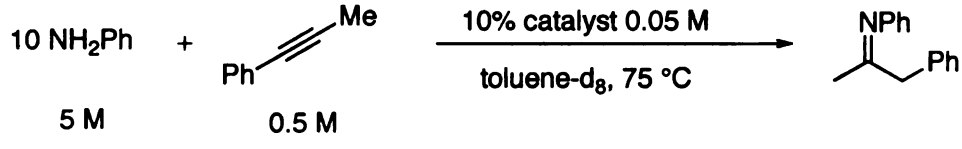

$$-\frac{d[\text{1-phenylpropyne}]}{dt} = k_{obs}t$$

From the data in Table 4.2, 3-aryl substitution on the dpm results in an increase in rate constant by a factor of about 3.5. As anticipated, adding electron-withdrawing groups without increasing steric congestion around the metal results in catalysis faster than $Ti(NMe_2)_2$(dpm) (**9**). The reaction of aniline and 1-phenylpropyne is smoothly catalyzed by **22** and **23** in ~1 h with rate constants of (6963 ± 582) and (6225 ± 614) × 10^{-7} s^{-1}.

Table 4.2. Representative catalysis rates for $Ti(NMe_2)_2(dpm)$ (**9**), $Ti(NMe_2)_2(NHMe_2)(3\text{-}dpm^{3,5\text{–}CF3})$ (**22**) and $Ti(NMe_2)_2(NHMe_2)(3\text{-}dpm^{C6F3})$ (**23**).

Entry	Catalyst	k_{obs} ($\times 10^{-7}$ s^{-1})[a]
1	$Ti(NMe_2)_2(dpm)$ **9**	1976 ± 130
2	$Ti(NMe_2)_2(NHMe_2)(3\text{-}dpm^{3,5\text{–}CF3})$ **22**	6963 ± 582
3	$Ti(NMe_2)_2(NHMe_2)(3\text{-}dpm^{C6F3})$ **23**	6225 ± 614

[a] Errors are based at 99% confidence level with at least 3 repeated runs.

4.3 Conclusions

Using readily prepared 3-substituted pyrroles, a route to 3,3'-diaryldipyrrolylmethanes has been developed where the synthesized pyrroles can be used as the limiting reagent in condensation with acetone. Placing these new ligands on titanium is readily accomplished by reaction with $Ti(NMe_2)_4$ (**3**), and the resulting complexes show η^1,η^1-coordination of the dipyrrolylmethane in the solid-state. The increased electrophilic nature of the metal center allows for dimethylamine retention.

Catalysis with these new complexes was faster than the dpm parent complex **9**, suggesting that electron-withdrawing groups increase hydroamination reactivity. However, strategic positioning of the electron-withdrawing groups did not result in a significant difference in catalysis rate, which can be attributed to the choice of electron-withdrawing substiuents. While CF_3 and F are good σ-withdrawing groups, it is possible for F to be a π-donor negating some of the electron-withdrawing ability. Investigations are currently underway with using just CF_3 substitution in *ortho/para* positions on the arene to see if there is a significant difference in catalysis rate.

4.4 Experimental

General Considerations: All manipulations of air sensitive compounds were carried out in an MBraun drybox under a purified nitrogen atmosphere. Anhydrous ether was purchased from Columbus Chemical Industries Inc. Pentane and toluene were purchased from Spectrum Chemical Mfg. Corp., were purified by sparging with dry N_2, then dried by running through activated alumina systems purchased from Solv-Tek. Hexanes and ethyl acetate were purchased from Mallinckodt Baker Inc. Pinacolborane was purchased from BASF and was used as received. 1-bromo-3,5-bis(trifluoromethyl)benzene and 2-bromo-1,3,5-trifluorobenzene were purchased from Matrix Scientific and dried by passed over a column of neutral alumina. N-Boc-pyrrole was purchased from Aldrich, vacuum distilled, and stored under a purified nitrogen atmosphere over molecular sieves. Aniline was purchased from Matheson Coleman and Bell Mfg. and was distilled twice from calcium hydride under vacuum. 1-phenylpropyne was purchased from GFS Chemical, distilled under vacuum, and then passed over two columns neutral alumina. $Ti(NMe_2)_4$,[7] was synthesized according to the literature procedure. Deuterated solvents were dried over purple sodium benzophenone ketyl (C_6D_6) or phosphoric anhydride ($CDCl_3$) then distilled under a nitrogen atmosphere. Deuterated toluene was dried by passing it through two columns of neutral alumina. ^1H and ^{13}C spectra were recorded on Inova-300 or VXR-500 spectrometers. All spectra were referenced internally to residual protiosolvent (^1H) or solvent (^{13}C) resonances.

General Considerations for X-ray Crystallography: Crystals grown from concentrated solutions in pentane at –35 °C were moved quickly from a scintillation vial to a microscope slide containing Paratone N. Samples were selected and mounted on a

glass fiber in wax and Paratone. The data collections were carried out at a sample temperature of 173 K on a Bruker AXS platform three-circle goniometer with a CCD detector. The data were processed and reduced utilizing the program SAINTPLUS supplied by Bruker AXS. The structures were solved by direct methods (SHELXTL v5.1, Bruker AXS) in conjunction with standard difference Fourier techniques.

General Considerations for Kinetics: All manipulations were done in an inert atmosphere drybox. In a 2 mL volumetric flask was loaded the catalyst (10 mol%, 0.1 mmol), aniline (0.931 g, 911 μL, 10 mmol), 1-phenylpropyne (0.116 g, 125 μL, 1 mmol), and ferrocene (0.056 g, 0.3 mmol) as an internal standard. The solution was then diluted to 2 mL with deuterated toluene. An ample amount of solution (~0.75 mL) was put into a threaded J. Young tube that was sealed with a cap and then wrapped with Teflon tape. The tube was then removed from the drybox and heated at 75 °C in the NMR spectrometer. The relative 1-phenylpropyne versus ferrocene concentration was monitored as a function of time.

For kinetics by reaction calorimetry, the same amounts of reagents were used. The solution was added to the reaction vial and sealed with a Teflon cap minus 1-phenylpropyne. The vial was taken out of the dry box and put in the calorimeter at 75 °C. Once the solution had reached 75 °C, the alkyne was added via syringe. The progress of the reaction was monitored by heat as a function of time, and the kinetic rates were verified by ^{1}H NMR spectroscopy.

The fits are to the exponential decay of the starting material or exponential growth of the heat using the scientific graphing programs Origin or KaleidaGraph. The exact expression used to fit the data was $Y_t = Y_\infty + (Y_0 - Y_\infty)\exp^{-k_{obs}t}$ where Y = [1-

phenylpropyne] at time = t (Y_t), infinity (Y_∞), or at the start of the reaction (Y_0).[8] The variables Y_∞, Y_0, and k_{obs} were optimized in the fits.

Synthesis of 3-(3,5-bistrifluromethylphenyl-1*H*-pyrrole) (3-Hpyrr$^{3,5-CF3}$)

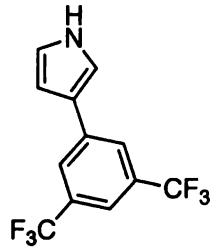

Under an atmosphere of dry N_2 an oven dried 250 mL Schlenk tube was loaded with a stirbar, $Pd(PPh_3)_4$ (0.536 g, 0.464 mmol) in DME (10 mL), 3,5-bis(trifluoromethyl)phenylbromobenzene (4.54 g, 15.5 mmol) and N-Boc-3-pinacolborylpyrrole (4.54 g, 15.5 mmol) in DME (20 mL). To that same vessel was added K_3PO_4 (6.16 g, 23.15 mmol). DME (7 mL) was used to wash the sides of the tube. The tube was then capped, removed from the drybox, and placed in an oil bath at 85 °C for 18 h. After the reaction was complete as judged by GC-FID, the reaction mixture was transferred to a separatory funnel with H_2O (100 mL). The aqueous layer was extracted and washed with ethyl acetate (3 × 75 mL). The combined organic layers were combined and dried with $MgSO_4$. The volatiles were removed in vacuo to yield a viscous brown oil. The oil was then transferred to that same 250 mL Schlenk tube with 1-butanol (35 mL) and K_3PO_4 (6 g, 23 mmol). The solution was then heated in an oil bath at 100 °C for 18 h. The resulting solution was then transferred to a separatory funnel with H_2O (75 mL) water. The aqueous layer was extracted and washed with ethyl acetate (3 × 75 mL). The combined organic layers were collected and dried with $MgSO_4$. The volatiles were removed in vacuo to yield a viscous brown oil. The product was then purified by column chromatography on basic alumina with an elution of hexanes:ethyl acetate (4:1) to yield the product as an off white solid. The product was purified further by sublimation to give

a bright white solid (2.7 g, 62.5 %). ^{1}H NMR ($CDCl_3$, 500 MHz): 8.37 (br s, 1 H), 7.90 (s, 2 H), 7.65 (s, 1 H), 7.18 (m, 1 H), 6.87 (q, 1 H), 6.58 (m, 1 H). ^{13}C {^{1}H} NMR ($CDCl_3$, 125 MHz): 138.04, 131.81 (q, J_{CF} = 31.51 Hz), 124.85 (dd), 123.77 (q, J_{CF} = 277.72 Hz), 122.53, 119.78, 118.77 (sep., J_{CF} = 4.63 Hz), 115.74, 106.63. Anal. (Found) Calcd: C, (51.63) 51.29; H, (2.53) 2.33; N, (5.02) 5.03.

Synthesis of 3-(2,4-bis(trifluoromethyl)phenyl)-1*H*-pyrrole ($Hpyr^{C8F6}$)

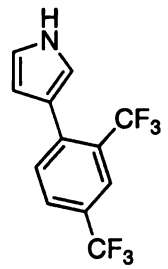

Under an atmosphere of dry N_2, a 200 mL Schlenk tube was loaded with 3-(pinacolboryl)-N-Boc-pyrrole (4.86 g, 16.5 mmol), K_3PO_4 (anhydrous) (3.51 g, 16.5 mmol), $Pd_2(dba)_3$ (0.216 g, 0.236 mmol) biphenyl-2-yldicyclohexylphosphine (0.165 g, 0.471 mmol) and a stirbar. The Schlenk tube was capped, removed from the drybox, and connected to a Schlenk line. The headspace was evacuated and back filled with N_2. The cap was removed quickly under a continuous flow of N_2 and replaced with a septum. A 60 mL syringe containing t-amyl alcohol (30 mL) and 1-bromo-2,4-bis(trifluoromethyl)benzene (3.46 g, 11.8 mmol) was inserted into the septum with the needle extending below the neck of the Schlenk tube, and the solution was added. The septum and needle were removed quickly, and the tube was sealed with a screwcap. The headspace was evacuated and filled with N_2. This procedure was repeated 6 times. The Schlenk tube was then placed in a 100 °C oil bath for 18 h. Once the reaction was complete as judged by GC-FID, K_3PO_4 (3 g, 14 mmol) and Bu^nOH (OH) were added. The reaction mixture was allowed to reflux for an additional 2 h at 100 °C. After the deprotection, the resulting solution was poured into a separatory funnel with H_2O (100 mL) and ethyl acetate (50 mL). The water layer was washed and extracted with ethyl acetate (3 × 75 mL). The combined organic layers were collected and dried over $MgSO_4$. The volatiles were removed in vacuo to give a viscous red oil. The product was then

purified by column chromatography on silica gel using an elutant of CH_2Cl_2:hexanes (7:3). This was followed by a second column on silica gel with hexanes:ethyl acetate (7:3) as elutants to give the product as a pale orange solid (2.6 g, 76%). M.p 27 - 30 °C ^{1}H NMR ($CDCl_3$, 500 MHz): 8.35 (br s, 1 H), 7.99 (s, 1 H), 7.75 (d, 1 H, J_{HH} = 8.14 Hz), 7.62 (d, 1 H, J_{HH} = 8.14 Hz), 7.00 (s, 1H), 6.87-6.85 (m, 1 H), 6.45 (app s, 1 H). ^{13}C {^{1}H} NMR ($CDCl_3$, 125 MHz): 140, 132.79, 128.28 (q, J_{CF} = 33 Hz), 128.34 (q, J_{CF} = 30 Hz), 128.14-128.05 (m), 123.87 (q, J_{CF} = 278 Hz), 123.77 (q, J_{CF} = 271 Hz), 123.66-123.49 (m), 120.93, 118.30, 117.91-117.83 (m), 109.88-109.83 (m). Anal. (Found) Calcd: C, (51.26) 51.63; H, (2.42) 2.53; N, (4.87) 5.02.

Synthesis of 3-(2,4,6-trifluorophenyl)-1*H*-pyrrole (3-Hpyrr^{C6F3})

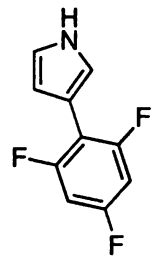

Under an atmosphere of dry N_2 a 200 mL Schlenk tube was loaded with 3-(pinacolboryl)-N-Boc-pyrrole (4.16 g, 14.2 mmol), K_3PO_4 (anhydrous) (2.81 g, 13.2 mmol), $Pd_2(dba)_3$ (0.156 g, 0.173 mmol), biphenyl-2-yldicyclohexylphosphine (0.119 g, 0.346 mmol) and a stirbar. The Schlenk tube was capped, removed from the drybox, and connected to a Schlenk line. The headspace was evacuated and back filled with N_2. The cap was removed quickly under a continuous flow of N_2 and replaced with a septum. A 60 mL syringe containing t-amyl alcohol (30 mL) and 2-bromo-1,3,5-trifluorobenzene (2 g, 9.5 mmol) was inserted into the septum with the needle extending below the neck of the Schlenk tube, and the solution was added. The septum and needle were removed quickly, and the tube was sealed with a screwcap. The headspace was evacuated and filled with N_2. This procedure was repeated 6 times. The Schlenk tube was then placed in a 100 °C oil bath for 18 h. Once the reaction was complete as judged by GC-FID, K_3PO_4 (2 g, 9.4 mmol) and Bu^{n}OH (8 mL) were added. The reaction mixture was refluxed for an additional 2 h at 100 °C. After the deprotection, the resulting solution was poured into a separatory funnel with H_2O (50 mL) and ethyl acetate (50 mL). The water layer was washed and extracted with ethyl acetate (3 × 75 mL). The combined organic layers were collected and dried over $MgSO_4$. The volatiles were removed in vacuo to give a viscous red oil. The flask containing the oil was connected to the Schlenk line and kept under

vacuum for 24 h. The product was then purified by column chromatography on silica gel using of CH_2Cl_2:hexanes (7:3) as elutants. A second column on silica gel with of hexanes:ethyl acetate (4:1) as elutants gave the product as an off white solid, (0.958 g, 52%). ^1H NMR ($CDCl_3$, 500 MHz): 8.38 (br s, 1 H), 7.28-7.27 (m, 1 H), 6.90-6.78 (m, 1 H), 6.77-6.71 (m, 3 H). ^{13}C {^1H} NMR ($CDCl_3$, 125 MHz): 161.14-160.65 (m), 159.16-158.69 (m), 118.74 (app t), 117.89, 110.76, 109.40 (app t), 100.54-100.09 (m). Anal. (Found) Calcd: C, (60.50) 60.92; H, (3.14) 3.07; N, (6.84) 7.10.

Synthesis of 5,5'-(propane-2,2-diyl)bis(3-(3,5-bis(trifluoromethyl)phenyl)-1*H*-pyrrole) (3-$H_2dpm^{3,5\text{-}CF3}$)

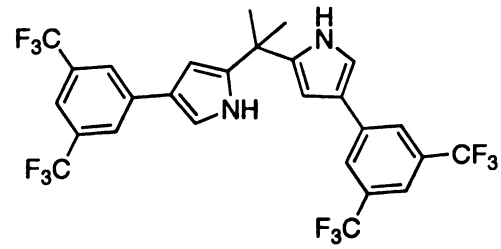

An oven dried pressure tube was loaded with 3-(3,5-bistrifluromethylphenyl-1*H*-pyrrole) (2.33 g, 8.35 mmol), acetone (13 mL, 10.27 g, 176 mmol), and a stirbar. To that tube was added $InCl_3$ (0.3 g, 1.3 mmol). The tube was then capped and placed in an oil bath at 40 °C for 24 h. Once the reaction was complete as judged by ^1H NMR spectroscopy, the solution was transferred to a 250 mL round bottom flask, and the volatiles were removed in vacuo. The resulting solid was put into a solution of hexanes:CH_2Cl_2 (7:3) (~35 mL). A column was made using hexanes:CH_2Cl_2 (7:3). Once the crude mixture was loaded onto the column, it was flashed with hexanes until spots appeared on the TLC plate. Once material started appearing on TLC the elutant was changed to hexanes:CH_2Cl_2 (7:3). Once the desired product appeared by TLC, the elutant was changed to just CH_2Cl_2 until all the product had been collected. The fractions were collected, and the volatiles were removed in vacuo to yield the product as a white solid, (1.9 g, 76 %) ^1H NMR ($CDCl_3$, 500 MHz): 8.03 (br s, 2 H), 7.87 (s, 4 H), 7.62 (s, 2 H), 7.06 (q, 2 H), 6.45 (q, 2 H), 1.74 (s, 6 H). ^{13}C {^1H} NMR ($CDCl_3$, 125 MHz): 140.67, 138.13, 132.09 (q, J_{CF} = 32.14 Hz), 124.88, 123.77 (q, J_{CF} = 272.73 Hz), 122.46, 118.99 (pent., J_{CF} = 4.11 Hz), 115.61, 102.73, 35.85, 29.19. Anal. (Found) Calcd: C, (53.88) 54.14; H, (3.31) 3.03; N, (4.51) 4.68.

Synthesis of 5,5'-(propane-2,2-diyl)bis(3-(2,4,6-trifluorophenyl)-1*H*-pyrrole) (3-H_2dpm^{C6F3})

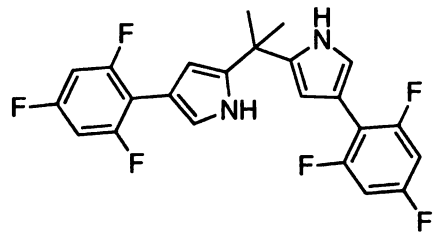

A threaded pressure tube was charged with $InCl_3$ (0.107 g, 0.0484 mmol), 3-(2,4,6-trifluorophenyl)-1*H*-pyrrole (0.952 g, 0.483 mmol), acetone (2.80 g, 3.55 mL, 4.83 mmol), and a stirbar. The tube was capped and placed in a 40 °C oil for 18 h. Once the reaction was complete as judged by ^1H NMR spectroscopy, the solution was transferred to a 100 mL round bottom flask, where the volatiles were removed in vacuo to yield a viscous orange oil. The product was purified by column chromatography on silica gel using hexanes:ethyl acetate (85:15) as elutants. The product was obtained as an off white solid, (0.450 g, 43 %). ^1H NMR (500 MHz, $CDCl_3$): 7.09 (s, 2H), 7.07-7.06 (m, 2 H), 6.75-6.65 (m, 4 H), 6.55-6.53 (m, 2 H). ^{13}C {^1H} NMR (125 MHz, $CDCl_3$): 161.12-160.67 (m), 159.12-158.72 (m), 138.68, 118.37 (t), 110.42, 110.05-109.83 (m), 105.12-105.01 (m), 100.63-100.15 (m), 35.35, 28.96. Anal. (Found) Calcd: C, (63.11) 63.60; H, (3.58) 3.31; N, (6.17) 6.48

Synthesis of $Ti(NMe_2)_2(NHMe_2)(3\text{-}dpm^{3,5\text{-}CF3})$ (22)

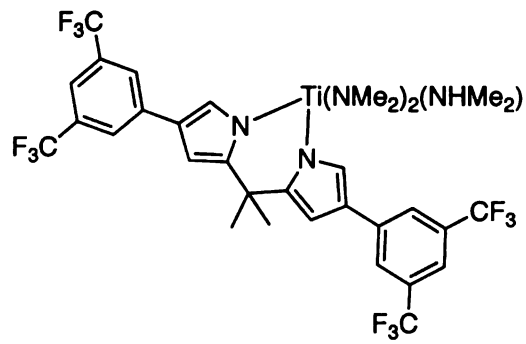

Under an atmosphere of purified N_2, a vial was loaded with $3\text{-}H_2dpm^{3,5\text{-}CF3}$ (0.503 g, 0.841 mmol) in OEt_2 (3 mL). A separate vial was loaded with $Ti(NMe_2)_4$ (**3**) (0.188 g, 0.840 mmol) in OEt_2 (3 mL). The two vials were placed in the cold well where they sat until frozen. To the thawing solution, $3\text{-}H_2dpm^{3,5\text{-}CF3}$ was added to the vial containing **3**. The solution was allowed to stir overnight. The next day, the volatiles were removed under reduced pressure to give a red oil. The oil was triturated with pentane thrice to give the product as a bright orange solid. The solid was crystallized from OEt_2/pentane to yield the title compound as an orange solid, (0.602 , 92%). ^1H NMR ($CDCl_3$, 500 MHz): 7.83 (s, 4 H), 7.53 (s, 2 H), 7.07 (s, 2 H), 6.40 (s, 2 H), 3.37 (s, 12 H), 2.61 (br s, 6 H), 1.72 (s, 6 H). ^{13}C $\{^1H\}$ NMR ($CDCl_3$, 125 MHz): 154.05 (m), 138.8, 131.5 (q, J_{CF} = 34 Hz), 124.4, 123.8 (q, J_{CF} = 270 Hz), 122.2, 121.8, 117.6, 100.9, 46.8, 40.5, 38.2, 31.1. Anal. (Found) Calcd: C, (50.75) 50.98; H, (4.89) 4.54; N, (9.04) 9.01.

Synthesis of $Ti(NMe_2)_2(NHMe_2)(3\text{-}dpm^{C6F3})$ (23)

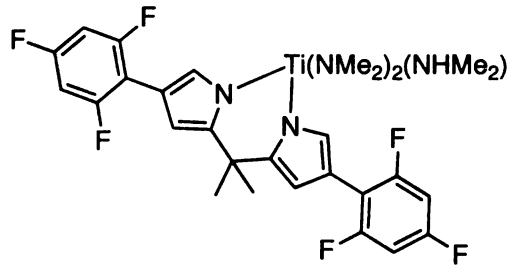

Under an atmosphere of purified N_2, a vial was loaded with $3\text{-}H_2dpm^{C6F3}$ (0.130 g, 0.3 mmol) in OEt_2 (3 mL). A separate vial was loaded with $Ti(NMe_2)_4$ (**3**) (0.067 g, 0. mmol) in OEt_2 (3 mL). The two vials were placed in the cold well, where they sat until frozen. To the thawing solution, $3\text{-}H_2dpm^{C6F3}$ was added to the vial containing **3**. The solution was allowed to stir overnight. The next day the volatiles were removed under reduced pressure to give a red oil. The oil was triturated with pentane twice to give the product as a bright orange solid. The solid was crystallized from OEt_2/pentane to yield the title compound as an orange solid, (0.157 g, 86%). M.p 110-112 °C. ^1H NMR ($CDCl_3$, 500 MHz): 7.32 (s, 2 H), 6.72-6.64 (m, 6 H), 6.63 (s, 2 H), 3.24 (s, 12 H), 2.49 (br s, 6 H), 1.73 (s, 6 H).

4.5 References

1. (a) Shi, Y.; Hall, C.; Ciszewski, J. T.; Cao, C.; Odom, A. L. *Chem. Commun.* **2003**, 586. (b) Ramanathan, B.; Keith, A.J.; D. Armstrong D.; Odom, A.L. *Org. Lett.*, **2004**, *6*, 2957. (c) Majumder, S.: Odom, A.L.; *manuscripts in preparation.*

2. Swartz, D.L.; Odom, A.L. *Organometallics*, **2006**, *26*, 6125.

3. (a) Tse M.K.; Cho, J-Y.; and Smith, III M.R. *Org. Lett.*, **2001**, *3*, 2831. (b) Paul, S.; Chotana, G.A.; Holmes, D.; Reichle, R.C.; Maleczka, R.E.; Smith III, M.R. *J. Am. Chem. Soc.* **2006**, *128*, 15552.

4. For a nice review on kinetics obtained using reaction calorimetry see. Blackmond, D. G. *Angew. Chem., Int. Ed.* **2005**, *44*, 4302.

5. For some additional reports on reaction calorimetry used in catalysis see. (a) Antonio Jinu C. F.; Mathew, J. S.; Blackmond, D. G.; *Ind. Eng. Chem. Res.*, **2007**, *46*, 8584. (b) Mathew, J. S.; Klussmann, M.; Iwamura, H.; Valera, F.; Futran, A.; Emanuelsson, E.A.C.; Blackmond, D. G.; *J. Org. Chem.*, **2006**, *71*, 4711. (c) Blackmond, D. G.; Ropic, M.; Stefinovic, M. *Org. Process Res. Dev.*, **2006**, *10*, 457. (d) Shekhar, S.; Ryberg, P.; Hartwig, J. F.; Mathew, J. S.; Blackmond, D. G.; Strieter, E. R.; Buchwald, S. L. *J. Am. Chem. Soc.*, **2006**, *128*, 3584.

6. Blackmond, D.G.; Rosner, T.; Pfaltz, A. *Org. Process Res. Dev.*, **1999**, *3*, 275.

7. Bradley, D.C.; Thomas, I.M.; J. Chem. Soc., **1960**, 3859.

8. Espenson, J. H. *Chemical Kinetics and Reaction Mechanisms*; McGraw-Hill: New York, 1995.

CHAPTER 5

Effects of 5,5-substitution on dipyrrolylmethane ligand isomerization

5.1 Introduction

Dipyrrolylmethane ligands on titanium provide catalysts capable of extremely fast hydroamination of alkynes with primary amines[1,2] and very efficient catalysts for iminoamination.[3] One of the most commonly employed dipyrrolylmethane derivatives is prepared from acetone and pyrrole in the presence of trifluoroacetic acid.[4] The product 5,5-dimethyldipyrrolylmethane (H_2dpm) can be placed on titanium by transamination with $Ti(NMe_2)_4$ (**3**) to provide $Ti(NMe_2)_2$(dpm) (**9**) (Scheme 5.1).[1,2]

Scheme 5.1 Synthesis of H_2dpm and $Ti(NMe_2)_2$(dpm) (**9**).

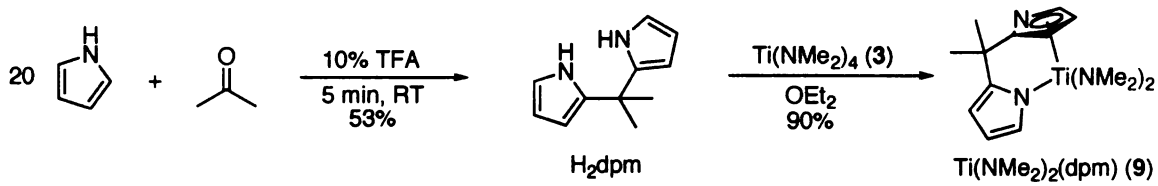

In the solid state and in solution, **9** has a structure where the two pyrrolyl substituents are inequivalent. One of the pyrrolyl rings adopts an η^5-geometry, and the other is η^1-bound. However, at room temperature in the ^{1}H NMR spectrum the two pyrroles appear equivalent due to fast exchange on the timescale of this spectroscopy. Our research group previously reported the barrier for pyrrolyl exchange as $\Delta G^{\ddagger} \sim 10$ kcal/mol.[1]

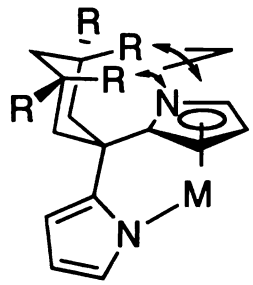

1,3 diaxial interactions

Figure 5.1 Use of 1,3-diaxial interactions to affect dipyrrolylmethane isomerizations barriers.

The most likely mechanism for pyrrole exchange is conversion of both rings to an η^1-geometry.[5] Methods for altering this barrier may provide clues for the active species in catalyses and allow control of complex structure.

Previously,[6] we have reported that altering the pyrrolyl ligand by placing aryl-substituents in the 2-position of the dpm framework lowers the barriers associated with pyrrolyl exchange, presumably by sterically destabilizing the η^5-bonding mode.[7] In fact placing a 3,5-bis(trifluoromethyl)phenyl or mesityl group in the 2-position of the pyrrole lowers the pyrrolyl exchange barriers below what can be measured by variable temperature NMR (<5 kcal/mol). However, addition of sterically hindered groups in these positions hinders access to the metal center as well, affecting catalysis rates.[7]

Scheme 5.2 Synthesis of H_2cpm, H_2tmcpm, $Ti(NMe_2)_2$(cpm) (**24**) and $Ti(NMe_2)_2$(tmcpm) (**24**).

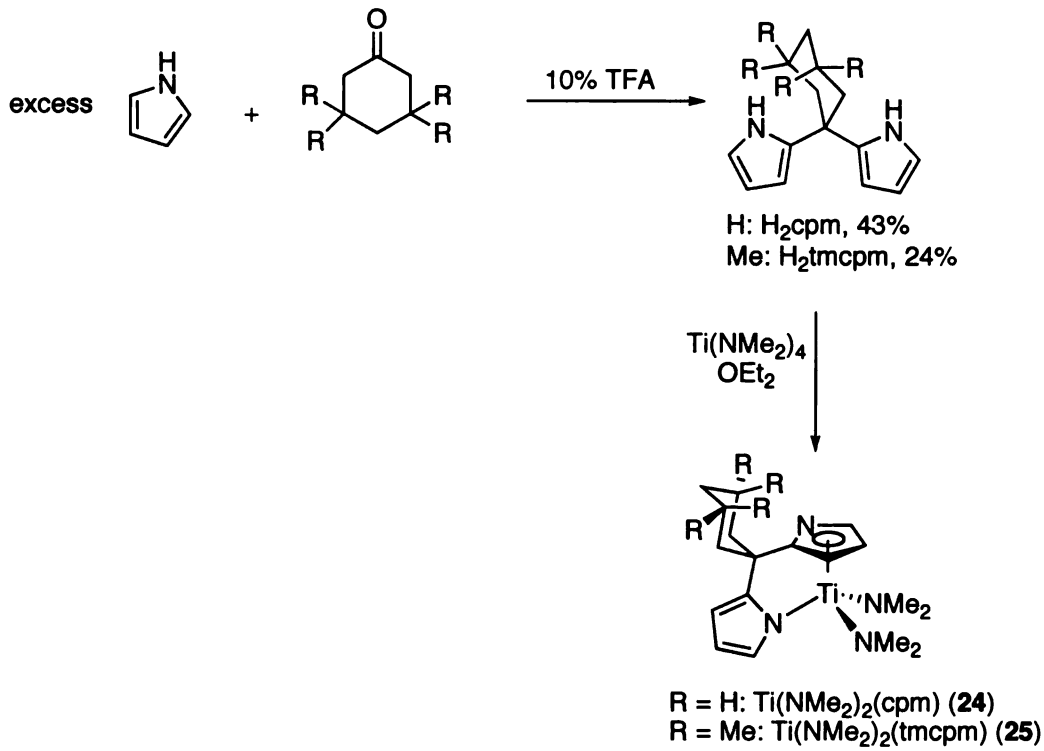

In an attempt to alter the pyrrolyl isomerization rates without blocking access to the metal I explored the use of substituents in the dpm backbone. The strategy was to use 1,3-diaxial interactions within a cyclohexyl ring to stabilize the η^5-bonding mode by sterically inhibiting pyrrolyl-ring rotation (Figure 5.1). The steric interaction will be with the axial pyrrolyl substituent, which will prefer to be in the η^5-bonding mode allowing it to present one side of the π-system to the cyclohexyl substituents rather than the larger ring edge. By using *gem*-disubstitution, the 1,3-diaxial interactions are required regardless of which ring is bound through the π-face. The size of R should affect the ease with which the η^5-bound ring can rotate to obtain the η^1-bonding mode.

This chapter discusses the synthesis of 1,1-bis(α-pyrrolyl)cyclohexane ligands, their titanium complexes, and the barriers for pyrrolyl exchange. The barriers were

determined using the Eyring method with kinetics from variable temperature spin saturation magnetization transfer NMR spectroscopy. Consequently, the enthalpic and entropic effects of this substitution were determined. All this data will be compared with the simple dimethyl compound **9**.

5.2 Ligand Isomerization Study

I examined two cyclohexyl-dpm derivatives, which were easily prepared using commercially available cyclohexanone and 3,3,5,5-tetramethylcyclohexanone as shown in Scheme 5.2. The 1,1-bis(α-pyrrolyl)cyclohexane (H_2cpm) and 1,1-bis(α-pyrrolyl)-3,3,5,5-tetramethylcyclohexane (H_2tmcpm) compounds were prepared in 43% and 24% isolated yields. The transamination reactions with $Ti(NMe_2)_4$ (**3**) and both of these cyclohexyl derivatives occurs in high yields to provide R = H $Ti(NMe_2)_2$(cpm) (**24**) and R = Me $Ti(NMe_2)_2$(tmcpm) (**25**).

The structure of the tetramethylcyclohexyl complex was determined by X-ray diffraction. An ORTEP diagram is shown in Figure 5.2. The metric parameters around titanium are quite similar to previously reported derivatives.[1,2] The cyclohexyl group has the expected chair-conformation with the η^5-pyrrolyl in the more sterically favorable axial position. This conformation puts the two axial methyl groups directly over the η^5-pyrrolyl.

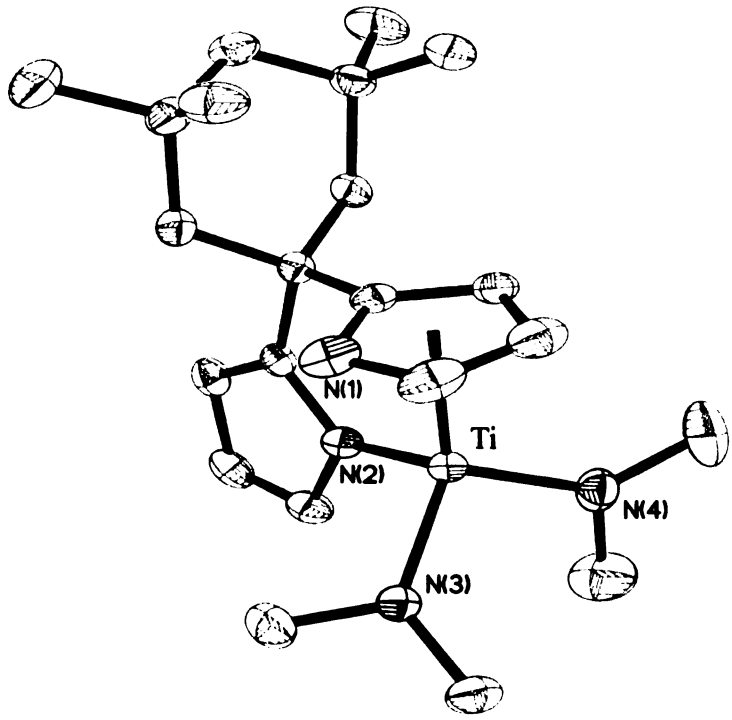

Figure 5.2 ORTEP diagram of the X-ray diffraction model for $Ti(NMe_2)_2$ (tmcpm) (**25**). Ellipsoids at the 50% probability level. Hydrogens are omitted for clarity. Selected bond distances (Å) and angles (°): Ti(1)-N(1) 2.292(2), Ti(1)-N(2) 2.023(1), Ti(1)-N(3) 1.901(1), Ti(1)-N(4) 1.895(2); N(4)-Ti(1)-N(3) 103.49(6), N(4)-Ti(1)-N(2) 107.01(6), N(3)-Ti(1)-N(2) 101.47(6).

The increased steric interaction between the axial cyclohexane substituent and the η^5-pyrrolyl π-face raises the barrier for pyrrolyl exchange as can be seen in the ^1H spectrum at room temperature. There is significant line broadening in the room temperature ^1H spectrum, which indicates that the coalesense point is nearly reached at this tempertature. Cooling a solution of **24** in $CDCl_3$ to –40 °C provided a spectrum of the η^1,η^5-complex. The ^1H NMR spectra of **24** at room temperature and at –40 °C is shown in Figure 5.3.

Variable temperature spin-saturation magnetization transfer was used to determine the barriers for pyrrolyl equilibration for $Ti(NMe_2)_2$(dpm) (**9**), $Ti(NMe_2)_2$(cpm) (**24**), and $Ti(NMe_2)_2$(tmcpm) (**25**). As an example, the Eyring plot for $Ti(NMe_2)_2$(tmcpm) (**25**) is shown in Figure 5.4.

Figure 5.3. ^1H spectra of **24** at room temperature and –40 °C in $CDCl_3$.

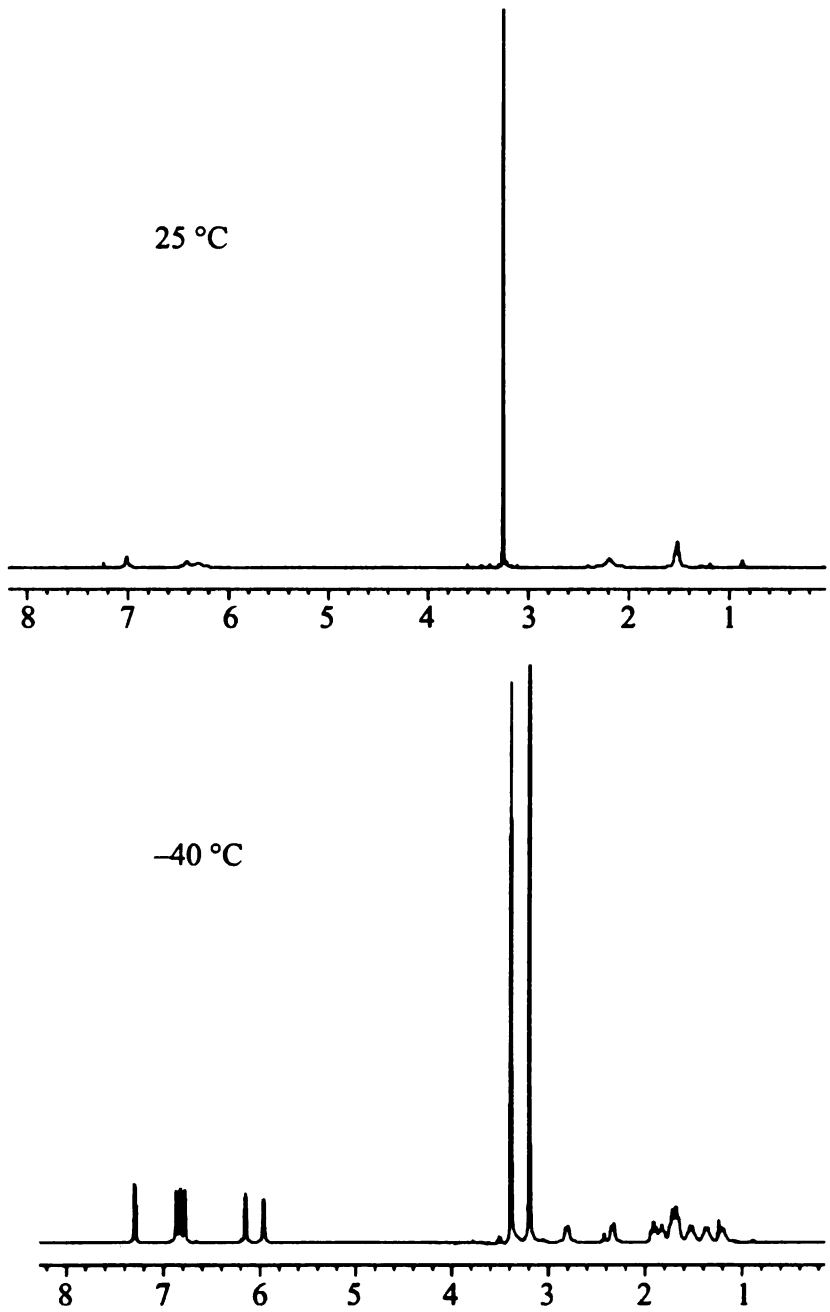

Figure 5.4 Eyring plot of pyrrolyl exchange in $Ti(NMe_2)_2(tmcpm)$ (**25**).

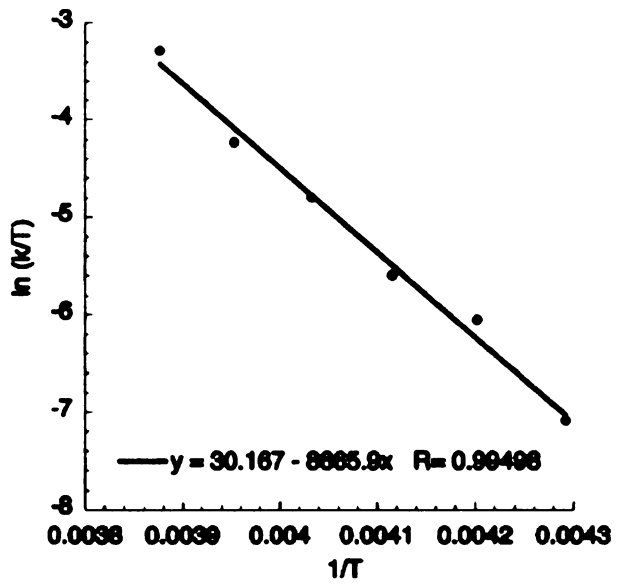

The plot in Figure 5.4 is of ln(k/T) versus 1/T and is used with the Eyring Equation (Equation 5.1), where k_B = Boltzmann constant and R is the gas constant, to determine the activation parameters under the usual assumptions of Transition State Theory.[8] Consequently, the slope (m) can be used to determine $\Delta H^{\ddagger}$ using Equation 5.2, and the intercept (b) can be used to determine $\Delta S^{\ddagger}$ using Equation 5.3.

$$\ln\left(\frac{k}{T}\right) = \frac{\Delta S^{\ddagger}}{R} + \ln\left(\frac{k_B}{h}\right) - \frac{\Delta H^{\ddagger}}{RT} \qquad (5.1)$$

$$\Delta H^{\ddagger} = -m \times R \qquad (5.2)$$

$$\Delta S^{\ddagger} = R\left[b - \ln\left(\frac{k_B}{h}\right)\right] \qquad (5.3)$$

The parameters for the pyrrolyl exchange in compounds **9, 24,** and **25** can be found in Table 5.1. The enthalpic barriers increase from approximately 12 kcal/mol to over 17 kcal/mol for **9, 24,** and **25** reflective of the greater steric interactions on attempting to rotate the η^5-pyrrolyl substituent during the exchange in the

tetramethylcyclohexyl complex.

Table 5.1 Parameters for pyrrolyl exchange for **9, 24,** and **25** at 25 °C.

	$\Delta H^{\ddagger}$ *(kcal/mol)*	$\Delta S^{\ddagger}$ *(cal/mol•K)*	$\Delta G^{\ddagger}$ *(kcal/mol)*
$Ti(NMe_2)_2$(dpm) **(9)**	11.8	5.2	10.3
$Ti(NMe_2)_2$(cpm) **(24)**	14.1	5.1	12.6
$Ti(NMe_2)_2$(tmcpm) **(25)**	17.2	12.7	13.4

The entropic parameters are the same, small and positive, for the 5,5-dimethyldipyrrolyl **9** and cyclohexyldipyrrolyl **24** during the exchange. The tetramethyl complex **25** shows a substantial increase in $\Delta S^{\ddagger}$ to 13 cal/mol•K, which is quite a large positive value for a unimolecular process. The increase in entropy in the transition state suggests that the ground state is highly ordered. This may be due to the single preferred conformation when one of the pyrroles is in the η^5-conformation as opposed to the more conformationally flexible η^1-conformation where neither chair conformer will be strongly favored and any C–C rotations difficult in the η^1,η^5-conformer will be more readily allowed.

As shown in Table 5.1, the difference in exchange barriers between **9** and **24** are largely enthalpic and presumably caused by the 1,3-diaxial interactions. In contrast, the difference in barriers between, **9** and **25**, is more complex. The enthalpic barrier to reach the transition state for exchange is ~5 kcal/mol higher for **3**, but the entropic term reduces the overall barrier to 13.4 kcal/mol.

5.3 Conclusion

Cyclohexyl substituents in the backbone of the dipyrrolylmethane ligand can be used to affect pyrrolyl exchange barriers. The difference in sterics for the η^5-pyrrolyl and η^1-pyrrolyl groups can be used to alter this barrier. While placing *gem*-dimethyl groups on the 3-carbon of the cyclohexyl ring increases the enthalpic cost to pyrrolyl exchange substantially (increased ~50% relative to **9**), the entropic factor for sterically hindered **25** cancels some of the enthalpic increases. Consequently, the free energy barrier only increased by a modest 3 kcal/mol using this strategy.

All three of these compounds were evaluated for catalysis using the same hydroamination test conditions used previously.[6] All three exhibited the same rate for catalysis, indicating that altering the isomerization barriers to the level possible here did not affect the catalysis rates, which is consistent with the rate limiting step not being associated with this isomerization. This is not unexpected as barriers associated with the isomerization are relatively small for this titanium system.

The same methodology used here may prove useful to study pyrrolyl coordination effects in systems where the isomerization has a much larger enthalpic barrier. In addition, this strategy using cyclohexane-based dipyrrolylmethanes potentially could be used to control complex chirality by using asymmetric cyclohexane substituents in systems with a larger tendency to stay in the η^1,η^5-coordination mode.

5.4 Experimental

General Considerations: Anhydrous ether was purchased from Columbus Chemical Industries Inc., and pentane and toluene was purchased from Spectrum Chemical Mfg. Corp., were purified by sparging with dry N_2, then water was removed by running through activated alumina systems purchased from Solv-Tek. Hexanes and ethyl acetate were purchased from Mallinckodt-Baker Inc. Reagent grade cyclohexanone and 3,3,5,5-tetramethylcyclohexanone were purchased from Acros Organics and used as received. Pyrrole was purchased from TCI, was refluxed with sodium, distilled under nitrogen, and then was stored in a purified nitrogen glove box. $Ti(NMe_2)_4$[9] was prepared using a modification of the literature procedure. Deuterated solvents were dried over purple sodium benzophenone ketyl (C_6D_6) or phosphoric anhydride ($CDCl_3$) and distilled under a nitrogen atmosphere. ^1H and ^{13}C spectra were recorded on a VXR-500 spectrometers. All spectra were referenced internally to residual protiosolvent (^1H) or solvent (^{13}C) resonances. Chemical shifts are reported in ppm, and coupling constants are reported in Hz. Typical coupling constants are not reported.

Procedure for Spin Saturation Transfer Experiments: The spin saturation transfer experiments were carried out using the method described by Kresge and co-workers.[10] The dimethylamido resonances were observed in the spin saturation transfer experiments. In order to correct for decoupler spill-over, off-resonance irradiation was carried out on the opposite side of the observation peak relative to the dimethylamido resonance being irradiated.

General Considerations for X-Ray Diffraction: Crystals grown from

concentrated toluene solutions at –35 °C were moved quickly from a scintillation vial to a microscope slide containing Paratone N. Samples were selected and mounted on a glass fiber in wax and Paratone. The data collections were carried out at a sample temperature of 173 K on a Bruker AXS platform three-circle goniometer with a CCD detector. The data were processed and reduced utilizing the program SAINTPLUS supplied by Bruker AXS. The structures were solved by direct methods (SHELXTL v5.1, Bruker AXS) in conjunction with standard difference Fourier techniques.

Synthesis of 1,1-bis(α-pyrrolyl)cyclohexane (H_2cpm)

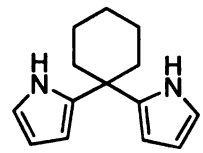

An oven dried 100 mL round bottom flask was charged with cyclohexanone (1 g, 10 mmol) and pyrrole (17 g, 253 mmol) and capped with a septum. The solution was then degassed with argon for 10 min. Trifluoroacetic acid (0.116 g, 1 mmol) was added via syringe. The reaction mixture was allowed to stir for 15 min under an argon atmosphere before being quenched with a 0.1 M NaOH (30 mL) solution. The solution was then transferred to a separatory funnel. It was extracted with OEt_2 and the aqueous layer was washed with OEt_2 (2 × 30 mL). The combined organic layers were dried with $MgSO_4$ and subjected to rotary evaporation to yield a viscous brown oil. The excess pyrrole was removed by distillation under vacuum (~1 torr). The product was purified by column chromatography on silica gel with an eluant of hexanes:ethyl acetate (7:3) to yield a white solid, (0.928 g, 43%). M. p. 104-106 °C. ^{1}H NMR ($CDCl_3$, 500 MHz): 7.61 (br s, 2 H), 6.58-6.55 (m, 2 H), 6.18-6.13 (m, 2 H), 6.13-6.11 (m, 2 H), 2.12-2.07 (m, 4 H), 1.62-1.53 (m, 4 H), 1.52-1.45 (m, 2 H). ^{13}C {^{1}H} NMR (125 MHz, $CDCl_3$): 137.81, 116.67, 107.78, 104.30, 39.77, 37.23, 25.91, 22.74. Anal. Found (Calc.) C: 78.21 (78.46); H: 8.91 (8.47); N: 12.83 (13.07).

Synthesis of 1,1-bis(α-pyrrolyl)-3,3,5,5-tetramethylcyclohexane (H_2tmcpm)

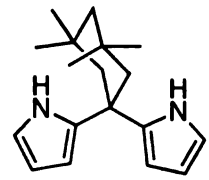

An oven dried 100 mL round bottom flask was charged with 3,3,5,5-tetramethylcyclohexanone (1.0 g, 6.5 mmol) and pyrrole (9.3 g, 138 mmol) and capped with a septum. The solution was then degassed with argon for 10 min. Trifluoroacetic acid (0.074 g, 0.65 mmol) was added via syringe. The reaction mixture was allowed to stir for 15 min under an atmosphere of argon before being quenched with 0.1 M NaOH (30 mL) solution. The solution was then transferred to a separatory funnel and was extracted with OEt_2. The aqueous layer was washed with OEt_2 (2 × 30 mL). The combined organic layers were dried with $MgSO_4$ and subjected to rotary evaporation to yield a viscous brown oil. The excess pyrrole was removed by distillation under vacuum (~1 torr). The product was purified by column chromatography on silica gel with an eluant of hexanes:ethyl acetate (7:3) to yield a white solid, 0.426 g (24%). M. p. 83-85 °C. ^{1}H NMR ($CDCl_3$, 500 MHz): 7.65 (br s, 2 H), 6.55 (dd, 2 H, J_{HH} = 2.5 Hz, J_{HH} =1.5 Hz), 6.13-6.07 (m, 4 H), 2.00 (s, 4 H), 1.27 (s, 2 H), 0.94 (s, 12 H). ^{13}C {^{1}H} NMR ($CDCl_3$ 125 MHz): 138.7, 116.4, 107.7, 104.0, 51.9, 47.9, 39.5, 32.7, 31.7. Anal. Found (Calc.) C: 80.17 (79.95); H: 9.94 (9.69); N: 10.46 (10.36).

Synthesis of $Ti(NMe_2)_2(cpm)$ (24)

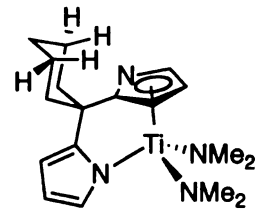

All manipulations were carried out in an inert atmosphere dry box filled with purified dinitrogen. A 20 mL scintillation vial was loaded with $Ti(NMe_2)_4$ (**3**) (0.222 g., 0.991 mmol) and 2 mL of ether. In a separate vial was loaded H_2cpm (0.212 g., 0.991 mmol) in 2.5 mL of ether. The two vials were placed in a liquid nitrogen cooled cold well where they sat until frozen. To a thawing solution, H_2cpm was added to $Ti(NMe_2)_4$ (**3**). The solution was allowed to warm to room temperature where it was left to react for 18 h. The volatiles were removed under reduced pressure, which provided the compound in pure form as judge by NMR and elemental analysis. M. p. 126-130 °C (dec). ^1H NMR ($CDCl_3$, 500 MHz, 25 °C) δ 7.01 (br s, 2 H), 6.41 (br s, 2 H), 6.30 (br s, 2 H), 3.24 (s, 12 H), 2.19 (br s, 4 H), 1.51 (br s, 6 H). ^1H NMR ($CDCl_3$, 500 MHz, –40 °C): 7.25 (app s, 1 H), 6.83 (app s, 1 H), 6.78 (app s, 1 H), 6.73 (app s, 1 H), 6.11 (s, 1 H), 5.93 (s, 1 H), 3.34 (s, 6 H), 3.15 (s, 6 H) 2.76 (d, 1 H, J_{HH} = 12 Hz), 2.29 (d, 1 H, J_{HH} = 14 Hz), 1.87 (app t, 1 H, J_{HH} = 15 Hz), 1.79 (app t, 1 H, J_{HH} = 8.5 Hz), 1.56-1.72 (m, 3 H), 1.42-1.56 (m, 1 H), 1.28-1.40 (m, 1 H), 1.18-1.26 (m, 1 H). ^{13}C NMR {^1H} ($CDCl_3$, 125 MHz, –40 °C): 163.35, 160.79, 126.54, 123.97, 118.13, 115.33, 106.27, 100.67, 48.12, 47.32, 43.93, 38.81, 37.62, 25.60, 23.37, 23.26. Anal. Found (Calcd.) C: 61.91 (62.07); H: 8.49 (8.10); N: 15.62 (16.08).

Synthesis of $Ti(NMe_2)_2$(tmcpm) (25)

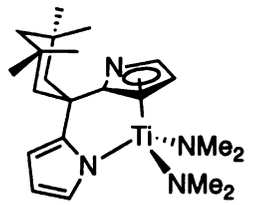

All manipulations were carried out in an inert atmosphere dry box filled with purified dinitrogen. In a 20 mL scintillation vial was loaded $Ti(NMe_2)_4$ (**3**) (0.195 g, 0.869 mmol) and 2 mL of ether. In a separate vial was loaded H_2tmcpm (0.270 g, 0.870 mmol) and 2.5 mL of ether. The two vials were placed in the cold well where they sat until frozen. To a thawing solution of $Ti(NMe_2)_4$ (**3**) was added H_2tmcpm. The solution was allowed to warm to room temperature, where it was left to react for 18 h. The volatiles were removed under reduced pressure, which provided the compound in pure form as judged by NMR and elemental analysis. M. p. 174-177 °C (dec). ^{1}H NMR ($CDCl_3$, 500 MHz, 25 °C): δ 6.97 (br s, 2 H), 6.37 (br s, 4 H), 3.24 (br s, 12 H), 2.6-1.6 (br s, 4 H), 1.25 (s, 2 H), 0.92 (br s, 12 H). ^{1}H NMR ($CDCl_3$, 500 MHz, –40 °C): 7.19 (app s, 1 H), 6.77-6.75 (m, 3 H), 6.11 (t, 1 H, J_{HH} = 2.6 Hz), 5.88 (dd, 1 H, J_{HH} = 1.83 Hz, J_{HH} = 1.09 Hz), 3.35 (s, 6 H), 3.12 (s, 6 H), 2.85 (d, 1 H, J_{HH} = 14.0 Hz), 2.29 (d, 1 H, J_{HH} = 15.0 Hz), 1.73 (d, 1 H, J_{HH} = 15.0 Hz), 1.63 (d, 1 H, J_{HH} = 14.0 Hz), 1.23 (br s, 2 H), 1.00 (s, 3 H), 0.93 (s, 3 H), 0.90 (s, 3 H), 0.63 (s, 3 H). ^{13}C {^{1}H} NMR ($CDCl_3$, 125 MHz) (–40 °C): 166.21, 162.59, 126.09, 123.93, 117.15, 115.16, 106.31, 101.06, 51.89, 50.05, 49.45, 48.16, 47.25, 43.43, 37.10, 35.82, 32.14, 31.91, 29.97, 27.40. Anal. Found (Calcd.) C: 65.13 (65.34); H: 8.91 (9.23); N: 13.62 (13.85).

5.5 References

1 . Y. Shi, C. Hall, J. T. Ciszewski, C. Cao, A. L. Odom *Chem. Commun.* **2003**, 586.

2. For some additional reports of dipyrrolylmethane ligands on transition metals see (a) A. Novak, A. J. Blake, C. Wilson, J. B. Love *Chem. Commun.*, **2002**, 2796 (b) S. Majumder, A. L. Odom *Organometallics*, **2008**, 1174 (c) J. B. Love, P. A. Salyer, A. S. Bailey, C. Wilson, A. J. Blake, E. S. Davies, D. J. Evans *Chem. Commun*, **2003**, 1390.

3. Majumder, S.; Odom, A.L. *submitted.*

4. Littler, B. J.; Miller, M. A.; Hung, C. H.; Wagner, R. W.; O'Shea, D. F.; Boyle, P. D.; Lindsey J. S. *J. Org. Chem.*, **1999**, *64*, 1391.

5. For a recent computational study on pyrrolyl isomerization see Dias, A. R.; Ferreira, A. P.; Veiros, L. F. *Comptes Rendus Chimie*, **2005**, *8*, 1444.

6. Swartz II, D. L.; Odom, A. L. *Organometallics*, **2006**, *25*, 6125.

7. Tanski, J. M.; Parkin, G. *Organometallics* **2002**, *21*, 587.

8. B. K. Carpenter, *Determination of Organic Reaction Mechanisms*, John Wiley & Sons: New York, 1984.

9. D. C. Bradley, I. M. Thomas, *J. Chem. Soc.* **1960**, 3859.

10. C. L. Perrin, J. D. Thoburn, J. Kresge, J. *J. Am. Chem. Soc.* **1992**, *114*, 8800.

CHAPTER 6

Uranium (VI) bis(imido) pyrrolyl complexes: synthesis, structure, and reactivity

6.1 Introduction

The metal-ligand multiple bond functional group has played a significant role in transition metal synthetic organometallic chemistry and catalysis.[1] This functionality has been far less developed for actinides. Since its discovery, the most widely studied metal ligand multiple bond in actinide chemistry is the uranyl ion, UO_2^{2+}. The reactivity of the uranyl ion has been generally limited to equitorial coordination sites due to the high degree of thermodynamic stability and kinetic inertness of the U–O bond.[2] Therefore, uranyl analogues are highly attractive to expand on the reactivity associated with metal ligand multiple bonds in actinides as well as investigate *f*-orbital involvement in bonding. Until the recent work done by Boncella and co-workers in developing a dependable synthetic strategy for uranium bis(imido) analogues,[3] the understanding of the extent to which the *f*-orbitals participate in U-element multiple bonding was limited to the uranyl ion and a hand full of uranium imido complexes.[4]

Analysis of chemical bonding using density functional theory (DFT) on uranium bis(imido) complexes suggests that there is a significant amount of covalency in the U–N bond, which goes against the paradigm of the actinide elements being highly ionic in nature.[5,6] The 6 orbitals involved in bonding in $U(NMe)_2I_2(THF)_2$, σ_u, σ_g, two π_g and π_u, are the same types involved in the uranyl ion, although the ordering differs, which is partly due to the higher electronegativity of the oxygen atom and larger involvement of the 6*p* orbital in uranyl.[5,7]

Unlike uranyl, the U–N multiple bond in $U(NBu^t)_2(THF)_2I_2$ is not kinetically inert. The U–N bond can undergo [2+2]-cycloaddition with aryl isocyanates to yield an array of uranium (bis)imido derivatives,[8] as well react with $B(C_6F_5)_3\bullet(H_2O)$ to yield an uranium oxo imido complex (Scheme 6.1).[9] Interestingly, the addition of $OPPh_3$ forces the iodide ligands trans.

Scheme 6.1 Exchange of imido ligand in $U(NBu^t)_2(THF)_2I_2$ and $U(NBu^t)_2(OPPh_3)_2I_2$.

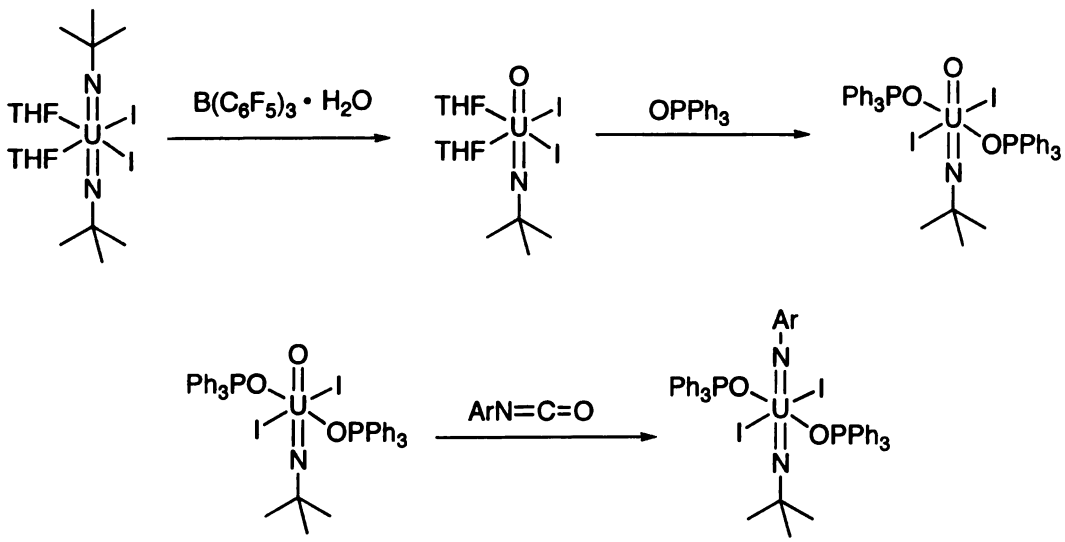

Among the many ancillary ligands employed in organoactinide chemistry, the most common are Cp-based ligands. Burns and Arney reported a *cis*-imido uranium complex $U(\eta^5\text{-}C_5Me_5)_2(NPh)_2$,[4c] while Boncella and co-workers reported $U(\eta^5\text{-}C_5H_5)_2(NBu^t)_2$ with the imidos in a *cis*-geometry. They also prepared a mono-Cp based system in $U(NBu^t)_2(dmpe)I(\eta^5\text{-}C_5H_5)$ with the imido ligands *trans*.[10]

Similar to Cp, pyrrolyl ligands can adopt bonding modes of η^5 or η^1 (Chart 6.1). Marks and co-workers reported a tetrakis(pyrrolyl) uranium complex where 3 of the

pyrrolyls are η^1-bound and the other is η^5-bound.[11] The fluxional behavior of pyrroles involving interchanging η^1- and η^5-coordination in their bonding hapticities is common in transition metals. Similarly at elevated temperatures the pyrrolyls interchange rapidly on the NMR timescale between η^5- and η^1-bound in Marks' uranium pyrrolyl complex.[11]

Our group has reported titanium ligated dipyrrolylmethanes as effective catalysts for hydroamination and multi-component coupling reactions.[12] Pyrrolyl ligands have proven to be a useful class of ancillary ligands for transition metals,[13] whereas their employment in actinide chemistry is relatively scarce and to the best of my knowledge there are no reports of dipyrrolylmethane ligands on uranium. I wanted to investigate the scope of dipyrolylmethane ligands as suitable ancillary ligands for uranium. This chapter discusses the synthesis, structure, and reactivity of uranium bis(imido) dipyrrolylmethane complexes.

Chart 6.1 Possible bonding modes of pyrrolyl and dipyrrolylmethane ligands to one metal center.

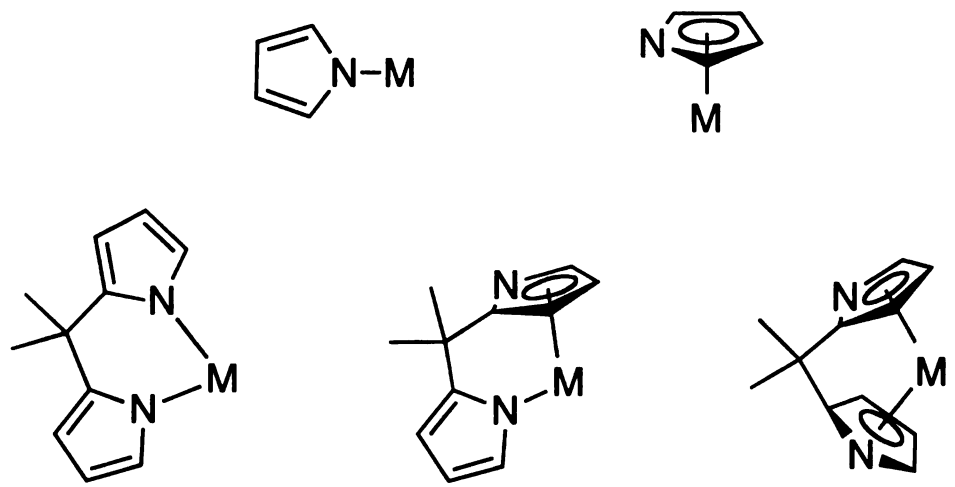

6.2 Uranium bis(imido) dipyrrolylmethane complexes

Encouraged by our previous results of pyrrolyl ligands supporting metal ligand multiple bonds on transition metals I sought to prepare novel uranium bis(imido) dipyrrolylmethane complexes. I was intrigued to investigate the bonding modes the ligand may adopt given the reports of Parkin and Tanski and our own research group that increased sterics lower the barrier for pyrrolyl exchange.[13a,14] Therefore, I thought to use a 2,2'-di(aryl)dipyrrolylmethane (H_2dpm^{mes}), where dpm^{mes} is 2,2'-bis(mesityl)-5,5-dimethyldipyrrolylmethane. The ligation of the dpm^{mes} on titanium shows pyrrolyls bound-η^1,η^5 in the solid state.[13a] While the pyrrolyl groups in $Ti(NMe_2)_2(dpm^{mes})$ (**13**) are inequivalent in the solid-state, the ^1H NMR is indicative of fast pyrrolyl exchange on the NMR timescale.[13a] I was interested to see if dpm^{mes} would exhibit this same fluxional behavior in uranium bis(imido) complexes and what ground-state geometry it would have in the solid-state.

Given the wonderful synthetic utility of $U(NBu^t)_2(THF)_2I_2$ in preparing a plethora of uranium bis(imido) derivatives, it was the practical synthon of choice in preparing dipyrrolylmethane uranium bis(imido) complexes. The addition of K_2dpm^{mes} to a stirring orange solution of $U(NBu^t)_2(THF)_2I_2$ in THF provides a black solution, from which $U(NBu^t)_2(dpm^{mes})$ (**26**) can be isolated as a black solid (Equation 6.1). Single crystals of **26** grown from hexane at –35 °C were suitable for X-ray diffraction. The structure of **26** is shown in Figure 6.1.

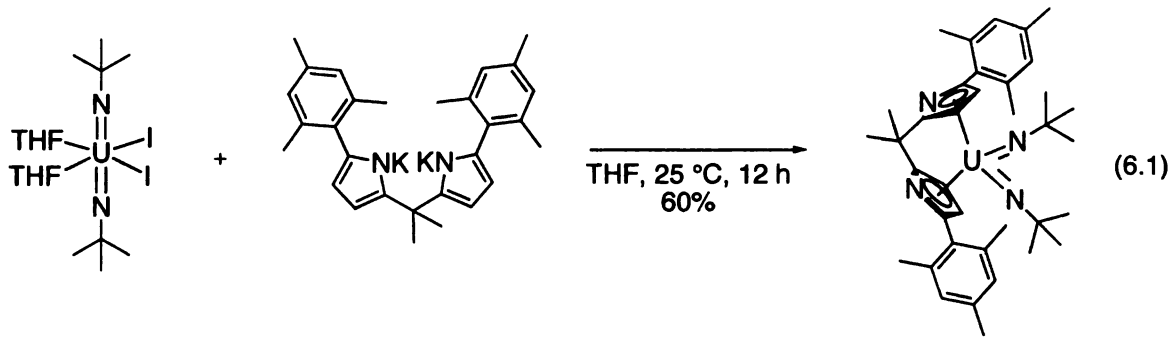

(6.1)

$U(NBu^t)_2(dpm^{mes})$ (**26**)

Complex **26** has C_2-symmetry with the pyrrolyls bound-η^5,η^5 in the solid state. The ability of the dpm^{mes} ligand to adopt an η^5,η^5-binding mode may be partly due to the sheer size of the uranium atom relative to the size of transition metals.

The geometry of the dpm^{mes} ligand forces the imido ligands cis with U-N bond lengths of 1.930(4) Å and 1.946(4) Å respectively. The average U-N(imido) bond length is significantly longer than the bond lengths found in $U(NBu^t)_2(THF)_2I_2$ which is probably due to an electronic effect.[3] The average U-N(imido) bond length is similar to the bond lengths found in η^5,η^5-bound $U(NBu^t)_2(C_5H_5)_2$, although the N-U-N imido angle in **26** is 116.06(15)°, which is significantly larger than the N-U-N imido bond angle in $U(NBu^t)_2(C_5H_5)_2$ (N-U-N = 103.4(3)°). This can be attributed to the chelated dpm^{mes} ligand.[10]

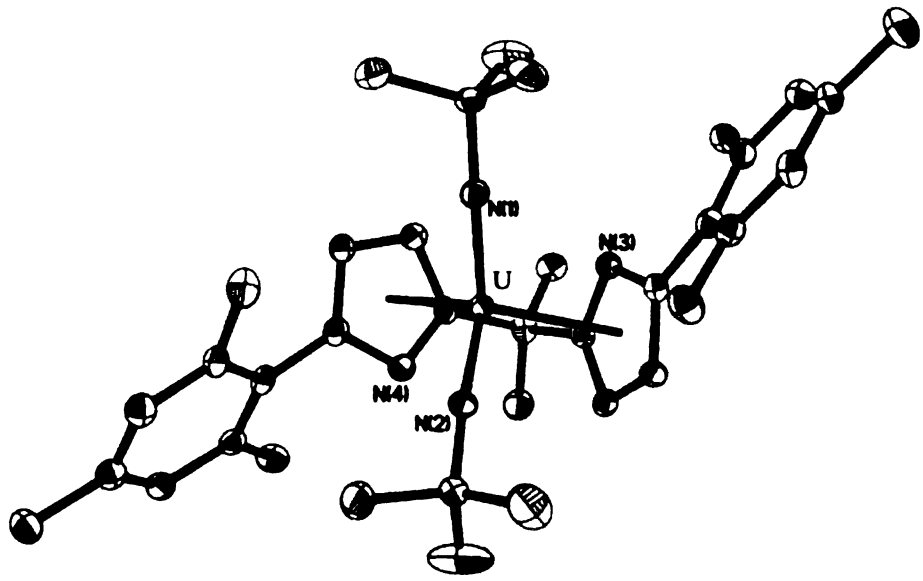

Figure 6.1 ORTEP structure of $U(NBu^t)_2(dpm^{mes})$ (**26**) from single crystal X-ray diffraction. Selected bond distances (Å) and angles (deg): U-N(1) 1.930(4), U-N(2) 1.946(4), U-N(3) 2.575(4), U-N(4) 2.592(4), N(1)-U-N(2) 116.06(15), N(1)-U-N(3) 91.90(14), N(1)-U-N(4) 131.47(13), N(2)-U-N(3) 130.79(13), N(2)-U-N(4) 94.11(14), N(3)-U-N(4) 95.72(12).

Uranium imidos are known to undergo [2+2]-cycloaddition to yield imido dervatives as well as react with $B(C_6F_5)_3 \bullet H_2O$ to produce an oxo imido uranium species.[8,10] Attempts to take advantage of this known reactivity with previously reported uranium imidos, showed disappointing imido reactivity in **26**, usually resulting in decomposition. Complex **26** is also sensitive to solvent. Leaving **26** in a solution of THF for extended periods of time resulted in decomposition as well, resulting in protio-ligand and new uranium resonances in the ^1H NMR spectrum. Unfortunately, the only solvent to facilitate the production of **26** from $U(NBu^t)_2(THF)_2(I)_2$ and K_2dpm^{mes} was THF, therefore particular attention to reaction times was required. Attempts to isolate the

uranium decomposition product were unsuccessful.

To probe the coordination chemistry of **26**, a handful of Lewis bases were examined (i.e. pyridine, $OPPh_3$, and dmpe). Most bases examined yielded no clean isolable products, however a reaction of **26** with dmpe, (dmpe = 1,2-bis(dimethylphosphino)ethane), in toluene yields $U(NBu^t)_2(dpm^{mes})(dmpe)$ (**27**) (Equation 6.2). A structure for **27** is shown in Figure 6.2. The addition of dmpe to **26** forces the imidos *trans*, and the increased sterics around the metal center forces the dpm^{mes} ligand to adopt an η^1,η^1-binding mode resulting in **27** taking on a pseudo-octahedral geometry.

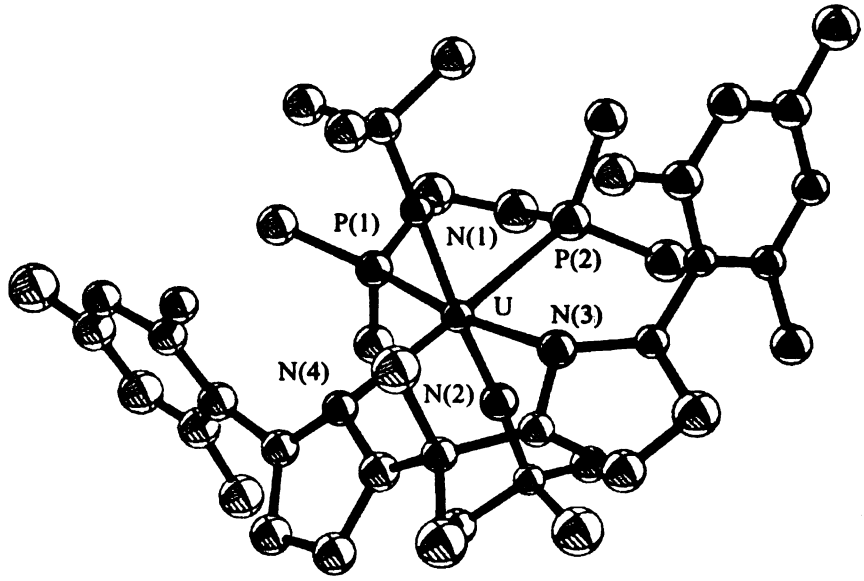

Figure 6.2 ORTEP structure of $U(NBu^t)_2(dpm^{mes})(dmpe)$ (**27**) from single crystal X-ray diffraction. Selected bond distances (Å) and angles (deg): U-N(1) 1.865(15), U-N(2) 1.857(14), U-N(3) 2.393(15), U-N(4) 2.431(15), U-P(1) 3.043(6), U-P(2) 3.116(6), N(1)-U-N(2) 165.9(6), N(1)-U-N(3) 97.10(6), N(1)-U-N(4) 98.2(6), N(2)-U-N(3) 92.7(6), N(2)-U-N(4) 91.4(6), N(3)-U-N(4) 93.1(5), N(2)-U-P(1) 84.1(5), N(1)-

U-P(1) 84.5(5), N(3)-U-P(1) = 169.4(4), N(4)-U-P(1) = 97.0(4), N(2)-U-P(2) = 80.6(5), N(1)-U-P(2) 87.3(5), N(3)-U-P(2) 102.2(4), N(4)-U-P(2) 163.0(4), P(1)-U-P(2) 67.39(15).

The average imido bond length in **27** is 1.861 Å, which is similar to the average bond lengths found in $U(NR)_2(THF)(I)_2$.[5] The N-U-N imido bond angle, 165.9(6)°, in **27** deviates from the ideal bond angle of an octahedral complex of 180°, which is likely due to steric effects. The average U-P bond distance of 3.079 Å is longer than the bond distance in $U(NBu^t)_2(dmpe)(\eta^5\text{-}C_5H_5)_2$ (U-P average = 2.99 Å), the only structurally characterized other uranium (VI) complex supported by the dmpe ligand.[10] The ^1H NMR spectrum of **27** shows an extremely broad singlet at 3.35 ppm, assigned to the *ortho*-methyl groups on dpm^{mes}, which could possibly be due to hindered rotation about pyrrolyl-mestiyl bond (See Appendix for the ^1H spectrum of **26** and **27**); however, fluxional behavior could also explain this phenomena. This broad singlet is also seen in complex **26**.

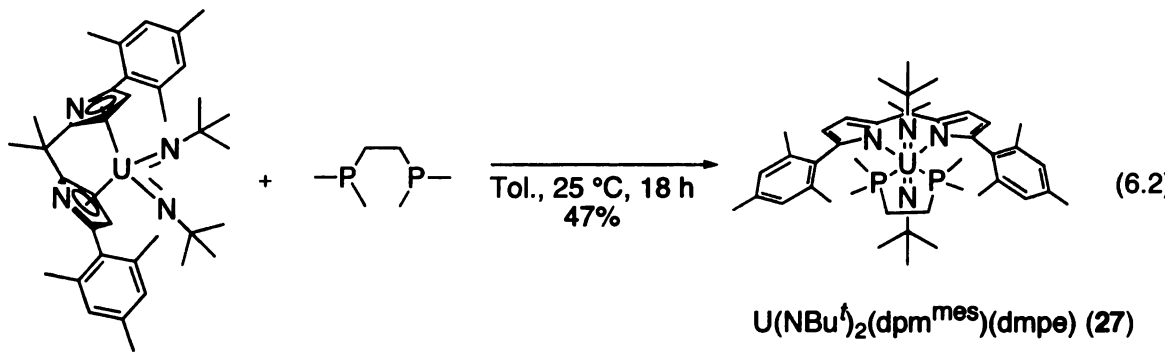

(6.2)

26

$U(NBu^t)_2(dpm^{mes})(dmpe)$ **(27)**

I also investigated the use of the sterically smaller ligand 5,5-dimethyldipyrrolylmethane (H_2dpm). The dry addition of K_2dpm to a stirred dilute orange stirring solution of $U(NBu^t)_2(THF)_2(I)_2$ in THF affords $U(NBu^t)_2(THF)_2(dpm)$

(**28**) as a red solid, which can be isolated in 42% using this synthetic procedure (Reaction 6.3). Crystallization of **28** from THF/hexane resulted in the growth of crystals suitable for X-ray diffraction. A structure of **28** is shown if Figure 6.3. The dilute reaction conditions for the production of **28** were required due to the low solubility of K_2dpm, which resulted in slightly longer reaction times.

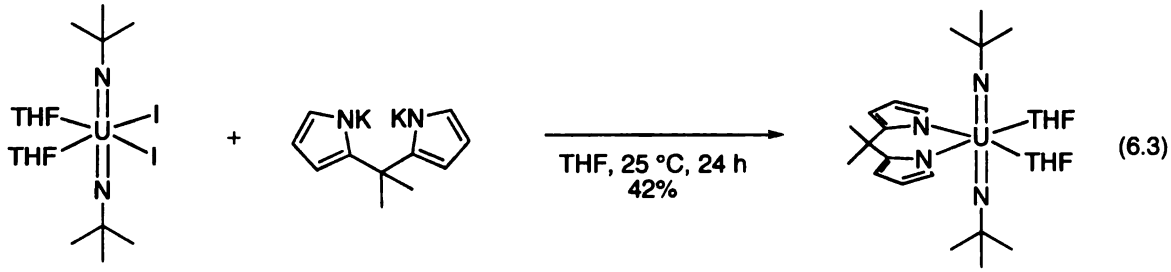

(6.3)

$U(NBu^t)_2(THF)_2(dpm)$ (**28**)

The pyrrolyls in the dpm ligand in **28** adopt an η^1,η^1-bonding mode. The ^1H NMR spectrum is consistent with the solid-state structure of **28** with the pyrrolyls being equivalent. The average imido bond length in **28** is 1.856(6) Å which is similar to the bond length found in **27** and other $U(NR)_2(THF)_2(I)_2$ complexes.[5] The imido bond angle in **28** is nearly linear with a bond angle of 172.8(3)°. The average U-N(pyrrolyl) bond length of 2.356(6) Å is similar to the U-N(pyrrolyl) average bond length in **28**, while the average U-O bond length in **28** is also similar to previously reported U-O bond lengths in $U(NR)_2(THF)_2(I)_2$ complexes.

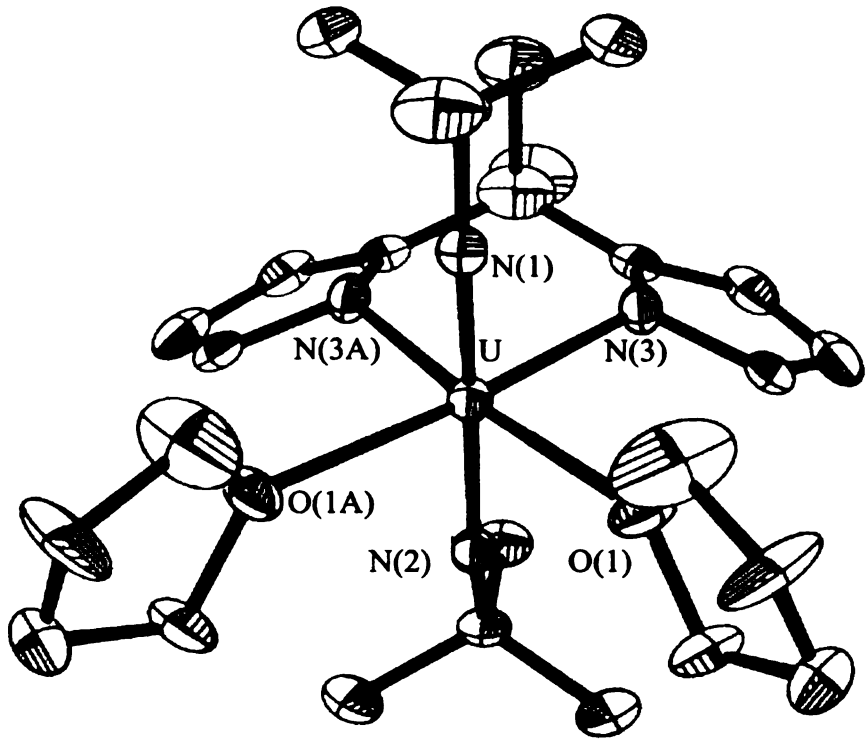

Figure 6.3 ORTEP structure of $U(NBu^t)_2(dpm)(THF)_2$ (**28**) from single crystal X-ray diffraction. Selected bond distances (Å) and angles (deg): U-N(1) 1.856(6), U-N(2) 1.856(7), U-N(3) 2.356(6), U-N(3A) 2.356(6), U-(O1) 2.461(4), U-O(1A) 2.461(4), N(1)-U-N(2) 172.8(3), N(2)-U-N(3A) 91.52(19), N(1)-U-N(3A) 94.23(19), N(2)-U-N(3) 91.52(19),

Complex **28** did not show the same sensitivity to solvent and temperature as **26**. Extended time in THF did not result in any new resonances is the ^1H NMR spectrum.

I also investigated the use of a 2-mesityl pyrrole ($Hpyrr^{mes}$) as an ancillary ligand. Reacting 2 equivalents of $Kpyrr^{mes}$ with $U(NBu^t)_2(THF)_2(I)_2$ did not afford the bis(pyrrolyl) uranium complex, instead a mono(pyrrolyl) uranium complex,

$U(NBu^t)_2(THF)_2(I)(pyrr^{mes})$ (**29**) was produced and structurally characterized by X-ray diffraction (Scheme 6.2). The structure of **29** is shown in Figure 6.4.

Scheme 6.2 Synthesis of $U(NBu^t)_2(THF)_2(I)(pyrr^{mes})$ (**29**).

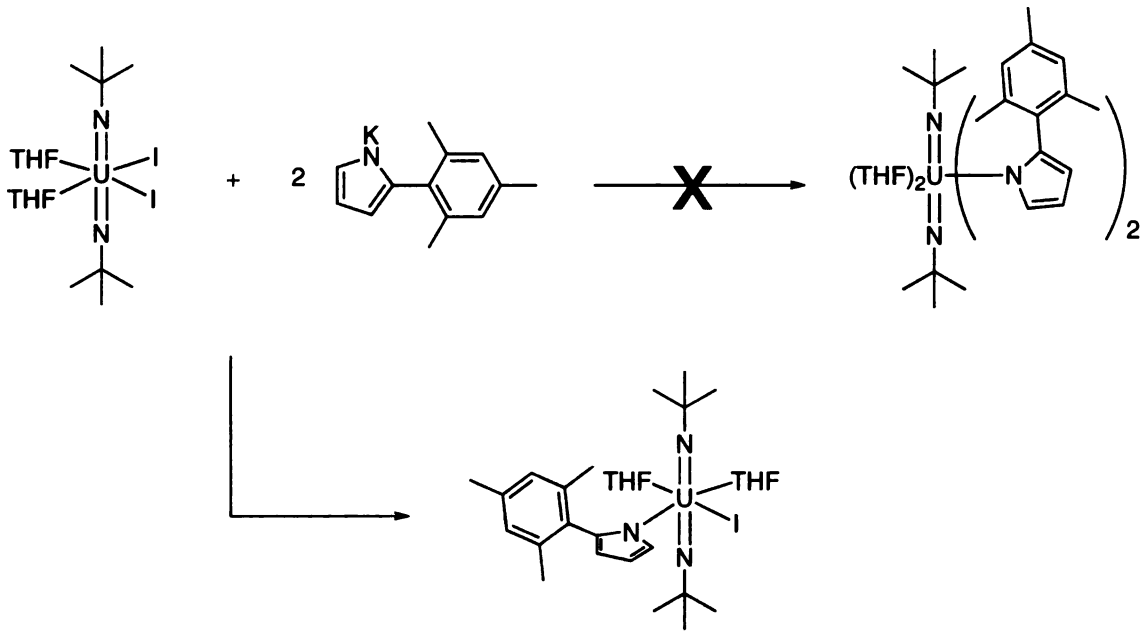

$U(NBu^t)_2(THF)_2(I)(pyrr^{mes})$ (**29**)

The ^1H NMR spectrum of the reaction mixture showed free $Hpyrr^{mes}$ peaks in the baseline in addition to a uranium complex. There were several attempts to reproduce **29** by reacting 1 equivalent of $Kpyrr^{mes}$ with $U(NBu^t)_2(THF)_2(I)_2$, but they yielded no isolable products resembling the structure of **29**. It is possible that the production of bis(2-mesitylpyrolyl) uranium complex disproportionates to give a mixture of mono(pyrrolyl) and other uranium complexes.[15]

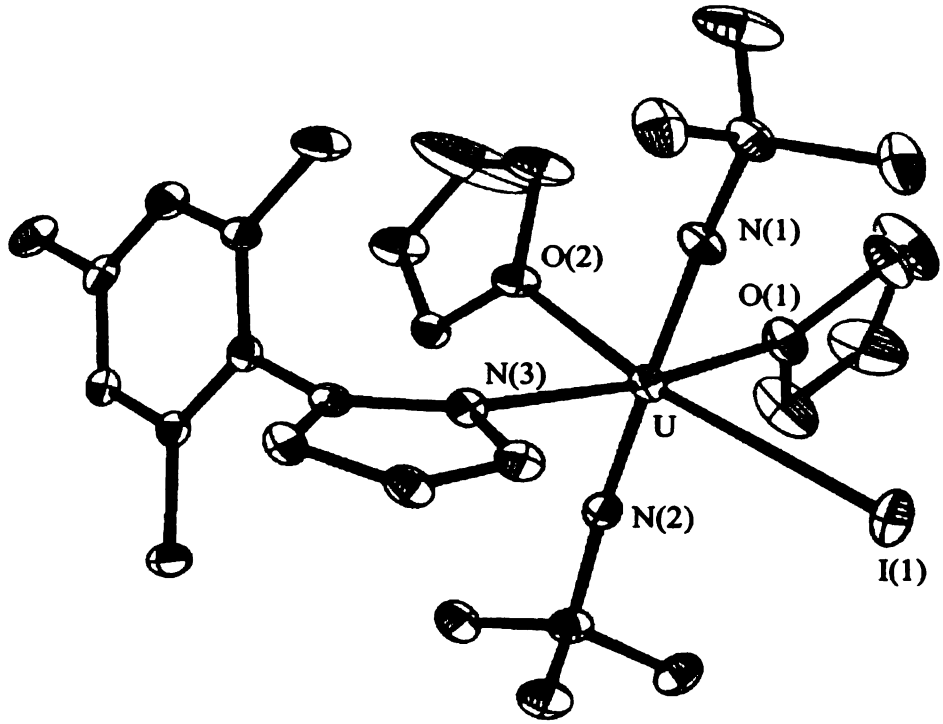

Figure 6.4 ORTEP structure of $U(NBu^t)_2(pyrr^{mes})(THF)_2(I)$ (**29**) from single crystal X-ray diffraction. Selected bond distances (Å) and angles (deg): U-N(1) 1.849(3), U-N(2) 1.841(3), U-N(3) 2.385(3), U-(O1) 2.467(3), U-O(2) 2.437(3), U-I 3.0721(4), N(1)-U-N(2) 175.06(13), N(2)-U-N(3) 91.41(12), N(1)-U-N(3) 92.69(12).

Complex **29** takes on a pseudo-octahedral geometry with the pyrroyl bonded η^1 in the solid state and imido ligands *trans* with a U-N bond angle of 175.06° and an average U-N bond distance of 1.844 Å, which are similar to previously reported $U(NR)_2(THF)_2(I)_2$ complexes. The average U-I and U-O bond distances are similar to previously reported complexes as well.[5]

6.3 Conclusion

In summary, a series of novel uranium bis(imido) dipyrrolylmethane complexes have been prepared by reacting the potassium salt of the dipyrrolylmethane ligand with $U(NBu^t)_2(THF)_2(I)_2$.

Binding the dpm^{mes} ligand to uranium results in the ligand adopting an η^5,η^5-coordination forcing the imido ligands *cis*. $U(NBu^t)_2(dpm^{mes})$ (**26**) showed disappointing reactivity towards alkynes, ketones, and isocyanates which typically resulted in decomposition. However, reacting **26** with one equivalent of dmpe, resulted in dmpe coordination. The increased steric interaction forced the imido ligands to adopt a *trans* geometry and pushed the dipyrrolylmethane ligand to an η^1,η^1-bonding mode.

Ligation of the dpm ligand to uranium resultd in a six coordinate complex with the imido ligands *trans* and the dipyrrolylmethane ligand adopting an η^1,η^1-binding mode. The possibility of fluxional behavior in **26** and **27** warrant further investigation.

These findings show that dipyrrolylmethanes support uranium(VI) bis(imido) complexes. In addition, the ability to take advantage of a dipyrrolylmethane ligand that adopts an η^5,η^5-bonding mode may prove useful in producing uranium bis(imido) complexes with the imido ligands in a *cis*-geometry that can be used in catalytic hydroamination reactions and other organoactinide catalysis.

6.4 Experimental

General Considerations. All manipulations of air sensitive compounds were carried out in an MBraun drybox under a purified nitrogen atmosphere. Anhydrous solvents were purchased from Acros Organics and were used as received. Deuterated solvents were dried over purple sodium benzophenone ketyl (C_6D_6) or phosphoric anhydride ($CDCl_3$) and distilled under a nitrogen atmosphere and stored over molecular sieves. $U(NBu^t)_2(THF)_2(I)_2$,[5] H_2dpm^{mes},[13a] and H_2dpm[16] were synthesized according to literature procedures. ^1H and ^{13}C spectra were recorded on Bruker-300 spectrometers. All spectra were referenced internally to residual protiosolvent (^1H) or solvent (^{13}C) resonances. ^1H and ^{13}C assignments were confirmed when necessary using two-dimensional ^1H–^1H and ^1H–^{13}C correlation NMR experiments. Chemical shifts are reported in ppm and coupling constants reported in Hz.

Synthesis of $U(NBu^t)_2(dpm^{mes})$ (26)

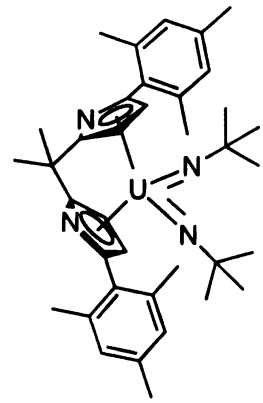

Under an atmosphere of dry N_2, a 20 mL scintillation vial was loaded with $U(NBut)_2(THF)_2(I)_2$ (1.24 g, 1.59 mmol) in THF (8 mL). In a separate vial was K_2dpm^{mes} (0.886 g, 1.59 mmol) in THF (6 mL). Both vials were put into the freezer where they sat for ~30 minutes. After that time, K_2dpm^{mes} was added to the vial containing $U(NBu^t)_2(THF)_2(I)_2$. The solution was allowed to stir overnight at room temperature. The following day the solution was filtered through a pipette filter with a thin pad of celite. The volatiles were removed by vacuum to give a viscous black oil. The oil was stirred in hexamethyldisiloxane (8 mL) for 8 h, after which the solution was filtered through a pipette filter. The solid remaining on the pipette filter was dissolved in toluene and put back into the vial containing the original solution. The volatiles were removed by vacuum to a black solid. The solid was triturated with hexane to give $U(NBu^t)_2(dpm^{mes})$ as a black solid, (0.750 g 60%). ^1H NMR (C_6D_6, 300 MHz): 7.03 (s, 4H), 6.31 (app s, 2 H), 5.68 (app s. 2H), 3.56 (br s, 12 H), 2.32 (s, 6 H), 2.24 (s, 6 H), 0.49 (s, 18 H).

Synthesis of $U(NBu^t)_2(dpm^{mes})$(dmpe) (27)

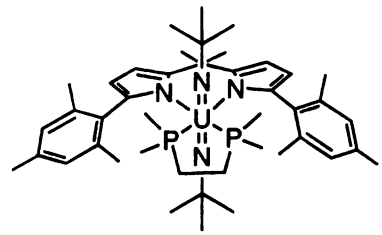

Under an atmosphere of dry N_2, a 20 mL scintillation vial was loaded with $U(NBu^t)_2(dpm^{mes})$ (0.075 g, 0.0951 mmol) in toluene (3 mL). To that vial was added dmpe (0.014 g, 0.0951 mmol). The solution was allowed to stir overnight. The next day the volatiles were removed in vacuo to give a black solid. The solid was dissolved in a minimal amount of hexane and put into the freezer to crystallize. The following day thin black needles were deposited on the side of vial. The crystals were dried in vacuo to give the title compound as a black solid, (0.047 g. 47%) ^{1}H NMR (C_6D_6, 300 MHz): 7.01 (s, 4 H), 6.37 (app s, 2 H), 3.36 (br s, 12 H), 2.44 (br s, 6 H), 2.26 (s, 6 H), 1.21 (br s, 4 H), 0.99 (br s, 12 H), 0.45 (s, 18 H).

Synthesis of $U(NBu^t)_2(dpm)(THF)_2$ (28)

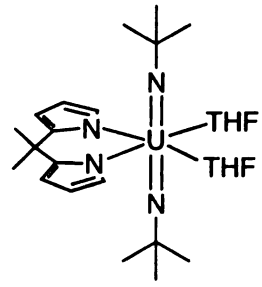

Under an atmosphere of dry N_2, a 20 mL scintillation vial was loaded with $U(NBu^t)_2(THF)_2(I)_2$ (0.050 g, 0.064 mmol) in THF (5 mL). To that vial was added K_2dpm (0.016 g, 0.064 mmol) dry. The solution was allowed to stir for 24 hours, after which it had turned deep red in color. The following day the solution was filtered through a pipette filter with a thin pad of celite. The volatiles were removed in vacuo to give a deep red solid. The solid was dissolved in THF and layered with an equal amount of hexane and put in the freezer to crystallize. The following day, red crystals were deposited on the side of the vial. The crystals were then dried to give the product as a red solid, (0.018 g 42%). ^1H NMR (C_6D_6, 300 MHz):7.37 (app s, 2 H), 7.22 (app s, 2 H), 6.59 (app s, 2 H), 3.61 (s, 4 H), 1.76 (s, 6 H), 1.41 (s, 4 H), 1.38 (s, 18 H).

Synthesis of $U(NBu^t)_2(dpm)(dmpe)$ (30)

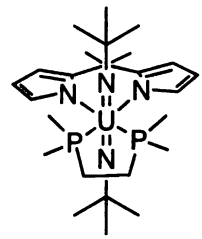

Under an atmosphere of dry N_2, a 20 mL scintillation vial was loaded with $U(NBu^t)_2(THF)_2(dpm)$ (0.050 g, 0.072 mmol) in toluene (2 mL). To that vial was added dmpe (0.0108 g, 0.072 mmol). The solution was allowed to stir overnight. The following day the volatiles were removed in vacuo to yield a red solid. The solid was dissolved in a minimal amount of THF and layered with an equal amount of hexane and put in the freezer to crystallize. Crystals formed as deep red blocks. The crystals were dried to give a deep red solid, 0.020 g (44 %). ^1H NMR (C_7D_8, 300 MHz) δ: 7.59 (app s, 2 H), 6.87 (app s, 2 H), 6.45 (app s, 2 H), 1.98 (app s, 4 H), 1.36 (s, 12 H), 1.27 (s, 18 H). ^{31}P NMR (C_7D_8, 300 MHz) δ: 79.57.

6.5 References

1. Mayer, J.M.; Nugent, W.A. *Metal Ligand Multiple Bonds*, Wiley, New York, 1988.

2. Morss, L. R.; Edelstein, N. M.; Fuger, J. *The Chemistry of the Actinide and Transactinide elements*, 3rd ed.; Springer Netherlends, New York, 2006, Vol 1.

3. Hayton, T. W.; Boncella, J. M.; Palmer, P. D.; Scott, B. L.; Batista, E. R.; Hay, P. J. *Science,* **2005**, *310*, 1941.

4. (a) Arney, D. S. J.; Burns, C. J.; Smith, D. C. *J. Am. Chem. Soc.* **1992**, *114*,10068 (b) Arney, D. S. J.; Burns, C. J. *J. Am. Chem. Soc.* **1995**, *117*, 9448. (c) Warner, B. P.; Scott, B. L.; Burns, C. J. *Angew. Chem., Int. Ed.* **1998**, *37*, 959. (d) Cramer, R. E.; Edelmann, F.; Mori, A. L.; Roth, S.; Gilje, J. W.; Tatsumi,K.; Nakamura, A. *Organometallics* **1988**, *7*, 841. (e) Ariyaratne, K. A. N. S.; Cramer, R. E.; Gilje, J. W. *Organometallics* **2002**, *21*, 5799.

5. Hayton, T. W.; Boncella, J. M.; Scott, B. L.; Batista, E.R., Hay, P. J. *J. Amer. Chem. Soc.*, **2006**, *128*, 10549.

6. Kaltsoyannis, N. *Inorg. Chem.* **2000**, *39*, 6009.

7. For an explanation of the "pushing from below" mechanism see. (a) Pepper, M.: Bursten, B. E. Chem. Rev. 1991, 91, 719. (b) Tataumi, K.; Hoffmann, R *Inorg. Chem.* **1980**, *19*, 2656.

8. Spencer, L. P.; Yang, P.; Scott, B. L. Batista, E. R.; Boncella, J.M. *J. Amer. Chem. Soc.* **2008**, *130*, 2930.

9. Hayton, T. W. Boncella, J. M.; Scott, B.L. Batista, E.R. J. Amer. Chem. Soc. **2006**, 128, 12622.

10. Spencer, L. P.; Gdula, R. L.; Hayton, T. W.; Scott, B. L.; Boncella, J. M. *Chem. Comm.* **2008**, 4986.

11. Marks, T.J. *Acc. Chem. Res.* **1976**, *9*, 223.

12. (a) Swartz II, D. L.; Odom, A.L. *Organometallics*, **2006**, *26*, 6125. (b) Majumder, S.; Odom, A.L; manuscript in preparation.

13. (a) A. Novak, A. J. Blake, C. Wilson, J. B. Love *Chem. Commun.*, **2002**, 2796 (b) S. Majumder, A. L. Odom *Organometallics*, **2008**, 1174 (c) J. B. Love, P. A. Salyer, A. S. Bailey, C. Wilson, A. J. Blake, E. S. Davies, D. J. Evans *Chem. Commun*, **2003**, 1390.

14. Tanski, J.M.; Parkin, G. *Organometallics* **2002**, *21*, 587.

15. Spencer, L.P. personal communication.

16. Littler, B. J.; Miller, M. A.; Hung, C. H.; Wagner, R. W.; O'Shea, D. F.; Boyle, P. D.; Lindsey, J. S. *J. Org. Chem.* **1999**, *64*, 1391.

APPENDIX A

Kinetic reaction plots for selected catalysts in Chapter 2

Figure A1.1 Representative plot of [1-phenylpropyne] versus time with 10 mol% $Ti(NMe_2)_2(dpm^{mes})$ (**12**) at 75 °C.

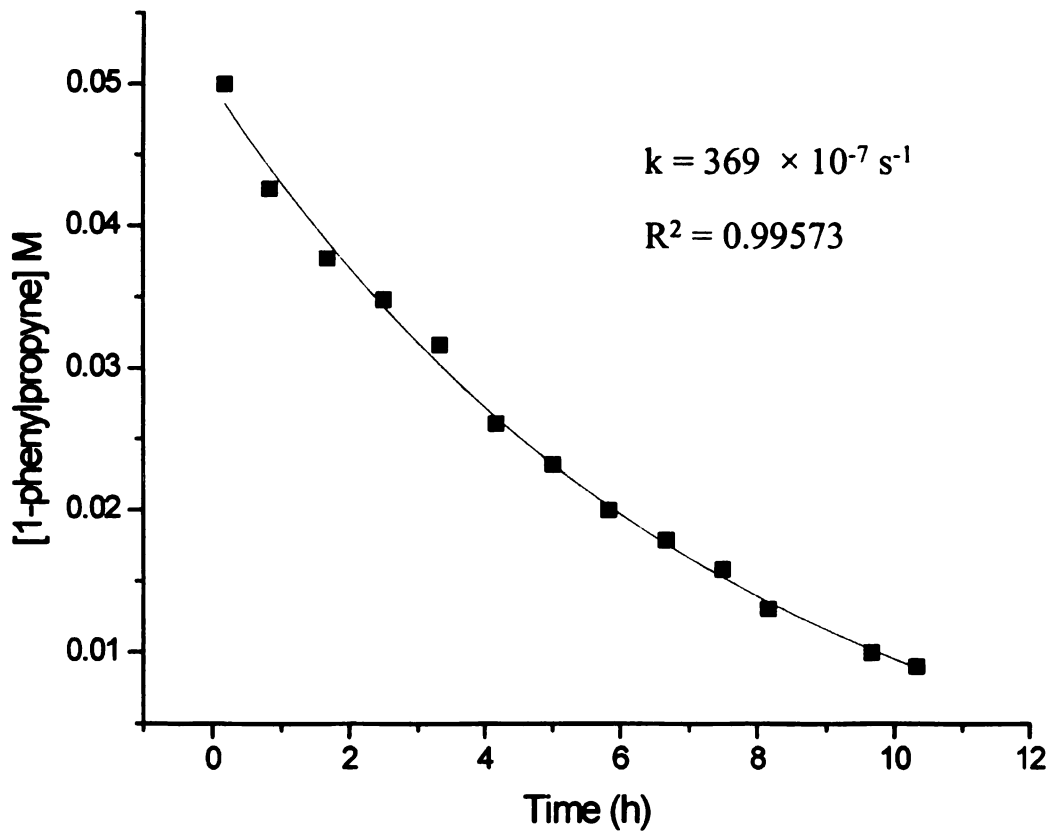

Figure A1.2 Representative plot of [1-phenylpropyne] versus time with 10 mol% $Ti(NMe_2)_2(dpm^{3,5-CF3})$ (**13**) at 75 °C.

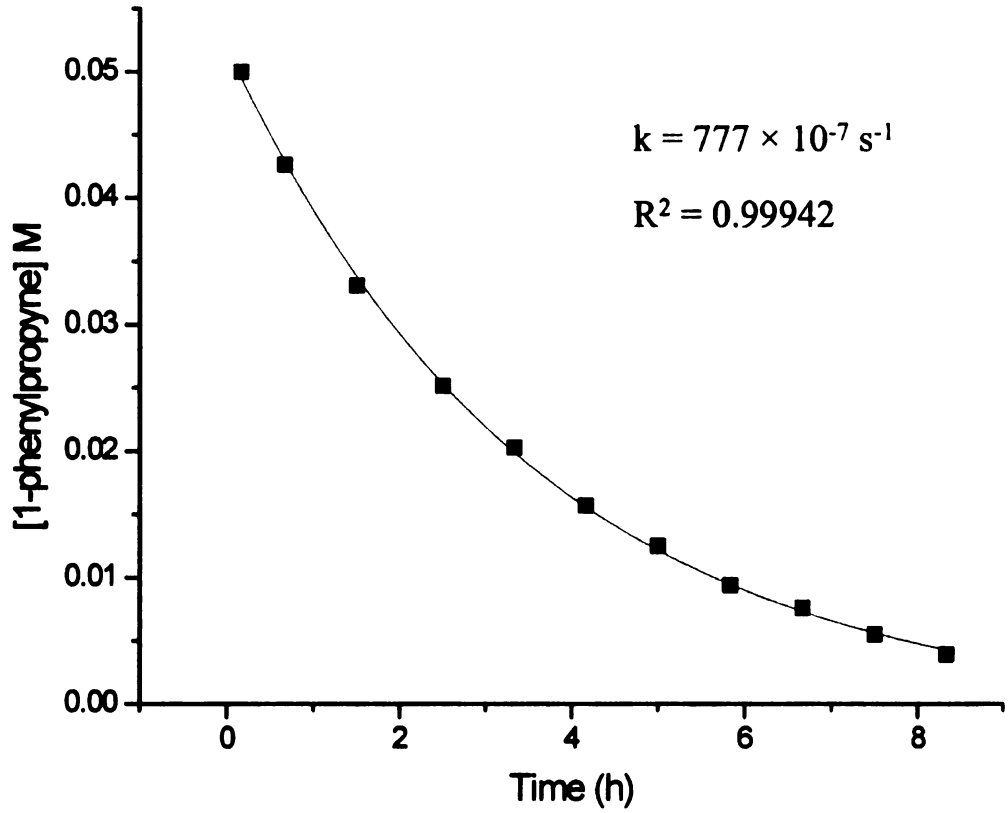

Figure A1.3 Representative plot of [1-phenylpropyne] versus time with 10 mol% $Ti(NMe_2)_2(pyrr^{3,5\text{–}CF3})_2$ (**14**) at 75 °C.

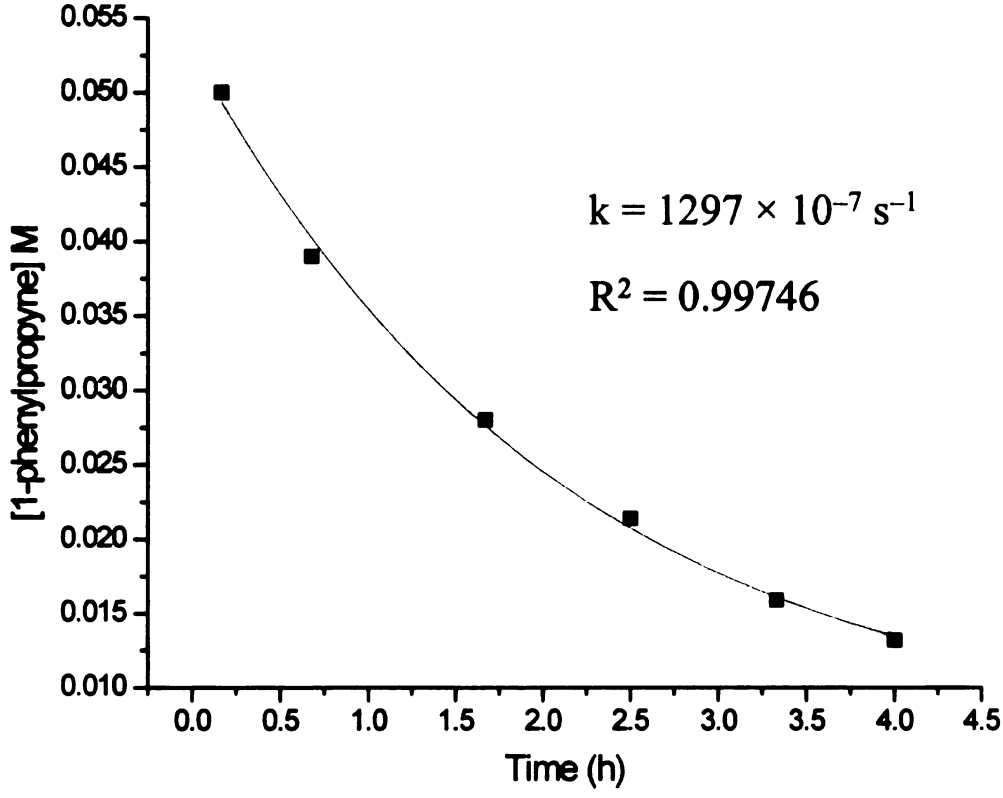

Figure A1.4 Representative plot of [1-phenylpropyne] versus time with 10 mol% $Ti(NMe_2)_2(pyrr^{mes})_2$ (**15**) at 75 °C.

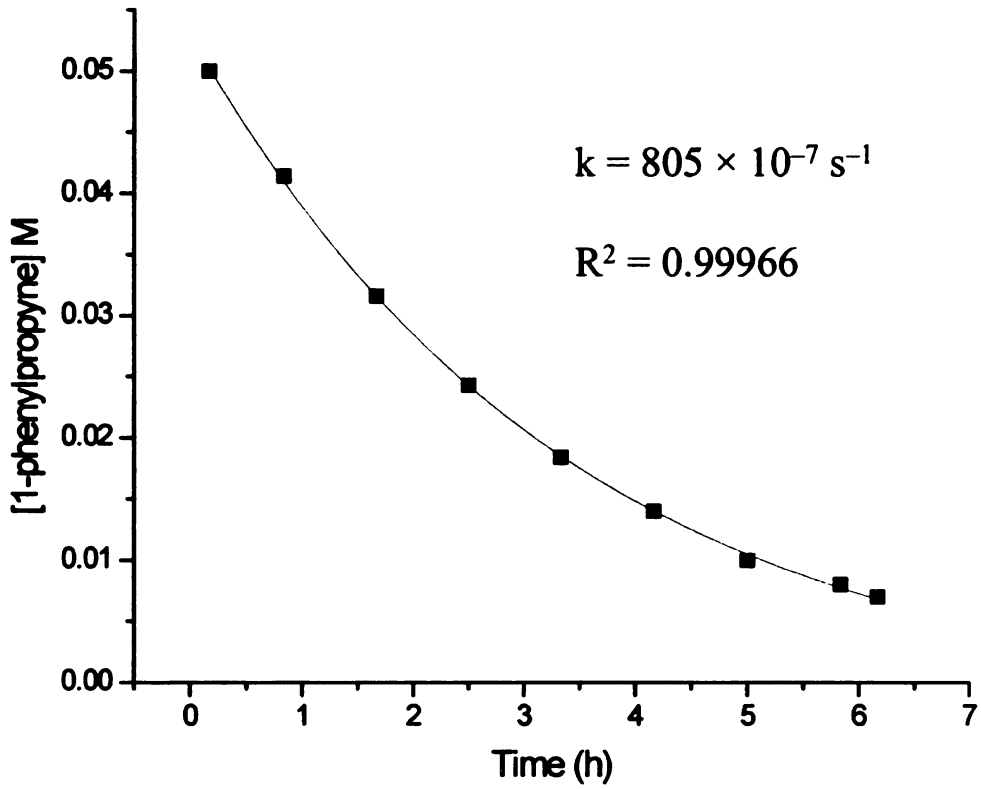

Figure A1.5 Representative plot of [1-phenylpropyne] versus time with 10 mol% $Ti(NMe_2)_2(pyrr^{4-CF3})_2$ (**16**) at 75 °C.

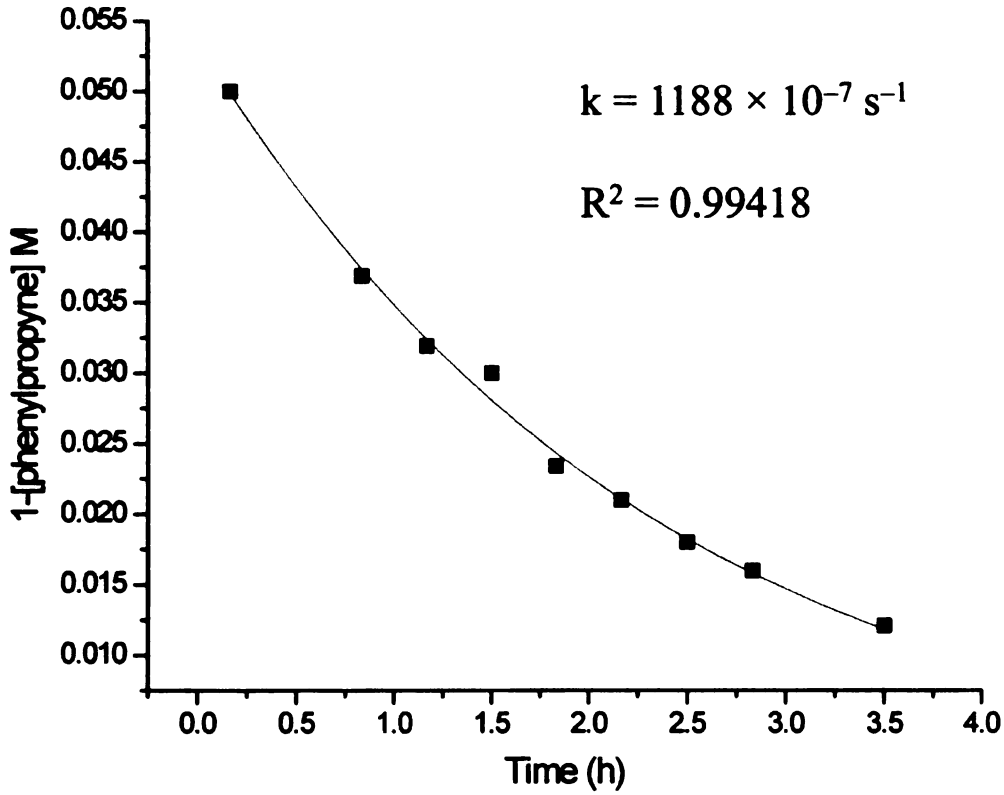

Figure A1.6 Representative plot of [1-phenylpropyne] versus time with 10 mol% $Ti(NMe_2)_2(pyrr^{tol})_2$ (**17**) at 75 °C.

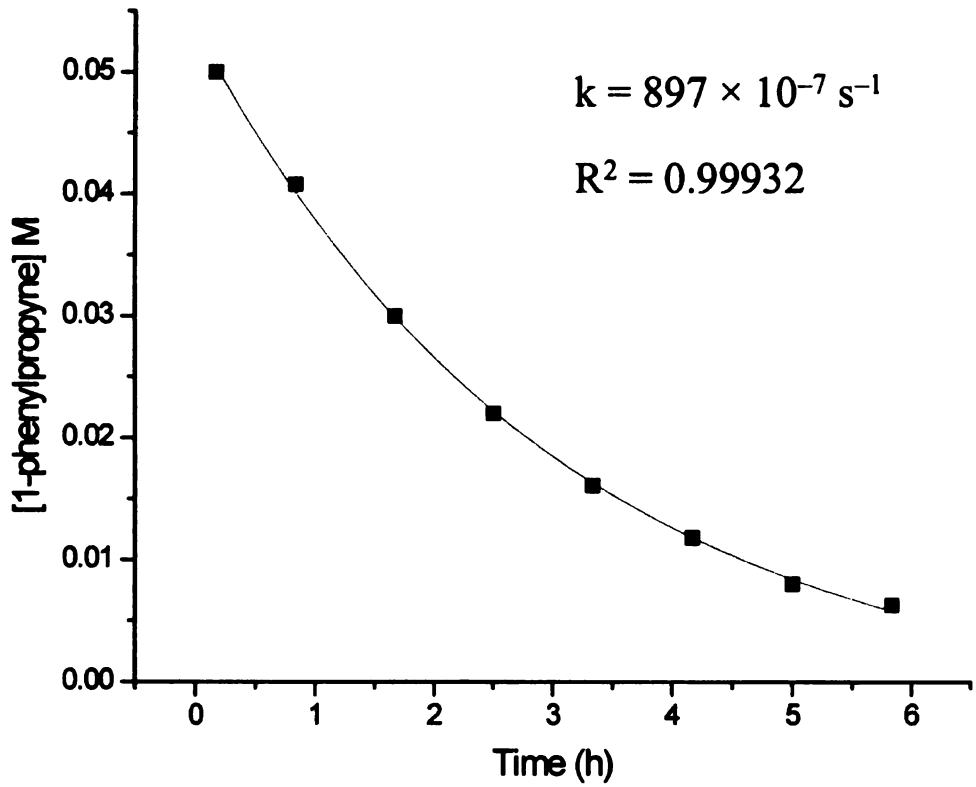

APPENDIX B

Kinetic plots for selected catalysts in chapter 3

Figure B1.1 Representative plot of [1-phenylpropyne] versus time with 10 mol% $Ti(NMe_2)_2(pyrr^{mes})_2$ (**15**) at 100 °C.

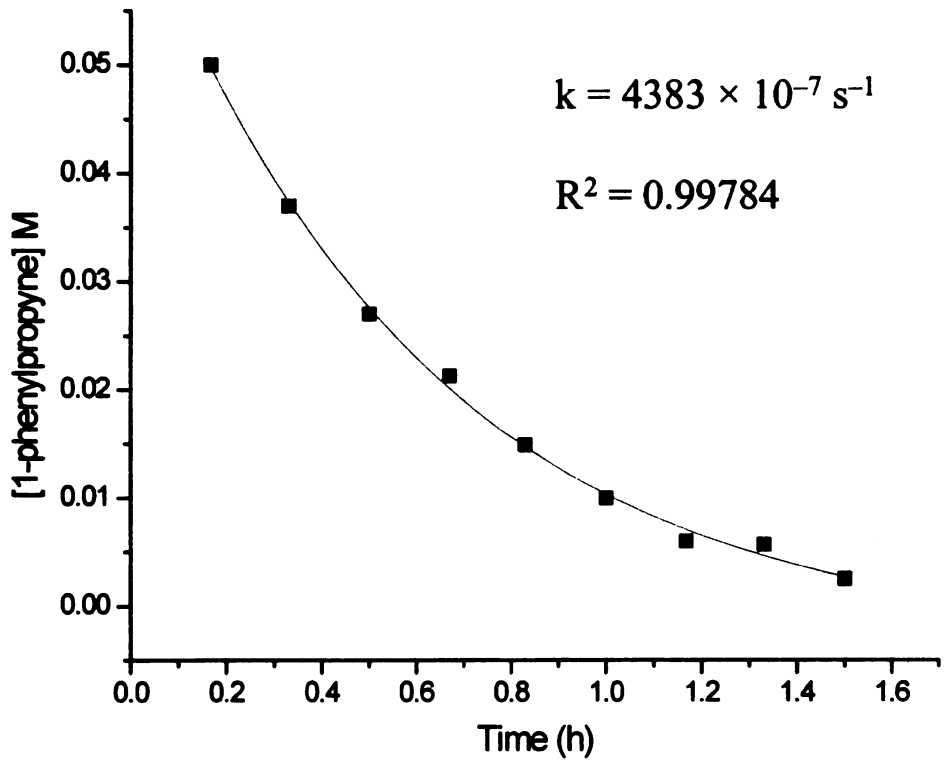

Figure B1.2 Representative plot of [1-phenylpropyne] versus time with 10 mol% Ti(indenyl)$_2$(Me)$_2$ (**21**) at 100 °C.

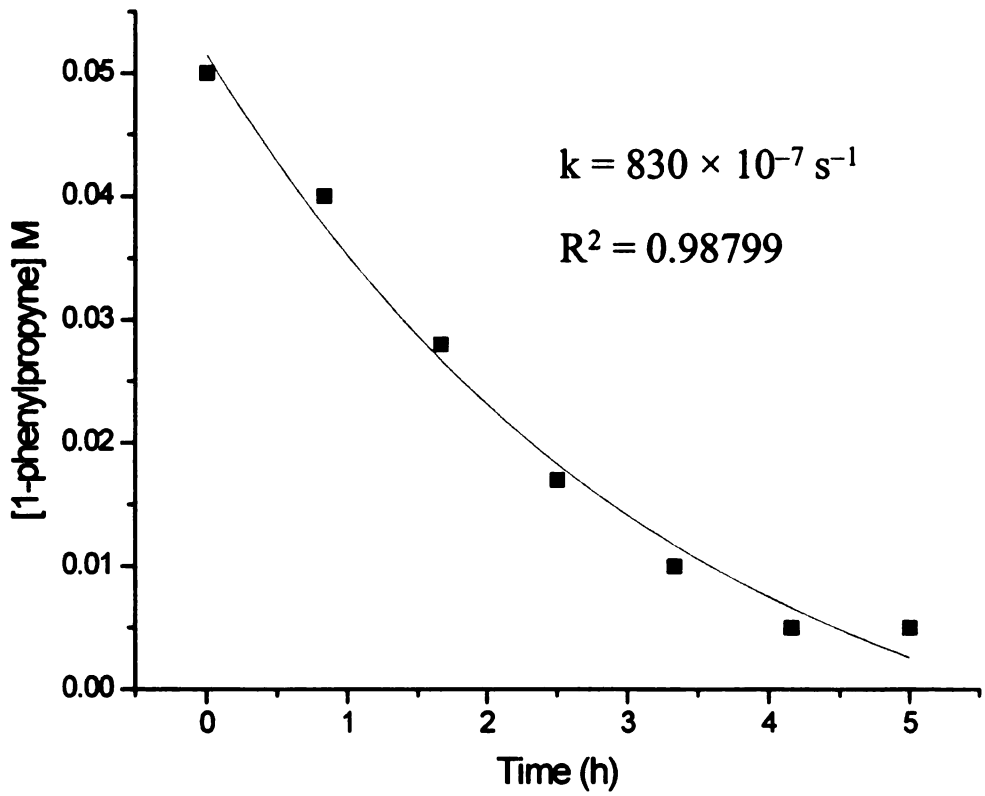

Figure B1.3 Representative plot of [1-phenylpropyne] versus time with 10 mol% $Ti(NMe)_3(pyr^{2\text{-}CF3\text{-}4C6F5})$ (**20**) at 100 °C.

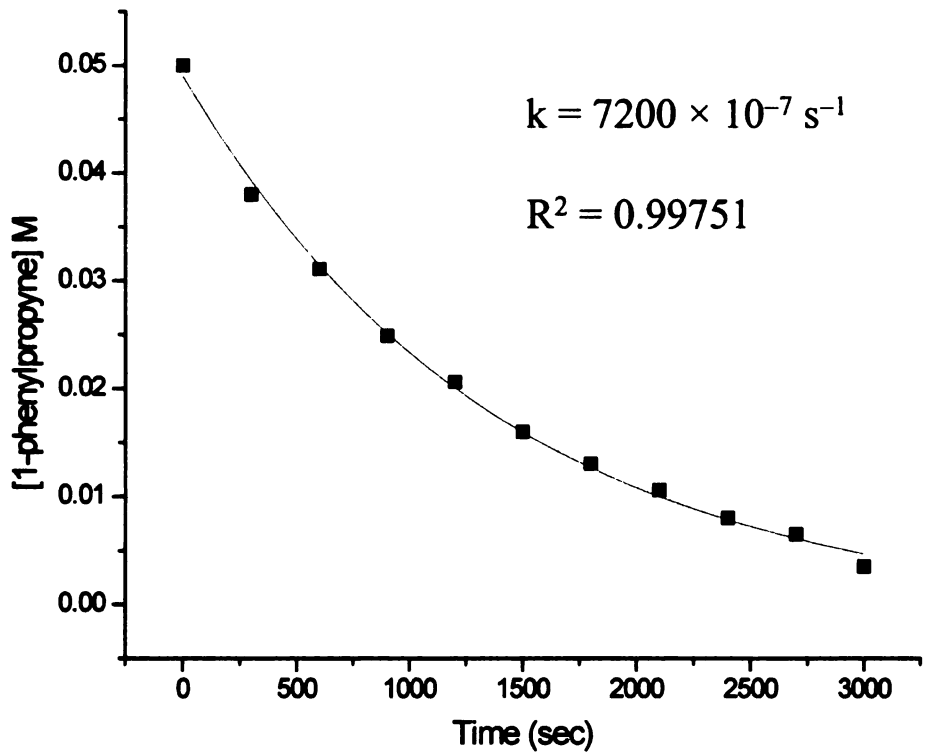

APPENDIX C

Kinetic plots for selected catalysts in chapter 4

Figure C1.1 Representative plot of [1-phenylpropyne] versus time with 10 mol% $Ti(NMe)_2(3\text{-}dpm^{3,5\text{-}CF3})$ (**22**) at 75 °C.

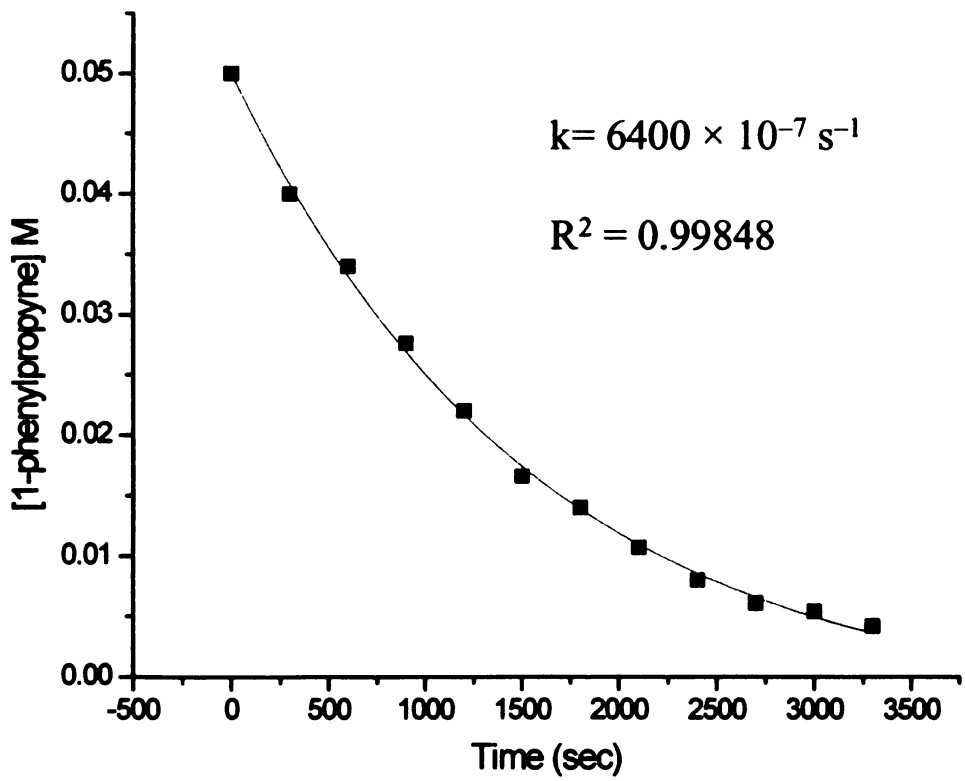

Figure C1.2 Representative plot of [1-phenylpropyne] versus time with 10 mol% $Ti(NMe)_2(3\text{-}dpm^{C6F3})$ (**23**) at 75 °C.

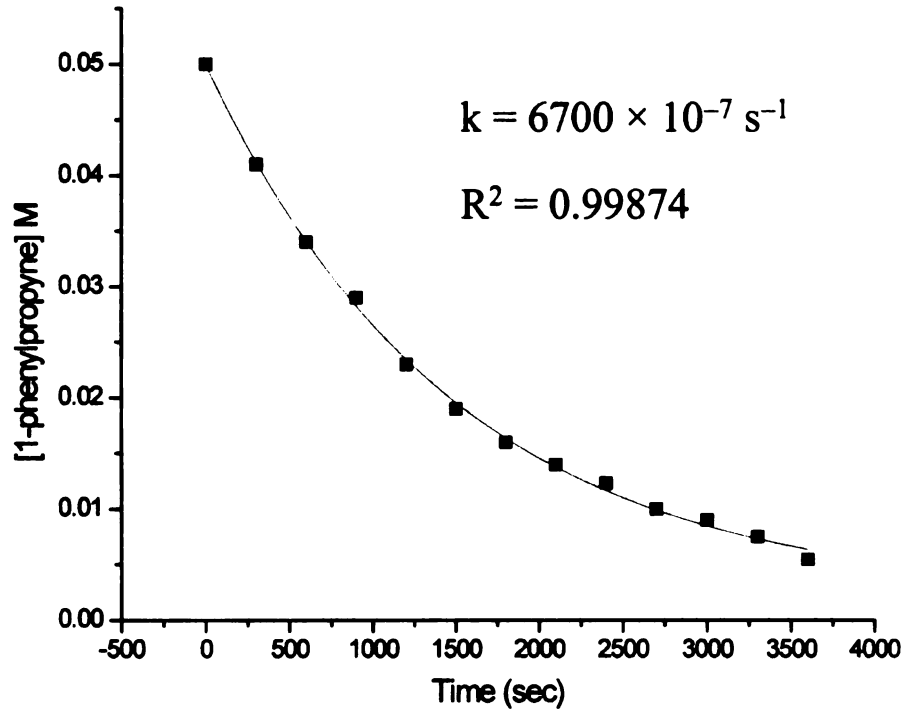

Figure C1.3 Representative plot of % conversion versus time with 10 mol% $Ti(NMe)_2(3\text{-}dpm^{3,5\text{-}CF3})$ (**22**) at 75 °C using reaction calorimetry.

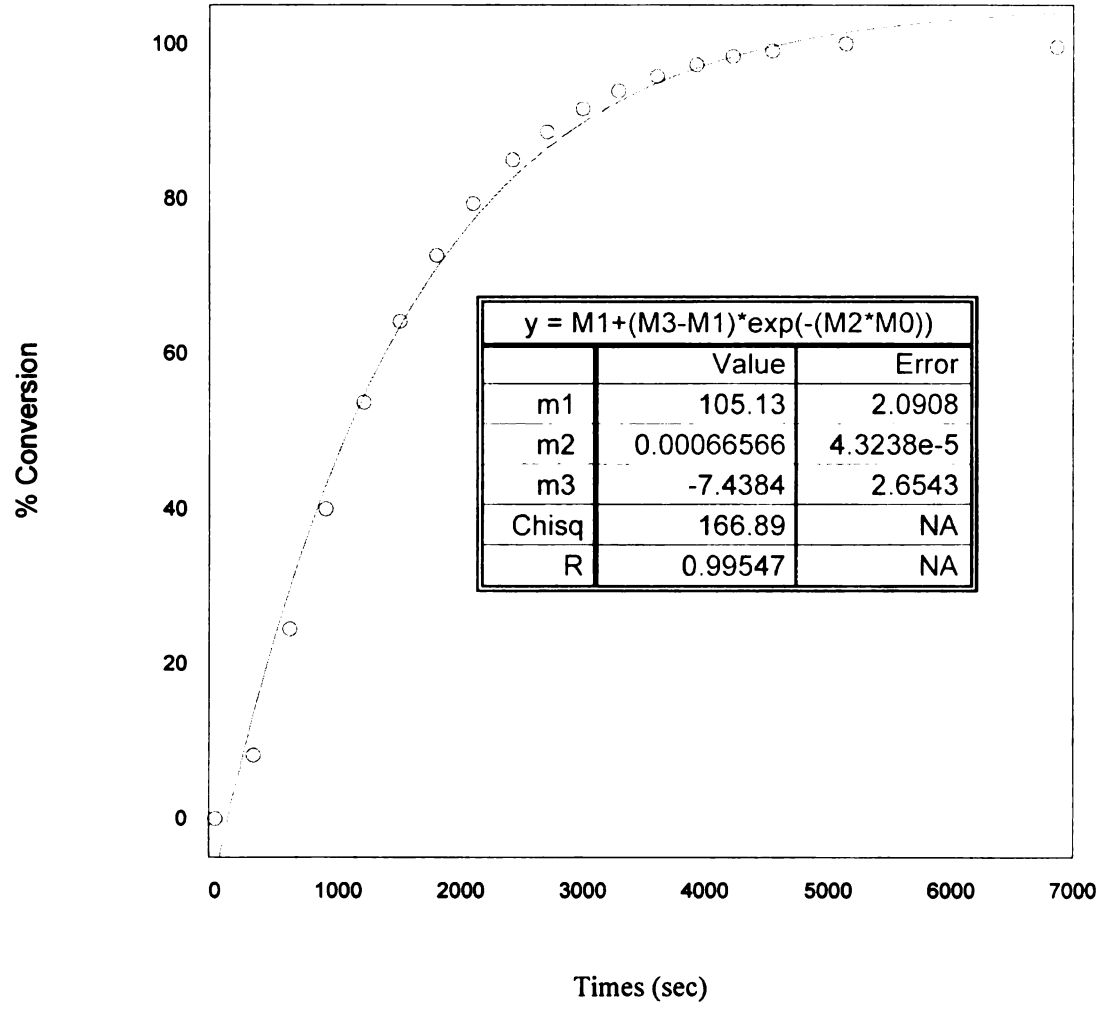

APPENDIX D

NMR spectra for selected compounds

Figure D1.1 ^{1}H spectrum for $Ti(NMe_2)_2(dpm^{mes})$ (**12**).

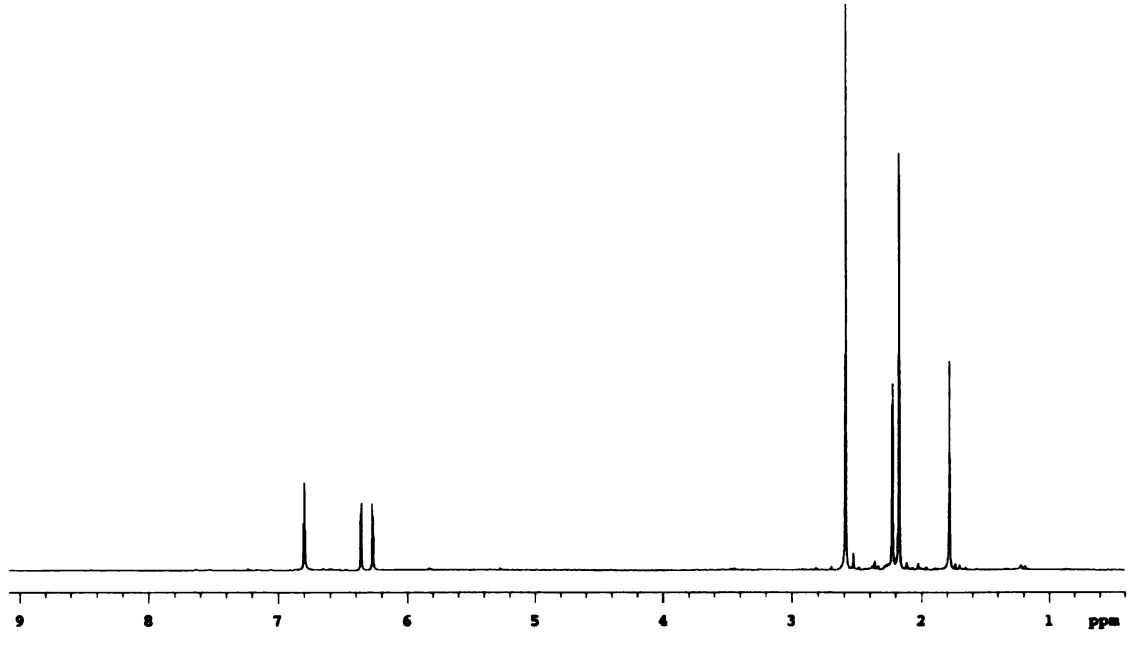

Figure D1.2 ^{13}C spectrum for $Ti(NMe_2)_2(dpm^{mes})$ (**12**).

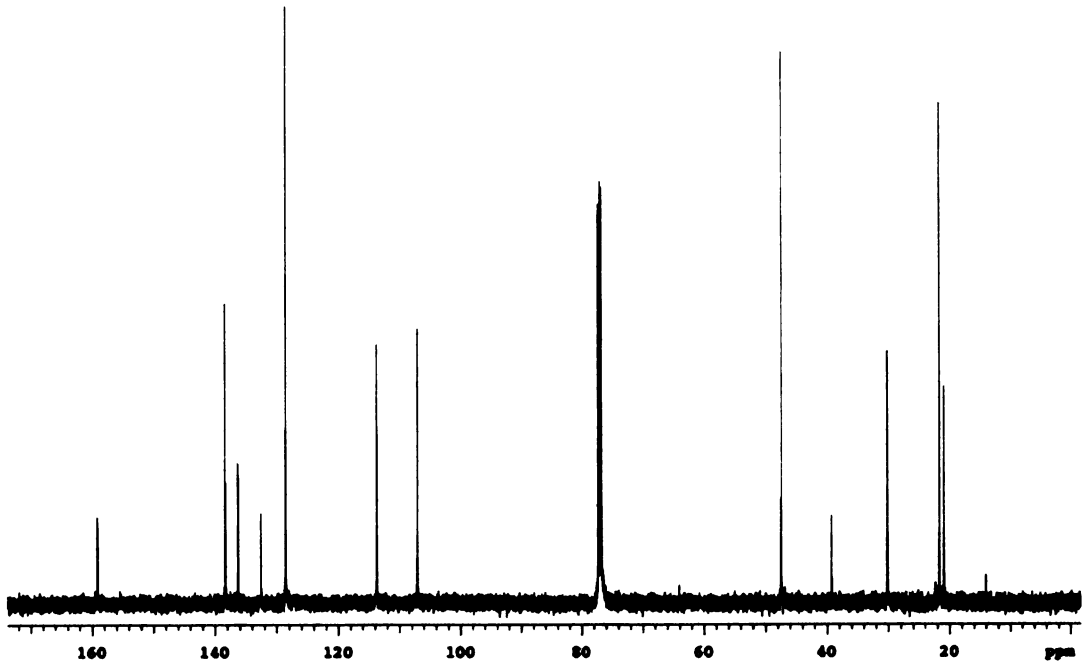

Figure D1.3 ^{1}H spectrum for $U(NBu^{t})_2(dpm^{mes})$ **(26)**.

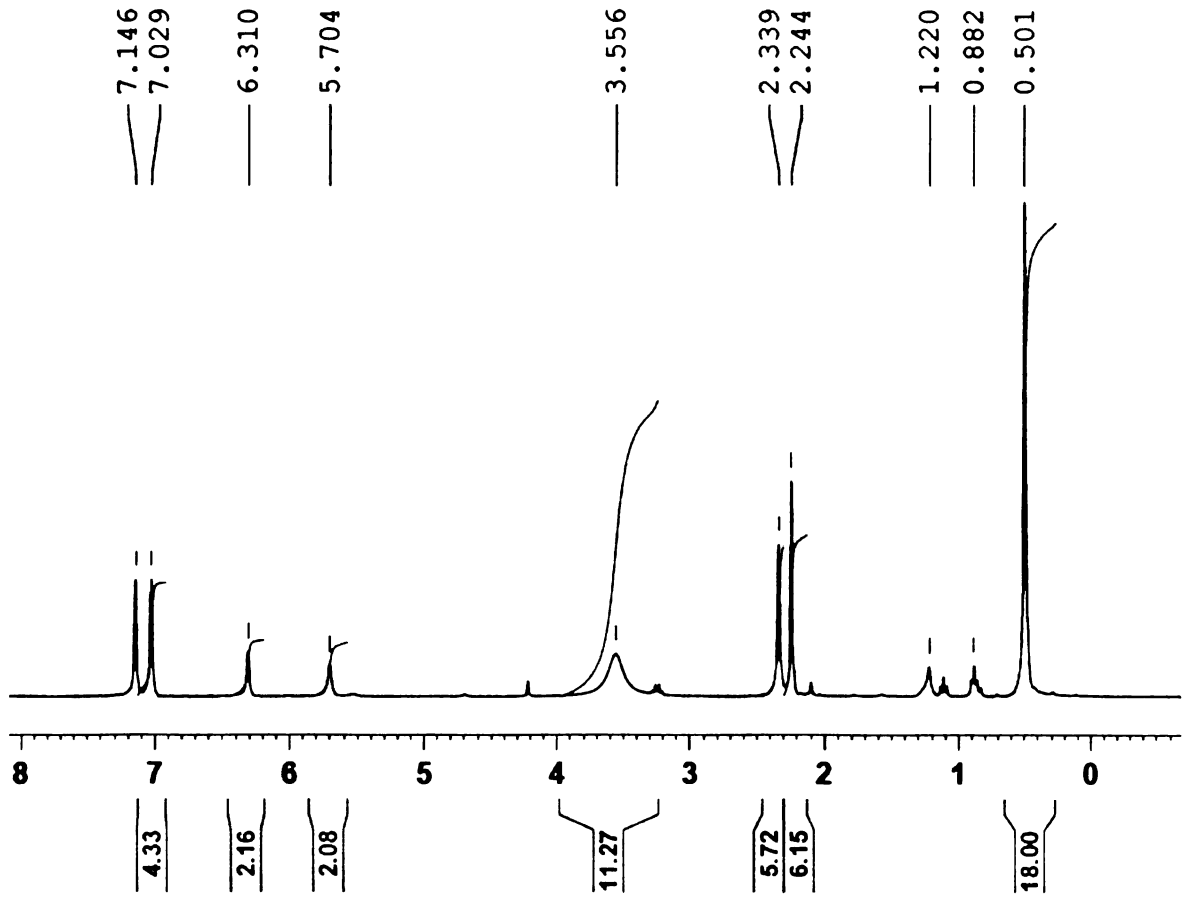

Figure D1.4 ^{1}H spectrum for $U(NBu^{t})_2(dpm^{mes})(dmpe)$ (**27**).

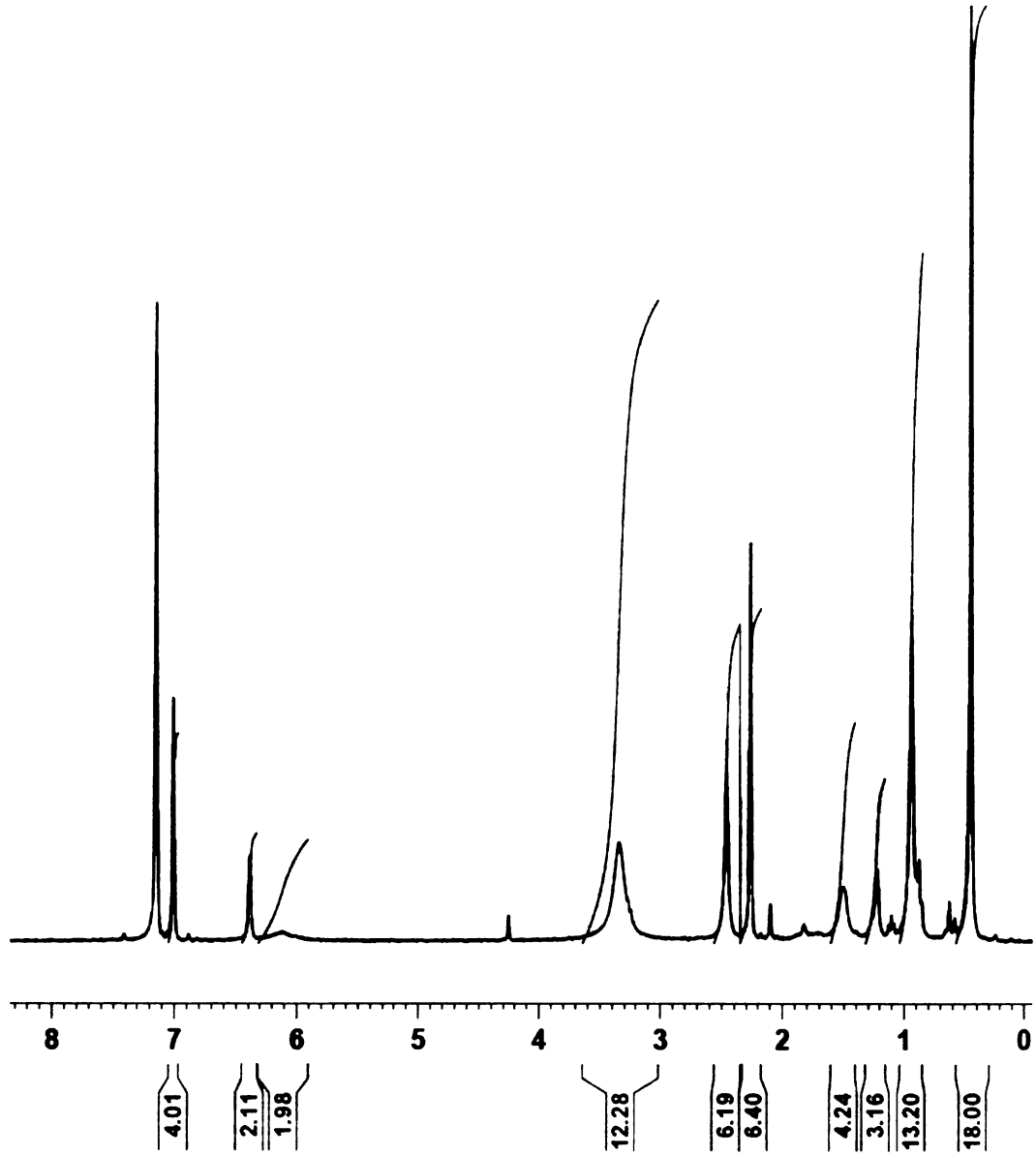

Figure D1.5 ^{31}P spectrum for $U(NBu^t)_2(dpm^{mes})(dmpe)$ (**27**).

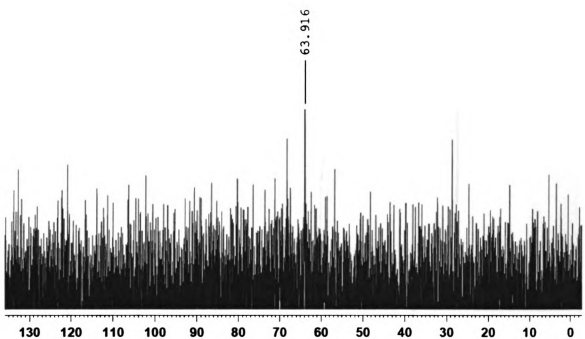

Figure D1.6 ^{1}H spectrum for U(NBu^{t})(THF)$_2$(dpm) (**28**).

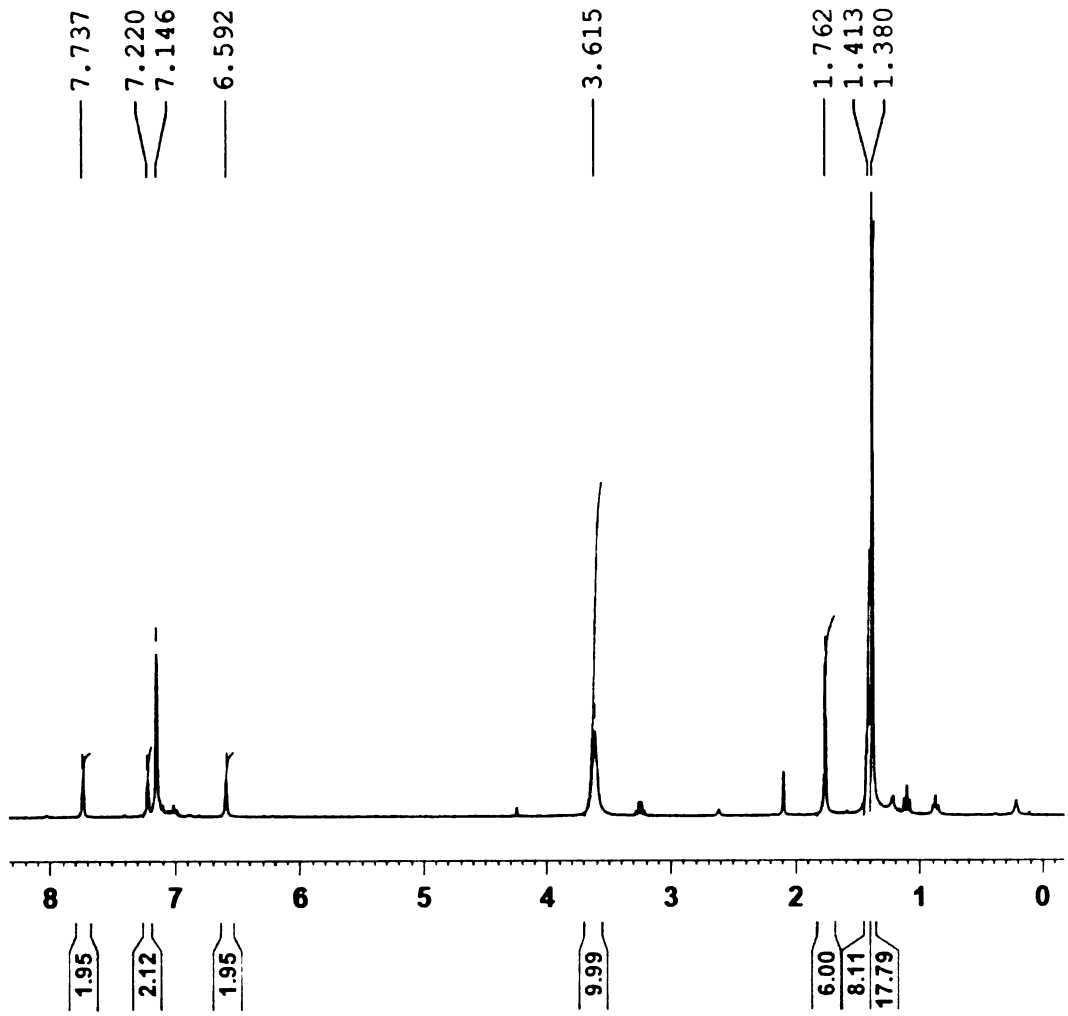

Figure D1.7 ^{13}C spectrum for $Ti(NMe_2)_2(NHMe_2)(pyrr^{3,5-CF3})_2$ (**19**) in $CDCl_3$.

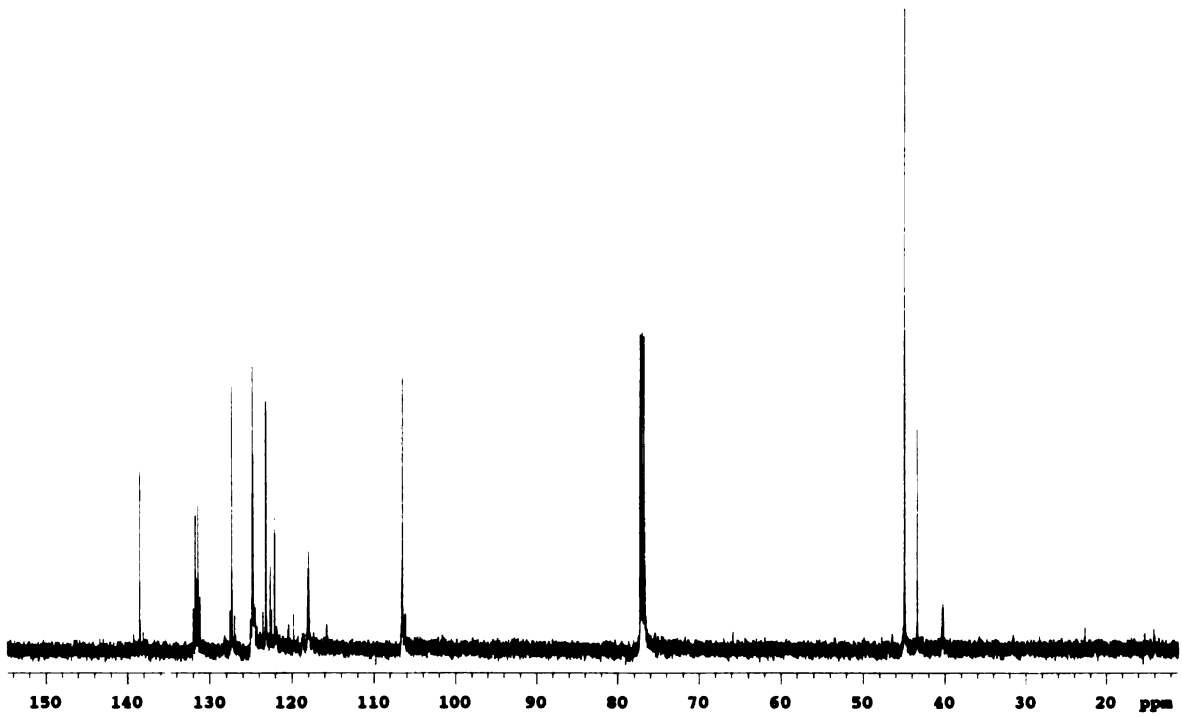

Figure D1.8 ^{1}H spectrum for $Ti(NMe_2)_2(NHMe_2)(pyrr^{3,5-CF3})_2$ **(19)** in $CDCl_3$.